OXFORD LIBRARY OF THE
PHYSICAL SCIENCES

ELECTROMAGNETIC STRUCTURE OF NUCLEONS

BY

S. D. DRELL

AND

F. ZACHARIASEN

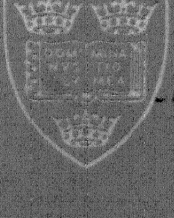

OXFORD UNIVERSITY PRESS

539.72 D77e 64-04549

Drell
Electromagnetic structure of
nucleons

~~MAIN~~

kansas city public library
kansas city, missouri

Books will be issued only
on presentation of library card.
Please report lost cards and
change of residence promptly.
Card holders are responsible for
all books, records, films, pictures
or other library materials
checked out on their cards.

3 1148 00613 6824

DATE DUE

MAI JUL 7 1979

FEB 10 1993

OXFORD LIBRARY OF THE PHYSICAL SCIENCES

Editors

B. BLEANEY
F. C. FRANK
M. H. L. PRYCE
D. H. WILKINSON

OXFORD LIBRARY OF THE PHYSICAL SCIENCES

Already published

THEORIES OF NUCLEAR MOMENTS
By R. J. Blin-Stoyle

THE SPECTRUM OF ATOMIC HYDROGEN
By G. W. Series

EXPANSION MACHINES FOR LOW TEMPERATURE PROCESSES
By S. C. Collins and R. L. Cannaday

STATISTICAL THEORY OF IRREVERSIBLE PROCESSES
By R. Eisenschitz

NUCLEAR PHOTO-DISINTEGRATION
By J. S. Levinger

THE FUNDAMENTAL ATOMIC CONSTANTS
By J. H. Sanders

ELECTROMAGNETIC STRUCTURE OF NUCLEONS

BY

S. D. DRELL and F. ZACHARIASEN
STANFORD UNIVERSITY,
STANFORD, CALIFORNIA

OXFORD UNIVERSITY PRESS
1961

Oxford University Press, Amen House, London, E.C.4
GLASGOW NEW YORK TORONTO MELBOURNE WELLINGTON
BOMBAY CALCUTTA MADRAS KARACHI KUALA LUMPUR
CAPE TOWN IBADAN NAIROBI ACCRA

© Oxford University Press 1961

Printed in Northern Ireland at The Universities Press, Belfast

PREFACE

This monograph is intended to provide a critical review and analysis of recent studies of the electromagnetic structure of nucleons. The first chapter is devoted to a precise definition of what is meant by the electromagnetic form factors. The different types of experiments which have given information on these form factors are discussed in Chapter II with emphasis on the theoretical assumptions and approximations made in analysing the experimental numbers in terms of form factors. Chapter III is devoted to the recent dispersion theoretic analyses of the form factors. The theoretical development here has the two goals of serving as a first introduction to the dispersion methods for physicists at the graduate level and of indicating clearly the various approximations made at present in implementing the dispersion theory approach. In Chapter IV the validity of quantum electrodynamics is discussed and it is shown how possible deviations in this theory alter the nucleon form factor analyses. Two appendices are included with formal developments.

We wish to thank the Air Force Office of Scientific Research, of the United States Air Force, for partial support in preparation of the manuscript.

S. D. D.
F. Z.

September 1960

KANSAS CITY (MO.) PUBLIC LIBRARY

6404549

50

CONTENTS

CHAPTER I. DEFINITION OF ELECTROMAGNETIC STRUCTURE OF NUCLEONS 1

CHAPTER II. THEORETICAL APPROXIMATIONS AND ASSUMPTIONS IN OBTAINING NUCLEON FORM FACTORS FROM EXPERIMENT 12

(1) Elastic electron-proton scattering 14
(2) Neutron-electron interaction 20
(3) Inelastic electron-deuteron scattering 23
(4) Elastic electron-deuteron scattering 40
(5) Electron production of pions from protons 44

CHAPTER III. CALCULATIONS OF NUCLEON FORM FACTORS 51

(1) The dispersion theory approach; illustration with Feynman diagram 51
(2) The absorptive amplitude and its high energy behaviour, thresholds, and (non-) positive definiteness 57
(3) Perturbation theory approximation 64
(4) Two pion approximation; static limit, selection rules, and unitarity limitations 69
(5) Form factor of the pion and $\pi-\pi$ scattering 74
(6) Annihilation amplitude for $\pi+\pi\rightarrow N+\bar{N}$ 78
(7) Completion of development and discussion of results 81

CHAPTER IV. VALIDITY OF QUANTUM ELECTRODYNAMICS AND EFFECT ON NUCLEON STRUCTURE INTERPRETATION 88

APPENDIX A 96

APPENDIX B 98

NOTES 101

CHAPTER I

DEFINITION OF ELECTROMAGNETIC STRUCTURE OF NUCLEONS

THE first step in any discussion of the electromagnetic structure of the nucleon is of necessity a precise definition of what is meant by such structure. For purposes of introducing and illustrating this definition, it will be convenient to fix attention, for the moment, on the scattering of electrons from protons; it is this experiment, after all, which has produced the present information on the proton's electromagnetic structure.

To lowest order in e, the electric charge, a single virtual photon is exchanged between the electron and the proton. The Feynman diagram representing this process is illustrated in Fig. I.1.

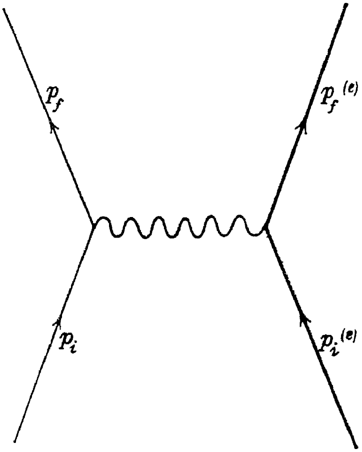

FIG. I.1. Feynman diagram for electron-proton scattering to order e^2. The proton is treated as a point Dirac particle. The line represents a proton, the heavy line, an electron, and the wavy line, a photon.

The transition amplitude corresponding to this diagram may be written [1]

$$\int \frac{d^4q}{(2\pi)^4} \langle p_f| \int j_\mu^{(P)}(x) e^{-iq.x}\, d^4x |p_i\rangle \frac{1}{q^2} \langle p_f^{(e)}| \int j_\mu^{(e)}(x) e^{iq.x}\, d^4x |p_i^{(e)}\rangle \tag{1.1}$$

where p_f, p_i and $p_f^{(e)}$, $p_i^{(e)}$ are the final and initial 4-momenta of the proton and electron, respectively, $q_\mu = (p_f - p_i)_\mu = (p_i^{(e)} - p_f^{(e)})_\mu$ is the 4-momentum transferred from electron to proton, and $j_\mu^{(P)}(x)$, $j_\mu^{(e)}(x)$ are the electromagnetic current operators of the proton and electron. The factor q^{-2} is the propagator for the virtual photon which is exchanged [2]. According to quantum electrodynamics, the current operator for the electron is given by,

$$j_\mu^{(e)}(x) = e_0 \bar{\psi}_e(x) \gamma_\mu \psi_e(x)$$

where $\psi_e(x)$ is the electron field, and e_0 is the unrenormalized charge. Thus, to lowest order,

$$\begin{aligned} \langle p_f^{(e)}| \int j_\mu^{(e)}(x) e^{iq.x}\, d^4x |p_i^{(e)}\rangle & \\ &= \frac{e_0}{\sqrt{(4E_f^{(e)}E_i^{(e)})}} (\bar{u}_{p_f}^{(e)}|\gamma_\mu|u_{p_i}^{(e)}) \int d^4x e^{i(p_f(e) - p_i(e) + q).x} \\ &= \frac{e_0}{\sqrt{(4E_f^{(e)}E_i^{(e)})}} (\bar{u}_{p_f}^{(e)}|\gamma_\mu|u_{p_i}^{(e)}) (2\pi)^4 \delta^4(p_f^{(e)} - p_i^{(e)} + q). \end{aligned} \tag{1.2}$$

Similarly, according to pure quantum electrodynamics, the proton current is

$$j_\mu^{(P)}(x) = e_0 \bar{\psi}_p(x) \gamma_\mu \psi_p(x) \tag{1.3}$$

so that, again to lowest order in e_0,

$$\begin{aligned} \langle p_f| \int j_\mu^{(P)}(x)\, e^{-iq.x}\, d^4x |p_i\rangle & \\ &= \frac{e_0}{\sqrt{(4E_f E_i)}} (\bar{u}_{p_f}|\gamma_\mu|u_{p_i}) \int d^4x e^{i(p_f - p_i - q).x}. \end{aligned} \tag{1.4}$$

The lowest order Feynman amplitude is then obtained by combining equations (1.1), (1.2), and (1.4). Now the basic assumption involved in deducing equation (1.4) is that the coupling of the proton to the virtual photon is described simply by quantum electrodynamics, in which the proton is a point particle of unit charge and the usual Dirac magnetic moment. It is clear, however, that this assumption is not at all valid—in particular the proton couples strongly to mesons and other particles, so that equation (1.3) for the electrodynamic current of the proton is certainly not correct. For example, since there is presumably a cloud of virtual mesons around the proton, one should add the meson current to $j_\mu^{(P)}$, i.e. one should write [3]

$$j_\mu^{(P)}(x) = e_0\bar{\psi}_p(x)\gamma_\mu\psi_p(x)+ie_0(\varphi(x)\nabla_\mu\varphi(x)^*-\varphi(x)^*\nabla_\mu\varphi(x)),$$

where $\varphi(x)$ is the meson field. Similarly more terms should be added corresponding to other particles which can appear virtually. All these virtual particles, then, produce effects which change the structure of the vertex at which the photon is absorbed by the proton; that is they change the form of equation (1.4). That such effects are not negligible is illustrated, for example, by observing that the proton's magnetic moment, $2.79e/2M$, differs greatly from the Dirac moment, $e/2M$.

One must therefore expect deviations from the result of equation (1.4). These deviations will, in general, be of two kinds. First, the fact that the proton's moment is not equal to the Dirac moment means that there will be a Pauli term of the form $\sigma_{\mu\nu}F_{\mu\nu}^{(e)}$ in addition to the simple $\gamma_\mu A_\mu^{(e)}$ term already included [4]. Second, because of the cloud of virtual mesons about the proton, the coupling of the photon to the proton may take place over an extended region in space—thus one should replace

$$\int d^4x e^{i(p_f-p_i)\cdot x}e^{-iq\cdot x}$$

in which the photon is absorbed on a point proton, by something like

$$\int d^4x' \int d^4x e^{i(p_f-p_i)\cdot x}F(x'-x)e^{-iq\cdot x'}.$$

This may be conveniently rewritten as

$$\int d^4x e^{i(p_f-p_i-q)\cdot x}F(q^2)$$

where

$$F(q^2) = \int d^4y e^{-iq\cdot y} F(y),$$

$$F(y) = \int \frac{d^4q}{(2\pi)^4} e^{iq\cdot y} F(q^2). \qquad (1.5)$$

Physically, one might interpret this by saying that if the spatial extension of the proton is, for example, due to a virtual meson cloud, then the photon could be absorbed at x' by a virtual meson emitted from the proton at x. $F(x-x')$ might therefore be expected to have the 'size' of the meson cloud around the proton. If these alterations are incorporated into equation (1.4), it becomes

$$\langle p_f|\int j_\mu^{(P)}(x) e^{-iq\cdot x} d^4x|p_i\rangle$$
$$= \frac{1}{\sqrt{(4E_fE_i)}}(\bar{u}_{p_f}|\gamma_\mu F_1(q^2) + i\sigma_{\mu\nu}q_\nu F_2(q^2)|u_{p_i})$$
$$\times \int d^4x e^{i(p_f-p_i-q)\cdot x}. \qquad (1.6)$$

Here a different spatial extent is associated with the original convection current coupling $\gamma_\mu A_\mu^{(e)}$, and with the subsequently introduced Pauli term $\sigma_{\mu\nu}F_{\mu\nu}^{(e)}$. Note that the charge e_0 has been included in F_1.

This form has been obtained on the basis of physical ideas about what effects could be produced by the presence of a meson cloud around the proton. It is in addition, however, the most general form which is allowed for the coupling of a photon to a physical proton by the requirements of gauge invariance and Lorentz invariance. This can be seen as follows. Consider the matrix element

$$\langle p_f|\int j_\mu^{(P)}(x) e^{-iq\cdot x} d^4x|p_i\rangle. \qquad (1.7)$$

The translational invariance of the theorists' world implies

$$j_\mu^{(P)}(x) = e^{iP.x} j_\mu^{(P)}(0) e^{-iP.x}$$

where P is the total energy momentum operator; thus equation (1.7) becomes

$$\int d^4x e^{i(p_f-p_i-q).x} \langle p_f|j_\mu^{(P)}(0)|p_i\rangle.$$

Now the matrix element $\langle p_f|j_\mu^{(P)}(0)|p_i\rangle$ must be of the form

$$\langle p_f|j_\mu^{(P)}(0)|p_i\rangle = \frac{1}{\sqrt{(4E_fE_i)}}(\bar{u}_{p_f}|O_\mu|u_{p_i}),$$

where O_μ is a Lorentz 4-vector, and is also a 4×4 matrix in the spinor space of the proton. The factor $\sqrt{(4E_fE_i)}$ appears here, incidentally, only for normalization purposes.

The matrix element is a function only of the 4-vectors p_f and p_i, which are subject to the restrictions $p_f^2 = p_i^2 = M^2$; from these one can construct only one scalar variable, which is chosen to be $(p_f-p_i)^2 = q^2$. The operator O_μ, then, must be constructed from the scalar q^2, the vectors $p_{f\mu}$ and $p_{i\mu}$, or equivalently the vectors q_μ and $P_\mu = (p_f+p_i)_\mu$, and the Dirac γ matrices. Since O_μ is a 4×4 matrix, it can always be written as a linear contribution of the 16 matrices

$$1,\quad \gamma_\mu,\quad \sigma_{\mu\nu},\quad \gamma_5\gamma_\mu,\quad \gamma_5;$$

since, in addition, it is not a pseudovector, the two γ_5 terms cannot appear.

The coefficients of the remaining terms are functions of whatever scalars can be formed; that is, of q^2, $\not{p}_f$ and $\not{p}_i$. By use of the commutation rules of the Dirac matrices, $\not{p}_f$ and $\not{p}_i$ can be moved to the left and right of the expression, respectively. But $\bar{u}_{p_f}\not{p}_f = \bar{u}_{p_f}M$, and $\not{p}_i u_{p_i} = Mu_{p_i}$; thus the $\not{p}_f$ and $\not{p}_i$ scalars can be eliminated and the most general form for O_μ is

$$O_\mu = a(q^2)q_\mu+b(q^2)P_\mu+c(q^2)\gamma_\mu+d(q^2)\sigma_{\mu\nu}q_\nu+e(q^2)\sigma_{\mu\nu}P_\nu.$$

Now the following identities are easily verified:

$$(\bar{u}_{p_f}|i\sigma_{\mu\nu}P_\nu|u_{p_i}) = (\bar{u}_{p_f}|-q_\mu|u_{p_i}),$$

$$(\bar{u}_{p_f}|i\sigma_{\mu\nu}q_\nu|u_{p_i}) = (\bar{u}_{p_f}|2M\gamma_\mu-P_\mu|u_{p_i}),$$

for free physical proton states which satisfy the Dirac equation $(\not{p}-M)u_p = 0$. Hence O_μ can be reduced to the form

$$O_\mu = a'(q^2)q_\mu+c'(q^2)\gamma_\mu+d'(q^2)\sigma_{\mu\nu}q_\nu,$$

where a', c', and d' are certain linear combinations of a, b, c, d, and e.

Up to this point only Lorentz invariance and the fact that the initial and final protons satisfy the free particle Dirac equation have been used. It is still necessary to impose the requirement of gauge invariance. This implies the continuity equation $\nabla_\mu j_\mu = 0$. Translating this into a condition on O_μ,

$$0 = \langle p_f | (\nabla_\mu j_\mu)_{x=0} | p_i \rangle = \frac{1}{\sqrt{(4E_f E_i)}} (\bar{u}_{p_f} | q_\mu O_\mu | u_{p_i});$$

therefore

$$0 = \frac{1}{\sqrt{(4E_f E_i)}} (\bar{u}_{p_f} | a'(q^2) q^2 + c'(q^2) \not{q} + d'(q^2) \sigma_{\mu\nu} q_\mu q_\nu | u_{p_i}).$$

The last term here is directly zero; the second vanishes because

$$(\bar{u}_{p_f} | \not{q} | u_{p_i}) = (\bar{u}_{p_f} | \not{p}_f - \not{p}_i | u_{p_i}) = (M - M)(\bar{u}_{p_f} | u_{p_i}) = 0.$$

Thus gauge invariance requires

$$q^2 a'(q^2) = 0.$$

Since in general, for virtual photons, $q^2 \neq 0$, it follows that $a'(q^2) = 0$. It is possible to show that $a'(0) = 0$ as well, by observing that the matrix element must be invariant under the transformation of interchanging p_f and p_i, and reversing the order of all γ matrices. This is most easily seen by an inspection of the relevant Feynman diagrams. The terms γ_μ and $\sigma_{\mu\nu} q_\nu$ are invariant to this, but the term q_μ changes sign.

The conclusion is that the most general form consistent with Lorentz invariance and gauge invariance, and with the fact that the two protons p_f and p_i satisfy the free Dirac equation, is

$$\langle p_f | j_\mu(0) | p_i \rangle = \frac{1}{\sqrt{(4E_f E_i)}} (\bar{u}_{p_f} | F_1(q^2) \gamma_\mu + i F_2(q^2) \sigma_{\mu\nu} q_\nu | u_{p_i}), \quad (1.8)$$

with the scalars c' and d' denoted here as F_1 and iF_2. Purely from these invariance arguments, then, it is clear that the form given in equation (1.6), on the basis of physical arguments is, in fact, the most general one possible. It is easy to see, in addition, from the fact that j_μ is a Hermitian operator, that the F's are real: explicitly,

$$
\begin{aligned}
&(\bar{u}_{p_i}|F_1{}^*\gamma_\mu - iF_2{}^*\sigma_{\mu\nu}q_\nu|u_{p_f}) \\
&\qquad = (\bar{u}_{p_f}|F_1\gamma_\mu + iF_2\sigma_{\mu\nu}q_\nu|u_{p_i})^* \\
&\qquad = \sqrt{(4E_fE_i)}\langle p_f|j_\mu(0)|p_i\rangle^* = \sqrt{(4E_fE_i)}\langle p_i|j_\mu(0)|p_f\rangle \\
&\qquad = (\bar{u}_{p_i}|F_1\gamma_\mu + iF_2\sigma_{\mu\nu}q'_\nu|u_{p_f})
\end{aligned}
$$

where $q' = p_i - p_f = -q$, so that $q'^2 = q^2$.

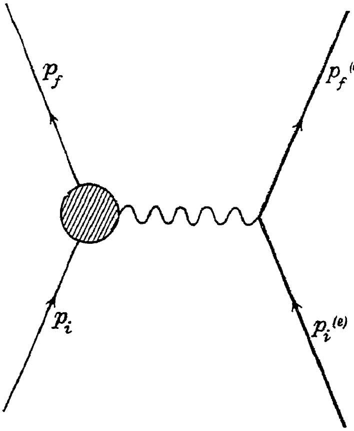

FIG. I.2. Diagram for electron-proton scattering to order e^2. The blob includes effects of all strongly interacting virtual particles.

The electron–proton scattering amplitude, to lowest order in the electric charge, is then given by

$$
\begin{aligned}
&(\bar{u}_{p_f}|\gamma_\mu F_1(q^2) + i\sigma_{\mu\nu}q_\nu F_2(q^2)|u_{p_i}) \times \frac{1}{q^2}(\bar{u}^{(e)}_{p_f}|e_0\gamma_\mu|u^{(e)}_{p_i}) \\
&\qquad \times \frac{1}{\sqrt{(16E_fE_iE^{(e)}_fE^{(e)}_i)}}(2\pi)^4\delta^4(p_f - p_i + p^{(e)}_f - p^{(e)}_i). \quad (1.9)
\end{aligned}
$$

This includes all possible effects due to clouds of virtual particles around the proton, and in fact, due to any contribution to the proton vertex which does not violate Lorentz invariance and gauge invariance.

The amplitude (1.9) may be interpreted as corresponding to a diagram like Fig. I.2 instead of Fig. I.1. The blob around the proton–photon vertex is supposed to indicate that no attempt is made to specify in detail how the interaction occurs—that is, the blob is meant to summarize all effects of any number of virtual particles as indicated in Fig. I.3.

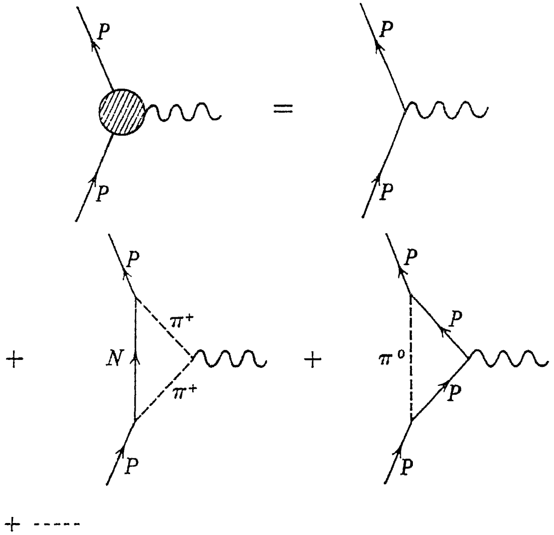

FIG. I.3. Examples of diagrams which contribute to the blob of Fig. I.2. The dashed lines represent pions.

The cross-section resulting from the amplitude of equation (1.9) is the Rosenbluth cross-section [5],

$$\frac{d\sigma}{d\Omega}=\frac{e^2}{4(4\pi)^2E_0^2}\,\frac{\cos^2(\frac{1}{2}\theta)}{\sin^4(\frac{1}{2}\theta)}\,\frac{1}{1+\dfrac{2E_0}{M}\sin^2(\frac{1}{2}\theta)}$$

$$\left\{F_1^2-\frac{q^2}{4M^2}(2(F_1+2MF_2)^2\tan^2(\tfrac{1}{2}\theta)+\{2MF_2\}^2)\right\}$$

where

$$q^2=-\frac{(2E_0\sin(\frac{1}{2}\theta))^2}{1+\dfrac{2E_0}{M}\sin^2(\frac{1}{2}\theta)}; \tag{1.10}$$

and E_0 denotes the incident energy and θ the scattering angle of the electron in the laboratory system.

If this formula is used to interpret the experimental results for electron–proton scattering, then F_1 and F_2 may be measured as functions of the invariant momentum transfer of the scattering. By definition, $F_1(0) = e$, the renormalized physically observed charge, and $F_2(0) = \mu_a = g(e/2M) = 1{\cdot}79\mu_B$, the anomalous magnetic moment [6].

A point particle of charge e and total magnetic moment $(g+1)\mu_B$ is a particle for which $F_1(q^2) = e$ and $F_2(q^2) = g\mu_B$ for *all* values of q^2; this is easily seen from equation (1.5). Thus by definition, a particle has electromagnetic structure—i.e. is not a point particle—if and only if the functions $F_1(q^2)$ and/or $F_2(q^2)$ are not constant. This is the precise definition of electromagnetic structure. The functions F_1 and F_2 are called respectively, the charge and moment form factors of the proton.

It should be noted that the definition of F_1 and F_2 in equation (1.8), is quite independent of the particular process of electron–proton scattering, but involves only the interaction of a real proton with a virtual photon. The same vertex appears in many other processes as well; it was only to make the physical meaning of the form factors a little clearer that their definition was introduced through the discussion of electron–proton scattering.

The functions $F_1(q^2)$ and $F_2(q^2)$ as defined in equation (1.8) from consideration of electron–proton scattering, are defined only for negative—i.e. spacelike—values of q^2, because $q^2 = (p_f-p_i)^2 = 2M^2-2p_f \cdot p_i \leqslant 0$. The definitions of F_1 and F_2 may be extended to include positive—i.e. timelike—values of q^2 by writing

$$\langle \overline{p}p'^{(-)}|j_\mu(0)|0\rangle = \frac{1}{\sqrt{(4\bar{E}E)}}\,(\bar{u}_{p'}|F_1(q^2)\gamma_\mu+iF_2(q^2)\sigma_{\mu\nu}q_\nu|v_{\overline{p}})$$

where $\langle \overline{p}p'^{(-)}|j_\mu(0)|0\rangle$ is the amplitude to create a proton–antiproton pair from a virtual photon. Here p' is the proton 4-momentum, $\overline{p}$ is the antiproton 4-momentum, $q = p'+\overline{p}$, and $\langle \overline{p}p'^{(-)}|$ is a proton–antiproton state with ingoing boundary conditions [7]. This definition gives F_1 and F_2 for $q^2 \geqslant 4M^2$.

It is possible to show that this definition of F_1 and F_2 in the region $q^2 \geqslant 4M^2$ coincides with the analytic continuation of the form factors defined in equation (1.8), treated as functions of the complex variable q^2. It will turn out that it is for many purposes more convenient to think of F_1 and F_2 in terms of this pair production process.

For spacelike q, where F_1 and F_2 may be thought of as related to the absorption of a virtual photon on a proton, it is possible to choose a co-ordinate system in which q has no time component. This is the barycentric system in which the incident (or outgoing) electron and proton have equal and opposite momenta. In this system, it is conventional to define spatial charge and moment densities by

$$\begin{aligned} e_1(r) &= \int \frac{d^3\mathbf{q}}{(2\pi)^3} F_1(-\mathbf{q}^2)e^{-i\mathbf{q}\cdot\mathbf{r}} \\ e_2(r) &= \int \frac{d^3\mathbf{q}}{(2\pi)^3} F_2(-\mathbf{q}^2)e^{-i\mathbf{q}\cdot\mathbf{r}}. \end{aligned} \tag{1.11}$$

It should be emphasized that this definition depends on a particular choice of Lorentz frame, in which the proton is not stationary, and therefore the relation of these densities to any real physical extension of the proton is quite unclear.

Note that

$$\int e_{1,2}(r)\, d^3\mathbf{r} = F_{1,2}(0).$$

The mean square radii of the spatial distributions are defined by

$$\begin{aligned} \langle r^2\rangle_{1,2} &= \int r^2 e_{1,2}(r)\, d^3\mathbf{r} \Big/ \int e_{1,2}(r)\, d^3\mathbf{r} \\ &= 6F'_{1,2}(-\mathbf{q}^2)|_{\mathbf{q}^2=0}/F_{1,2}(0). \end{aligned}$$

Therefore, for small q^2, one gets, in the special co-ordinate system:

$$\begin{aligned} F_{1,2}(-\mathbf{q}^2) &= F_{1,2}(0) - \mathbf{q}^2F'_{1,2}(-\mathbf{q}^2)|_{\mathbf{q}^2=0} + \dots \\ &= F_{1,2}(0)(1 - \tfrac{1}{6}\mathbf{q}^2\langle r^2\rangle_{1,2} + \dots). \end{aligned}$$

This may clearly also be written covariantly in any co-ordinate system: thus

$$F_{1,2}(q^2) = F_{1,2}(0)(1 + \tfrac{1}{6}q^2\langle r^2\rangle_{1,2} + \dots).$$

The mean square radius, then, just measures the slope of the form factor as $q^2 \to 0$; if the form factor is a very smooth function of q^2, this slope may give a way of simply summarizing its properties. If, however, the form factor does not have a fairly constant slope, the value of the rms radius is quite independent of its overall behaviour and therefore may in general not be a very useful concept.

Up to this point the discussion has been limited to the form factors and electromagnetic structure of the proton. It must now be expanded to recognize the existence of neutrons as well. The first step in accomplishing this is to affix an index P, for proton, onto all the form factors, densities, and radii so far defined.

The same considerations given above for the proton may also be made for the neutron; explicitly, define

$$\langle n_f|j_\mu(0)|n_i\rangle = \frac{1}{\sqrt{(4E_fE_i)}}\,(\bar{u}_{n_f}|F_1^N(q^2)\gamma_\mu + iF_2^N(q^2)\sigma_{\mu\nu}q_\nu|u_{n_i})$$

where $q = n_f - n_i$, and n_f, n_i are the 4-momenta of the neutron after and before absorbing the virtual photon. Equivalently, for timelike $q^2 \geqslant 4M^2$, the pair production amplitude is

$$\langle \bar{n}, n'^{(-)}|j_\mu(0)|0\rangle = \frac{1}{\sqrt{(4E'\bar{E})}}\,(\bar{u}_{n'}|F_1^N(q^2)\gamma_\mu + iF_2^N(q^2)\sigma_{\mu\nu}q_\nu|v_{\bar{n}})$$

where $q = n' + \bar{n}$, and n', $\bar{n}$ are the 4-momenta of the neutron and antineutron produced by the photon. Then the static limits for the neutron fix [8]

$$F_1^N(0) = 0$$
$$F_2^N(0) = \mu_N = -1{\cdot}91\,\frac{e}{2M}\,.$$

These equations, together with the analogous ones for protons, may be combined into one as follows: write

$$\langle p_f|j_\mu(0)|p_i\rangle = \frac{1}{\sqrt{(4E_fE_i)}}\,(\bar{u}_{p_f}|(F_1^s(q^2) + \tau_3F_1^v(q^2))\gamma_\mu + i(F_2^s(q^2) + \tau_3F_2^v(q^2))\sigma_{\mu\nu}q_\nu|u_{p_i}) \quad (1.11)$$

where p_f and p_i now refer to the 4-momenta of the final and initial nucleons, τ_3 is the z-component of the isotopic spin operator for the nucleon, and has the value $+1$ if p_f, p_i refer to a proton, and -1 if p_f, p_i represent a neutron. F_1^s and F_2^s are called the isotopic scalar charge and moment form factors, F_1^v and F_2^v are called the isotopic vector charge and moment form factors.

Evidently the following correspondence obtains:

$$\begin{aligned} F_1^P &= F_1^s+F_1^v \\ F_2^P &= F_2^s+F_2^v \\ F_1^N &= F_1^s-F_1^v \\ F_2^N &= F_2^s-F_2^v. \end{aligned} \tag{1.12}$$

Therefore

$$\begin{aligned} F_1^s(0) &= F_1^v(0) = e/2 \\ F_2^s(0) &= \frac{\mu_P+\mu_N}{2} = -0{\cdot}06\,\frac{e}{2M} \\ F_2^v(0) &= \frac{\mu_P-\mu_N}{2} = 1{\cdot}85\,\frac{e}{2M}. \end{aligned}$$

This decomposition into isotopic scalar and vector form factors is useful in the theoretical discussions which are based on the assumption of charge independence in the strong couplings between mesons and nucleons [7]. In all theoretical analyses presented in the succeeding chapters, charge independence, i.e. conservation of isotopic spin, will be assumed.

CHAPTER II

THEORETICAL APPROXIMATIONS AND ASSUMPTIONS IN OBTAINING NUCLEON FORM FACTORS FROM EXPERIMENT

It was remarked in Chapter I that the definition of the form factors F_1 and F_2 involves only the interaction of a real nucleon with a virtual photon. Thus any experimental arrangement which replaces the 'question box' of Fig. II.1 by a known interaction probes electromagnetic structure of the nucleon. Five types of experiments which have been carried out to determine the nucleon form factors are discussed in this chapter. These are:

1. Elastic electron–proton scattering for information on proton structure.

$$e+P \rightarrow e+P$$

2. Neutron–electron interaction for information on neutron structure.

$$N+e \rightarrow N+e$$

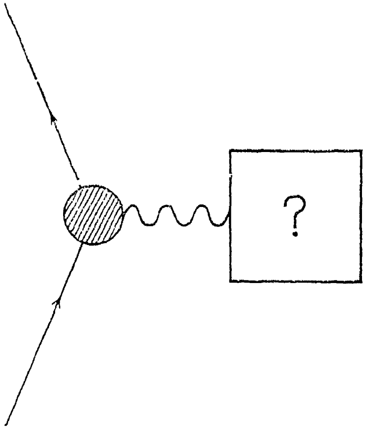

Fig. II.1. General process for measuring nucleon form factors.

3. Inelastic electron–deuteron scattering for information on neutron structure.

$$e+D \rightarrow e'+N+P$$

4. Elastic electron–deuteron scattering for information on neutron structure.

$$e+D \rightarrow e+D$$

5. Electron production of pions from protons primarily for information on neutron structure.

$$e+P \rightarrow \begin{cases} N+\pi^+ \\ P+\pi^0 \end{cases}$$

Theoretical assumptions and approximations which are required in order to extract values for $F_1(q^2)$ and $F_2(q^2)$ from these experiments are analysed in what follows.

1 [9]. For elastic electron–proton scattering the 'question box' of Fig. II.1 is replaced by an electron vertex, Fig. I.2. Hence this process gives the form factors of the proton, F_1^P and F_2^P, directly so long as it is adequate to treat the electromagnetic interaction between electron and proton in lowest-order perturbation theory, i.e. with one-quantum exchange.

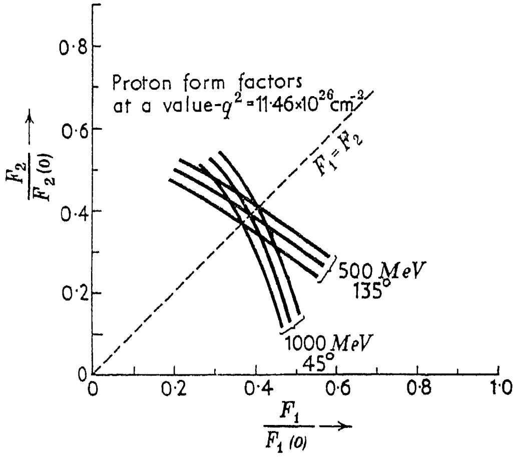

Fig. II.2. Curves for the independent determination of the charge and moment form factors of the proton. (Taken from R. Hofstadter; see [9].)

If the validity both of the Born approximation treatment of the electromagnetic interaction and of quantum electrodynamics is assumed, then the experiments on elastic scattering of electrons from protons must give a cross-section of the form of the Rosenbluth formula. Comparison of this formula with the experiments at various energies and angles then yields $F_1^P(q^2)$ and $F_2^P(q^2)$ directly for space-like momentum transfers. Evidently two measurements at different energies and angles, but fixed q^2, provide separate information on F_1 and F_2.

Charge scattering, or F_1, is of greater importance at small angles and moment scattering at large angles. Fig. II.2 shows the sensitivity with which two measurements at different energies E and angles θ, corresponding to the same q^2, determine F_1 and F_2 independently. Drawn in Fig. II.2 are portions of ellipses in the F_1-F_2 plane which correspond to a given cross-section value for fixed E and θ. A single cross-section measurement gives possible values of (F_1, F_2) along the arc of the ellipse corresponding to a given value of E and θ. The intersection with a second ellipse [10] for different values of E and θ but for the same q^2 then uniquely specifies (F_1, F_2). The figure is drawn for a particular pair and the family of three ellipses shows the latitude resulting from an experimental uncertainty of 10 per cent. If one continues this procedure and performs a third (or more) measurement with yet another pair of energy and angle values with the same q^2 there results a consistency check on the analysis.

Since the form factor analysis of the electron–proton scattering experiments are based on the Rosenbluth formula, it is appropriate to analyse next its quantitative validity, within the framework of quantum electrodynamics. The only possible corrections are then due to higher-order electromagnetic effects.

First of all there is the radiative correction to the electron current as calculated by Schwinger [11]. The Feynman diagrams corresponding to this correction appear in Fig. II.3. The emission of soft photons in the last two diagrams is allowed as consistent with the experimental energy resolution. For the high resolution used in the work of Hofstadter *et al.* [9], this correction may be as large as 15%–20% and it is taken into account in reducing the experimental data for comparison with the Rosenbluth formula. The analogous radiative correction to the proton current is negligible in present experiments due to the large proton mass.

A second class of possible corrections to the form factor interpretation corresponds to the exchange of more than one photon between the electron and proton. If the proton is treated as a rigid structure this correction is negligible, the difference between an exact phase shift calculation and the Born approximation being $\approx 0{\cdot}25\%$ [12]. However there exists the possibility of electron-induced polarizability of the proton's charge and current cloud [13]. Thus to order e^4 in the matrix element the electron may exchange two photons with the proton, virtually exciting isobaric states of the proton corresponding to resonances in the pion photoproduction cross-section. A diagram contributing to this virtual compton scattering by the proton is shown in Fig. II.4. Although they contribute corrections of order $\alpha = 1/137$ to the main term, Fig. I.2, terms of this type may be significant in the electron scattering analysis since in the compton scattering of real photons by protons they are responsible for the large resonance in the cross-section. Approximate evaluation of this polarizability correction has been carried out using a static 3–3 resonance model for the proton compton scattering [14] and it was established that the form factor analysis according to the

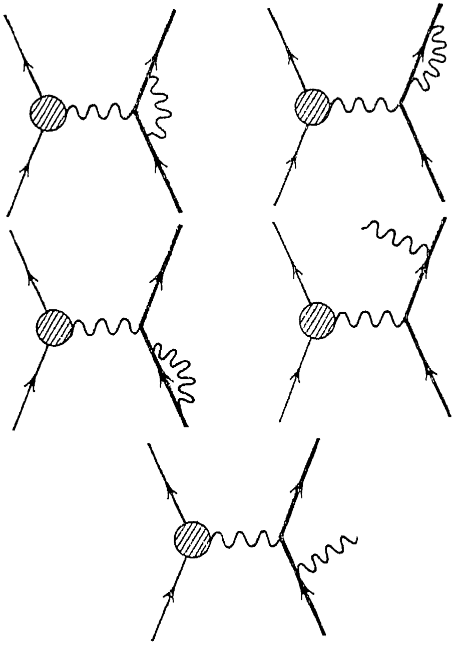

FIG. II.3. Feynman diagrams for radiative corrections to the electron current in electron-proton scattering.

Rosenbluth formula is valid to order $\alpha = 1/137$ up to energies $\approx$1 BeV for electron-proton scattering. However, as the laboratory energies for electron–proton scattering studies increase into the multi-BeV range the virtual compton amplitudes may be expected to play a more significant role. At higher energies there will be many important intermediate channels in Fig. II.4 for photon absorption to compete with the rapidly decreasing amplitude for the one-photon exchange.

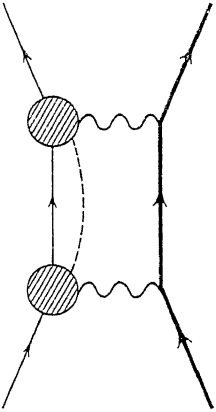

FIG. II.4. Diagram for an e^4 contribution corresponding to virtual compton scattering.

This result that compton scattering of the virtual photons in the electron–proton scattering plays a minor role at present energies whereas the compton scattering of real photons exhibits a big resonance [15] can be understood with a simple classical picture. Consider a monochromatic light wave, $a \cos \omega t$, incident on a proton which is represented as a charged oscillator with resonant frequency ω_r and damping constant γ. The constants ω_r and γ correspond to the total energy at resonance and the width of the 3–3 resonance in the meson–nucleon interaction. The charge of the proton scatters the light wave with no change in phase, the amplitude for charge scattering being proportional to $\cos \omega t$. The dipole moment induced in the proton by the incident radiation gives rise to dipole radiation which is phase-shifted relative to the incident wave and is proportional to

$$\frac{(\omega_r^2-\omega^2)\cos\omega t+\gamma\omega\sin\omega t}{(\omega_r^2-\omega^2)^2+\gamma^2\omega^2}. \tag{2.1}$$

The first term in (2.1) is in phase with and interferes with the direct charge-scattering term. It is the term of interest since this interference term is, to order α, the polarizability correction. However this in-phase term is seen to be odd about the resonant frequency $\omega = \omega_r$ and thus is largely cancelled in the integral over the virtual photon spectrum of the scattered electron. It is the second or out-of-phase term in equation (2.1) which gives rise to the resonant peak in the proton compton effect. For electron scattering its contribution is enhanced at resonance but nonetheless it is of negligible importance since it is of order α^2 relative to the leading or direct charge-scattering term.

Evidently electrons and photons are complementary tools for the study of nucleon structure. In compton scattering it is the polarizability of the structure that is studied whereas electron scattering measures the form factors F_1 and F_2. A connection between the form factors and polarizability emerges only as a detailed consequence of specific meson theories and models. Whereas the nucleon is real and on the physical mass shell both before and after absorbing the virtual photon at the vertex in Fig. II.1, in the compton process, Fig. II.4, it leaves the mass shell in the intermediate state which may contain pions and other strongly coupled states.

In résumé, the above discussion shows that in the range of present laboratory measurements, electron–proton scattering may be interpreted in terms of nucleon form factors using the Rosenbluth formula plus the radiative correction of Schwinger to the electron current. Measured form factors from some recent experimental data are shown in Fig. II.5.

For elastic scattering $q^2<0$ and so electron–proton scattering measurements yield direct information on the form factors for space-like momentum transfers only. In order to measure the form factors for time-like $q^2>0$, which is of interest in itself as well as for dispersion theory discussions of the nucleon form factors, as will be evident in Chapter III, it is necessary to turn to annihilation experiments

$$e^-+e^+\leftrightarrow P+\bar{P}, \tag{2.2}$$

in which case $q^2>[4(M)^2]$. It is hoped that such events will soon be within the scope of quantitative laboratory study. At this time they are not feasible because of energy and intensity limitations. Reaction (2.2) proceeding left to right requires $\geqslant 2$ BeV in the centre-of-mass system of the colliding electron and positron; proceeding to the left it requires an intense anti-proton beam as well as sensitive detectors in order to give an observable counting rate since the branching ratio for this process is $\leqslant\alpha^2=(1/137)^2$.

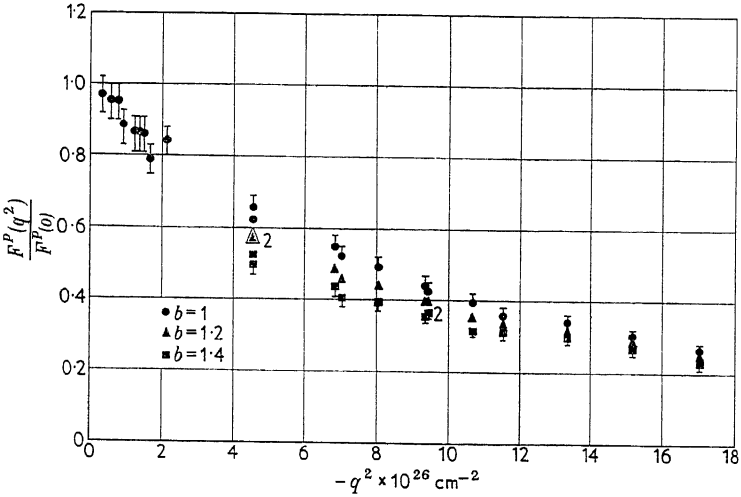

FIG. II.5. Experimental data on proton form factors. For $-q^2>4\times10^{26}$ cm^{-2} what is drawn is $F_2^P(q^2)/F_2^P(0)$; what is determined by experiment is essentially the combination $F_1^P+2MF_2^P$. At $-q^2=+4\cdot6$ and $+9\cdot4\times10^{26}$ cm^{-2}, the ratio $b=F_1^P/2MF_2^P$ has been measured by comparing experiments at different energies and angles, for fixed q, and found to be $1\cdot2\pm0\cdot2$. The experimental points display $F_2^P(q^2)/F_2^P(0)$ corresponding to three possible ratios $b=1\cdot0$, $1\cdot2$, and $1\cdot4$. For small $-q^2<2\times10^{26}$ cm^{-2} what is drawn is $F_1^P(q^2)/F_1^P(0)$; the magnetic contribution is negligible in this region.

2 [16]. Since there are no free neutron targets, present information on neutron form factors is in general less precise and complete than that available for the proton. However one aspect of the neutron structure, the mean square radius of the neutron's charge distribution, $\langle r^2 \rangle_{1,N}$, was the first experimental result on nucleon structure. It was originally measured in 1947 by scattering of slow neutrons from atoms, and it remains today as perhaps the most puzzling of all the nucleon structure properties.

Experimental measurements of $\langle r^2 \rangle_{1,N}$ have utilized the coherence between the spin and velocity independent part of the neutron–electron scattering amplitude with the coherent nuclear scattering of the neutron in the atom to which the electron is bound. This coherence has been observed in the laboratory in three different ways:

(1) For neutron wavelength comparable with atomic size, the interference term exhibits an angular dependence described by an atomic form factor since the nuclear scattering is isotropic and the superposition of scattered waves from the different electrons gives a form factor variation. Measurement of an angular asymmetry, when combined with known atomic form factors and coherent nuclear scattering amplitudes, yields $\langle r^2 \rangle_{1,N}$. An experiment of this type was first performed by Fermi and Marshall [17] using noble gases so that corrections in the analysis of the data from induced polarization effects in the closed electronic shells are negligible.

(2) Similarly this interference term gives rise to an energy, or wavelength, variation of the total cross-section, which can be measured and from which $\langle r^2 \rangle_{1,N}$ can be extracted in the same way as above. Such experiments were first carried out by Havens, Rabi, and Rainwater [18] in liquid lead.

(3) The coherent scattering amplitude a for forward scattering of neutrons in a medium is related to the index of refraction of the medium for neutrons by $n^2 = 1+(\lambda^2/\pi)Na$, where λ is the neutron wavelength and N

the number of atoms per unit volume. By measuring the critical angle of reflection at the interface between two media it is then possible to determine their relative index of refraction, and hence coherent scattering amplitudes, since $\cos\theta_c = n_1/n_2$ where θ_c is measured relative to the interface. Thus for $\theta_c \ll 1$ and $n^2-1 \ll 1$,

$$\theta_c^2 = 2(n_2-n_1) = \frac{\lambda^2}{\pi}(N_2a_2-N_1a_1). \qquad (2.3)$$

For a precise determination of the coherent neutron–electron amplitude two materials are sought for which the product density times nuclear scattering amplitude is approximately equal but for which the atomic numbers are very different. Then the importance of the neutron–electron amplitude in determining the critical angle is enhanced in (2.3). This method has been developed by Hughes and co-workers [19] who used bismuth and oxygen as the two substances in forming their neutron 'mirrors.'

Precision measurements by each of these quite different techniques, carried out on different materials under different physical conditions are consistent with one another. This lends great confidence both to the experimental accuracies and to their theoretical interpretation in terms of a neutron charge radius. In order to see how the neutron charge radius emerges from these coherence measurements it is necessary to return to the expression given in equation (1.8) for the current 4-vector of a neutron and take the non-relativistic limit of its interaction with an external electric field representing an electron charge cloud. This gives for the neutron's charge density

$$(\bar{u}_{p_f}|F_1^N(q^2)\gamma_0+iF_2^N(q^2)\sigma_{0\nu}q_\nu|u_{p_i}),$$

upon dropping terms of higher order than q^2 and reducing to two component Pauli spinors, χ,

$$(\chi_f^*\chi_i)\left[F_1^N(0)+q^2F_1^{N'}|_{q^2=0}+\frac{q^2}{2M}F_2^N(0)+\dots\right]$$
$$= e(\chi_f^*\chi_i)\frac{q^2}{6}\left[\langle r^2\rangle_{1,N}+\frac{3}{2M^2}k_N\right] \qquad (2.4)$$

where $k_N = -1{\cdot}91$ is the neutron moment in units of nuclear magnetons.

The second term in the above expression has been discussed and interpreted by Foldy and the reader is referred to his fine review [16] of the neutron–electron interaction for more details. Present measurements are quoted there with an accuracy of 5% and yield

$$\langle r^2\rangle_{1,N}+\frac{3}{2M^2}k_N = [-0{\cdot}126\pm{\cdot}006]\times 10^{-26}\ \text{cm}^2$$

or

$$\langle r^2\rangle_{1,N} = (0\pm{\cdot}006)\times 10^{-26}\ \text{cm}^2.$$

An alternative and more usual expression of these results is in terms of a constant potential well of depth V_0 and classical electron radius $r_0 = \alpha/m = 2{\cdot}8\times 10^{-13}$ cm, which gives rise to the same scattering amplitude—viz.

$$\begin{aligned} V_0 &= \frac{1}{2}\frac{\alpha}{r_0^3}\left[\langle r^2\rangle_{1,N}+\frac{3}{2M^2}k_N\right] \\ &= -4{\cdot}07\ \text{keV}\left(1+\frac{2}{3k_N}M^2\langle r^2\rangle_{1,N}\right). \end{aligned}$$

Translating the experimental results into these units,

$$V_0(\text{exptl}) = -(4{\cdot}05\pm 0{\cdot}2)\ \text{keV}.$$

The smallness of the observed charge radius of the neutron, $\langle r^2\rangle_{1,N}$ defies any simple interpretation with meson theory. It is to be contrasted with the form factor behaviour of the proton given in Fig. II.5. Though the mean square charge radius of the proton is not directly measured and may in fact vanish also, a smooth extrapolation of the data to $q^2 = 0$ suggests radii $\langle r^2\rangle_{1,P} \approx (\frac{1}{2}-1)\times 10^{-26}\ \text{cm}^2$ in closer accord with intuitive notions based on meson theory.

The discussion of this section has assumed that the electromagnetic interaction between electron and neutron need be treated only in Born approximation. Again, as in the previous electron–proton scattering analysis, polarizability corrections corresponding to the exchange of two photons, can be computed and as found earlier, are entirely negligible here.

3 [20]. For information on the neutron's moment structure as well as for further details of its charge distribution it is necessary to consider large momentum transfer experiments. To this end an extensive program of high energy electron–deuteron elastic and inelastic scattering experiments has been pursued at Stanford. In order to interpret these measurements in terms of neutron electromagnetic structure, one must have a reliable subtraction procedure to remove all effects of the spectator proton in the deuteron. In the absence of a relativistic theory of two bound nucleons a precise reduction of the observed deuteron cross-sections to a neutron form factor is impossible. Uncertainties in the present analyses are discussed here along with proposals for their eventual elimination.

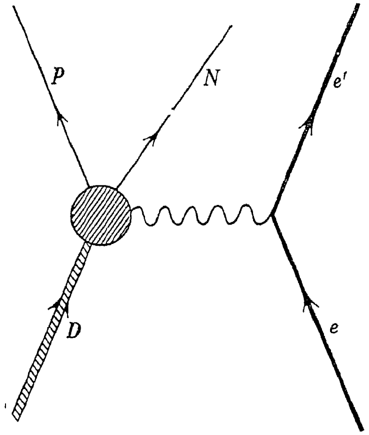

FIG. II.6. Diagram for inelastic scattering of electrons from deuterons. The deuteron is represented with a fat cross-hatched line.

Consider first the inelastic scattering process $e+D \rightarrow e'+N+P$ of Fig. II.6, which Yearian and Hofstadter [20], and Sobottka [21] have studied in detail for information on the neutron magnetic form factor. This process leads to three final particles and thus to a continuous energy spectrum of electrons at each scattering angle. Measurements have been made of the differential cross-sections for the number

$d^2\sigma_D/dE_{e'}\, d\Omega_{e'}$, of electrons emerging in a given energy interval $dE_{e'}$ and into a solid angle $d\Omega_{e'}$, and (by counting all electrons emerging in a given solid-angle element) of the integrated cross-section, $\int (d^2\sigma_D/dE_{e'}\, d\Omega_{e'})\, dE_{e'}$ as well. At the large momentum transfers required to probe nucleon structure, it is a very good approximation to neglect interference between scattering amplitudes from the neutron and the proton and to express the cross-section as a sum of single-particle cross-sections. This is because the interference term is reduced in amplitude by the fourier transform of the deuteron wave function which is very small at these large momenta.

There is an approximate sum rule expressing the integrated cross-section, i.e. the area under the inelastic curve, as the sum of free nucleon cross-sections for the same solid angle [22]:

$$\int dE_{e'} \frac{d^2\sigma_D}{dE_{e'}\, d\Omega_{e'}} = \frac{d\sigma_P}{d\Omega_{e'}} + \frac{d\sigma_N}{d\Omega_{e'}}. \tag{2.5}$$

This relation is useful for large enough momentum transfers so that the neutron contribution to (2.5) is comparable to that of the proton [23]. There are, however, significant corrections for these conditions which severely limit the reliability with which the neutron form factor can be deduced from (2·5) [22], [24]. Some of these corrections can be calculated, such as kinematical corrections arising from the width of the momentum distribution in the deuteron. However, mesonic corrections from exchange currents in the deuteron and from final state interactions can only be estimated in the absence of a satisfactory theory of the deuteron. By relating these effects with their important observed role in the photodisintegration of the deuteron at high energies corrections to (2.5) of the order of 10% are estimated [25].

These same estimates suggest that it is possible to avoid the main uncertainties from the meson exchange current corrections by considering the value of the sharply peaked maximum in the differential cross-section (see Fig. II.7). Uncertainties which remain in the theoretical interpretation of the peak value come from the final state interaction between the outgoing nucleons, to which the sum rule for the integrated cross-section is insensitive, and from the deuteron wave function. Durand [22] has extended the original calculations of Jankus and given an approximate calculation of the effect of final state interaction, using the Signell–Marshak phase shifts, and found that it serves to reduce the peak value of $d^2\sigma_D/dE_{e'}\, d\Omega_{e'}$ by $\approx 5\%$ for current laboratory parameters. At the same time the peak is broadened so that the area under the inelastic curve tends to remain constant.

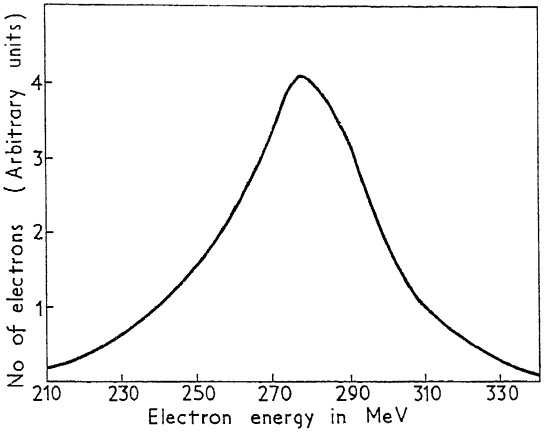

Fig. II.7. Spectrum of inelastically scattered electrons from deuterium as a function of the energy of the scattered electron for an incident electron energy of 600 MeV and a scattering angle of 135°.

The deuteron wave function is, of course, related to the final state interaction. Its effect on the peak value, calculated by comparing with the matrix element for transitions from the deuteron ground state to non-interacting final particles, was found to be $\lessdot 5\%$. It arises as follows: the peak in the inelastic electron spectrum at a given angle occurs at an energy which is, with neglect of the deuteron binding energy, the same energy as for scattering by a free nucleon. Upon integration over the undetected recoil nucleons, this peak acquires a major contribution from the possibility that one nucleon in the deuteron remains at rest as a spectator, and the other one, serving as the 'target' in the matrix element, recoils with the full momentum. This particular contribution is proportional to the zero-momentum amplitude of the deuteron wave function, i.e. to the normalization of the asymptotic wave

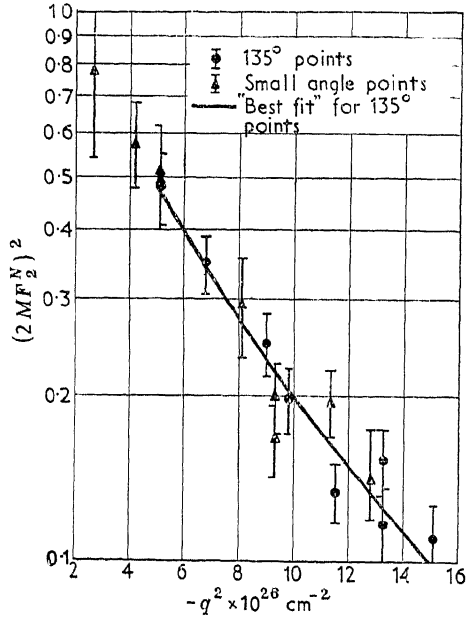

FIG. II.8. Experimental measurement of the neutron magnetic distribution from inelastic scattering of electrons from deuterium. The data is plotted assuming a vanishing neutron charge distribution. (Taken from S. Sobottka and R. Hofstadter [21], and see [9].)

function. In the integration over all nucleon recoils, there are in addition contributions to the cross-section which are proportional to the fourier transform of the deuteron wave function for the various momentum values available to the recoiling 'spectator nucleon.'

The experimental situation [20], [21], [26] at present is such that uncertainties in the measurements and in the theoretical interpretations are comparable. The latest work of Sobottka has been summarized in Figs. II.8 and II.9. Plotted here are data taken both at large and small angles in order to permit in a preliminary way separation of the charge and moment structures. Fig. II.8 is plotted assuming that the neutron charge distribution vanishes identically, an assumption consistent with but not required by the vanishing of the mean square radius $\langle r^2\rangle_{1,N}$ in the neutron–electron experiments discussed earlier. Fig. II.9 places limits on the ratio $F_1^N(q^2)$ to $2MF_2^N(q^2)$ deduced from these same data.

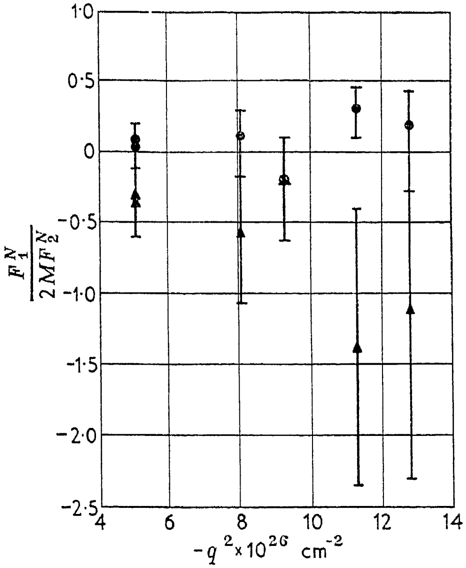

FIG. II.9. Ratio of charge to magnetic form factors of the neutron. (Taken from S. Sobottka and R. Hofstadter [21], and see [9].)

Note that these data are consistent with a similar magnetic moment structure for neutron and proton, as is not surprising in view of equation (1.12). Thus in terms of isotopic states

$$F_2^P(q^2) = F_2^v(q^2)(1+F_2^s(q^2)/F_2^v(q^2))$$

$$F_2^N(q^2) = -F_2^v(q^2)(1-F_2^s(q^2)/F_2^v(q^2))$$

and $F_2^s(0)/F_2^v(0) \equiv -0{\cdot}06/1{\cdot}85 \approx -3\,\%$. For the largest measured q^2, $F_2^N(q^2) \geqslant 0{\cdot}3F_2^N(0)$ so that even for a point structure for the iso-scalar moment, the corrections should be no more than 10 %. This is not the case for the charge form factor, for which $F_1^s(0) = F_1^v(0) = \frac{1}{2}e$.

In order to sharpen the above conclusions it is necessary to push the present experiments to greater accuracy or to turn to more exotic coincidence arrangements. The limitation in the former case comes from the fact that the peak and the area of the inelastic spectrum are the sums of two parts, the larger of which is due to the electron–proton interaction. The neutron form factors emerge with magnified errors when expressed as the difference of two experimental numbers, for deuteron and for proton scattering, respectively. This is evident in the preceding two figures which are computed from the electron–deuteron inelastic peak which is measured with a 5 % accuracy and from the electron–proton scattering known to better than 10 %.

Coincidence experiments may be designed to avoid this need of subtraction by selecting those nucleon recoils which correspond predominantly to neutron scattering, with the proton in the deuteron as idle spectator. This possibility can be seen easily from the following expression for the transition amplitude T. Denote by $\mathbf{k}_0$ the initial electron momentum, in the laboratory system, by $\psi_g(\mathbf{r}_P-\mathbf{r}_N)$, the wave function of the deuteron initially at rest, by $\mathbf{k}_f = \mathbf{k}_0-\mathbf{q}$, the final electron momentum, by $\mathbf{p}_P$ and $\mathbf{p}_N$, the asymptotic free particle momenta for the proton and neutron respectively, and by $f(\mathbf{r}_P-\mathbf{r}_N)$, a final state nucleon correlation:

$$\begin{aligned} T(\mathbf{k}_f\mathbf{p}_P\mathbf{p}_N;\,\mathbf{k}_0) &= \delta(k_0+M_D-k_f-E_P-E_N) \\ &\int d^3r_P\, d^3r_N\, d^3r_e e^{i\mathbf{q}.\mathbf{r}_e}\, e^{-i\mathbf{p}_P.\mathbf{r}_P-i\mathbf{p}_N.\mathbf{r}_N} f^*(\mathbf{r}_P-\mathbf{r}_N) \\ &\qquad [t_P(\mathbf{r}_P-\mathbf{r}_e)+t_N(\mathbf{r}_N-\mathbf{r}_e)]\psi_g(\mathbf{r}_P-\mathbf{r}_N). \end{aligned}$$

Here $t_i(\mathbf{r}_i-\mathbf{r}_e)$ is the matrix element for the two-body interaction of the electron with the ith nucleon and contains all spin and normalization factors. Re-expressing T in terms of centre-of-mass and relative co-ordinates, with $\mathbf{r} \equiv \mathbf{r}_P-\mathbf{r}_N$, and extracting the statement of overall momentum conservation, there results

$$\begin{aligned} T &= (2\pi)^3\delta^3(\mathbf{p}_P+\mathbf{p}_N-\mathbf{q})\,\delta(k_0+M_D-k_f-E_P-E_N) \\ &\quad\times\Big\{\Big[\int e^{-i\mathbf{q}.\mathbf{x}}\,t_P(\mathbf{x})\,d^3\mathbf{x}\Big]\int d^3\mathbf{r}f^*(\mathbf{r})e^{i\mathbf{p}_N.\mathbf{r}}\psi_g(\mathbf{r}) \\ &\qquad+\Big[\int e^{-i\mathbf{q}.\mathbf{x}}\,t_N(\mathbf{x})d^3\mathbf{x}\Big]\int d^3\mathbf{r}f^*(\mathbf{r})e^{i\mathbf{p}_P.\mathbf{r}}\psi_g(\mathbf{r})\Big\}. \end{aligned} \tag{2.6}$$

The two terms above express contributions to the transition amplitude arising from electron–proton and electron–neutron scattering, respectively. Consider an experiment in which the scattered electron is detected with a given final energy and angle corresponding to a large momentum transfer q as is desired for the nucleon structure analysis. The first term is the dominant contribution for a proton emerging with the full momentum transferred from the electron while the neutron stays at rest as spectator. This is due to the fact that for $\mathbf{p}_N \to 0$, the integral $\int d^3 r f^*(\mathbf{r})e^{-i\mathbf{p}_N.\mathbf{r}}\psi_g(\mathbf{r})$ receives important contributions out to $r \sim$ radius of the deuteron. On the other hand for $\mathbf{p}_N \sim \mathbf{q}$, the integrand oscillates rapidly for $r \gtrsim 1/q$ and so it is expected that the ratio

$$\left|\int d^3\mathbf{r}f^*(\mathbf{r})e^{i\mathbf{q}.\mathbf{r}}\psi_g(\mathbf{r})\right| \Big/ \left|\int d^3\mathbf{r}f^*(\mathbf{r})\psi_g(\mathbf{r})\right|$$

$$\approx \frac{1}{|\mathbf{q}|^2\ (\text{radius of deuteron})^2} \ll 1.$$

The second matrix element dominates for the neutrons emerging with the full recoil, and with the proton as the idle spectator. Evidently the relative magnitudes of these two terms can be controlled by experimental arrangements which fix the values of the recoil momenta $\mathbf{p}_P$ and $\mathbf{p}_N$ subject to the constraint $-\mathbf{q}+\mathbf{p}_P+\mathbf{p}_N = 0$. By fixing $|\mathbf{p}_P| \ll |\mathbf{p}_N|$ it is possible to emphasize the neutron–electron scattering amplitude by a large factor relative to that for the proton. One can thereby avoid the difficulties of the subtraction procedure as applied in the analysis of the peak height of the inelastic spectrum.

While the coincidence arrangement removes the subtraction difficulty by making one of the two terms in (2.6) dominant, both terms there exhibit a dependence on the final state interactions between the emerging nucleons which is expressed approximately (with dependence on exchange and spin operators suppressed) by the correlation factor $f(\mathbf{r}_N-\mathbf{r}_P)$. Durand [22] has proposed a programme of feasible coincidence experiments which to a large extent removes the uncertainty due to final state interaction by constructing appropriate cross-section ratios. His method yields the ratio of the neutron to the proton form factors at a fixed value of 4-momentum transfer q^2 from a measurement of the ratio of the number of neutrons to the number of protons emerging in a narrow conical region about the direction of the electron 3-momentum transfer $\mathbf{q}$. Thus, neutrons emerging in a narrow cone about $\mathbf{q}$ lead to small values of proton recoil, $\mathbf{p}_P = \mathbf{q}-\mathbf{p}_N$ and are predominantly the recoil neutrons from electron–neutron scattering. The ratio of the numbers of neutrons to protons involves the same matrix element, containing the deuteron ground state and final inter-nucleon correlation function, both in the numerator and denominator. To the accuracy with which one of the two terms in (2.6) dominates the other for the experimental parameters of interest, this ratio depends only on nucleon form factors and calculable kinematical factors. Up to corrections of order $1/M^2$ in the nucleon interaction Hamiltonian, Durand finds for the ratio R of the number of neutrons to the number of protons scattered into a given conical region about $\mathbf{q}$, corresponding to scattering angle θ of the electron,

$$R = \frac{\begin{array}{l} F_1^N(q^2)^2+\dfrac{|\mathbf{q}|^2}{4M^2} \\ \quad\times[2(F_1^N(q^2)+2MF_2^N(q^2))^2\tan^2(\tfrac{1}{2}\theta)+\{2MF_2^N(q^2)\}^2] \end{array}}{\begin{array}{l} F_1^P(q^2)^2+\dfrac{|\mathbf{q}^2|}{4M^2} \\ \quad\times[2(F_1^P(q^2)+2MF_2^P(q^2))^2\tan^2(\tfrac{1}{2}\theta)+\{2MF_2^P(q^2)\}^2] \end{array}}$$

or just the ratio of Rosenbluth cross-sections altered by the appearance here of 3-momenta $|\mathbf{q}|$ due to the nonrelativistic treatment of nucleons with a 2-component Pauli equation. Corrections to R arising from interference between the neutron and proton terms in (2.6) were calculated by Durand and typically found to be very small. For example, at the peak of the inelastic spectrum for the scattering of 500 MeV electrons through 75°, Durand finds, with neglect of final state interaction and with an S-wave Hulthén deuteron model that the interference term contributes less than $\frac{1}{2}\%$ when integrated over a cone of half-angle 30° about the $\mathbf{q}$ direction in the centre-of-mass system of the outgoing nucleons. When final state interactions are included the interference between the two amplitudes in (2.6) becomes somewhat more important due to the presence of high momentum amplitudes in the Fourier transform of $f(\mathbf{r}_N - \mathbf{r}_P)$. Durand has shown by approximate calculation with the Signell–Marshak phase shifts that this correction serves to increase R for the above values of experimental parameters by no more than $\approx 5\%$. The effect at larger scattering angles is further reduced [27].

Durand's analysis of the ratio R points to a way of obtaining greater accuracy in the determination of neutron electromagnetic structure from experiments on deuteron targets. His programme can be carried through either by comparing numbers of protons and neutrons in a cone about $\mathbf{q}$, or by comparing numbers of protons in forward relative to backward cones in the centre-of-mass system of the emerging nucleons about $\mathbf{q}$. The most difficult points in these two experiments are the requirements of counting fast neutrons in the first arrangement and of counting slow protons in the second. One may avoid these by subtracting the cross-section for protons in the forward cone about $\mathbf{q}$ from the total one $d^2\sigma/dE_{e'}\, d\Omega_{e'}$ for the same $\mathbf{q}$, thereby obtaining directly the cross-section integrated over the backward cone to good accuracy. The advantage of this subtraction procedure in comparison with the one now used for the peak height of the inelastic spectrum derives from the facts that it is made within one experiment and that the final state interaction $f(r)$ appears in all matrix elements. It is of course absent in the electron–proton scattering now used in carrying through a subtraction programme.

In principle it is possible to push the coincidence technique one step further and, by an extrapolation procedure, free the analysis entirely of corrections due to non-relativistic approximations, binding, and final state interactions between the two nucleons. Chew and Low [28] have described a general method for such a programme which is based on the possibility of analytically continuing the scattering amplitude

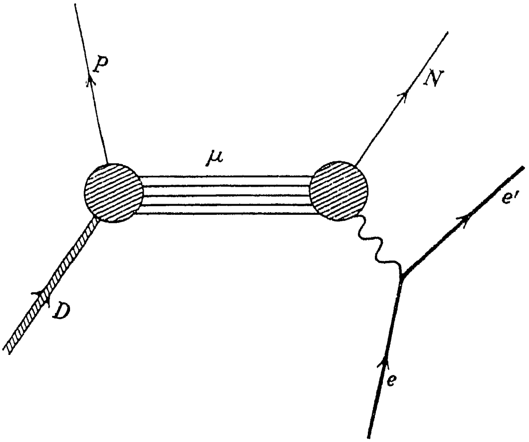

FIG. II.10. A possible decomposition of the Feynman diagram for the reaction $e+D \rightarrow e+N+P$. The series of parallel lines, labelled μ, represents all possible intermediate states coupling the two parts of the diagram.

$$e+D \rightarrow e'+N+P$$

to a pole, the existence of which and the residue at which can be plausibly conjectured from field theory. To be specific for the present application, consider Fig. II.6 for the amplitude of interest and dissect it as indicated in Fig. II.10. Here μ represents all possible states coupling the two parts of the diagram; for example μ represents a neutron, or neutron plus pion, etc. (only the strong couplings are included). Consider now the amplitude for this process as a function of the invariant square of the four-momentum difference between incoming deuteron and emerging 'spectator' proton:

$$\begin{aligned}\Delta^2 = (p_D - p_P)^2 &= M_D^2 + M_P^2 - 2p_D \cdot p_P \\ &= (M_D - M_P)^2 - 2M_D T_{P_l} \qquad (2.7)\end{aligned}$$

where the subscript on the 4-momentum p and on the mass M indicates deuteron (D), proton (P), or neutron (N), and where T_{P_l} is the proton recoil kinetic energy in the lab system. The basic assumption is that the analytic continuation of this amplitude as a function of Δ^2 has a simple pole at $\Delta^2 = M_N^2$ for the single particle one-neutron state and a branch cut starting at the point $\Delta^2 = (M_N + m_\pi)^2$ corresponding to the state of one neutron plus one pion. The practical value of this continuation procedure depends on the possibility of extrapolating the experimental measurements to this pole and, hence depends on the proximity of the pole to the physical range of scattering parameters and on its separation from other singularities in the scattering amplitude. It is of interest then to analyse further the kinematical questions relating to this process and to locate other singularities in the scattering amplitude. The general recipe for locating these singularities follows from the work of Mandelstam [29] and may be stated simply as follows: Consider first the states which can be reached with p_D and $-p_P$ the incident particles. The outgoing proton is replaced by its anti-particle as incident in the process, and so

$$\begin{aligned}\text{deuteron} + \text{anti-proton} \rightarrow\ &\text{neutron} \\ &\text{neutron} + \text{pion} \\ &\text{etc.}\end{aligned}$$

There is a pole in the amplitude for $\Delta^2 = (p_D - p_P)^2 = M_N^2$, the square of the mass of the one-particle intermediate state that can be reached, and branch cuts starting at the squared masses of all multi-particle states, the nearest one in this case being $(M_N + m_\pi)^2$. This gives the spectrum of singularities for p_D and $-p_P$ incident. For the remaining singularities consider the crossed reaction with incident deuteron plus anti-neutron, $(p_D - p_N)^2 = \sigma^2$:

$$\text{deuteron} + \text{anti-neutron} \rightarrow \begin{array}{l}\text{proton}\\ \text{proton and pion}\\ \text{etc.}\end{array}$$

There is then a pole for $\sigma^2 = M_P^2$ and a branch cut starting at $(M_P + m_\pi)^2$. By relating σ^2 and Δ^2 through the total energy of the reaction $E^2 = (p_P + p_N)^2$, where E is the total energy of the final nucleons in their centre-of-mass system $(\mathbf{p}_P^0 + \mathbf{p}_N^0 = 0)$, the singularities in the crossed spectrum are expressed in the Δ^2 plane. It follows from the relation

$$\sigma^2 + \Delta^2 + E^2 = M_D^2 + M_P^2 + M_N^2 + q^2$$

that the pole in the crossed spectrum lies at

$$\Delta^2 = -E^2 + M_N^2 + M_D^2 + q^2$$

and that the branch cut starts at

$$\Delta^2 = -E^2 + M_N^2 + M_D^2 + q^2 - 2M_P m_\pi (1 + m_\pi / 2M_P).$$

This spectrum of singularities is readily transcribed in terms of $\cos\theta$ where θ is the angle between the direction of 3-momentum transfer $\mathbf{q}$ and of the neutron in the centre-of-mass system of the emerging nucleons; i.e. $\cos\theta = \mathbf{q}^0 \cdot \mathbf{p}_N^0 / |\mathbf{q}^0||\mathbf{p}_N^0|$ in the system $\mathbf{p}_N^0 + \mathbf{p}_P^0 = 0$. ($E_D$ denotes the total energy of the deuteron in this system.) By overall energy–momentum conservation

$$\begin{aligned}\Delta^2 = (p_D - p_P)^2 &= (q - p_N)^2 \\ &= M_N^2 + q^2 - 2q_0^0 E_N + 2|\mathbf{q}^0||\mathbf{p}_N^0|(\cos\theta).\end{aligned}$$

The pole at $\Delta^2 = M_N^2$ corresponds to $\cos\theta_0 = \dfrac{2q_0^0 E_N - q^2}{2|\mathbf{q}^0||\mathbf{p}_N^0|}$, i.e.

$$\cos\theta_0 = \frac{EE_D - M_D^2}{\sqrt{(E_D^2 - M_D^2)}\sqrt{(E^2 - 4M_N^2)}} > 1.$$

The branch cut starting at $(M_N + m_\pi)^2$ corresponds to

$$\cos\theta_1 = \frac{EE_D - M_D^2 + m_\pi(2M_N + m_\pi)}{\sqrt{(E_D^2 - M_D^2)}\sqrt{(E^2 - 4M_N^2)}}.$$

The pole in the crossed spectrum at $\Delta^2 = -E^2+M_N^2+M_D^2+q^2$ and the corresponding branch cut appear symmetrically at $\cos(\pi+\theta) = -\cos\theta$. In the $\cos\theta$ plane the analyticity domain is as shown in Fig. II.11.

The amplitude is analytic in the physical region with an isolated pole just beyond the boundary of the real physical variables in both the forward and backward cones about $\mathbf{q}$ and with branch cuts further out. That the pole lies outside the physical region is nothing more than a stability statement for the deuteron ground state. Equivalently from equation (2.7), at the pole $\Delta^2 = M_N^2$ the recoil kinetic energy of the spectator proton in the laboratory system is [30], [29]

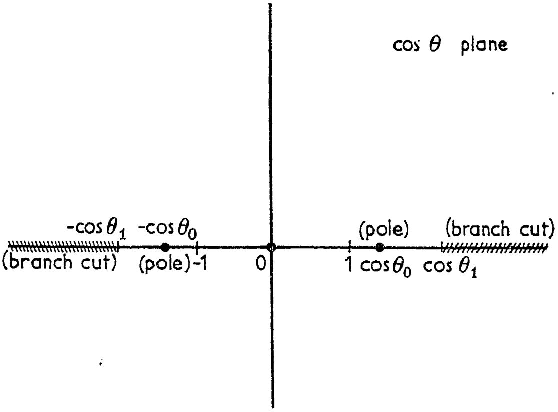

FIG. II.11. Poles and branch cuts in the cos θ plane for the amplitude of the reaction $e+D \rightarrow e+N+P$.

$$T_{Pl_0} = \tfrac{1}{2}(M_D-M_P-M_N) = -1{\cdot}1\text{ MeV};$$

the corresponding energy for the first branch point lies at

$$T_{Pl_1} = \tfrac{1}{2}(1+m_\pi/M_D)\,(M_D-M_P-M_N-m_\pi) \approx -70\text{ MeV}.$$

The singularities in the crossed spectrum are as above with the recoil neutron kinetic energy T_{N_l} replacing T_{P_l}. The pole corresponding to the one-nucleon intermediate state in Fig. II.11 is thus well separated from the other singularities and lies quite close to the edge of the physical region. It is to this pole that one extrapolates by detecting protons in the backward cone about $\mathbf{q}$ and studying the cross-section for fixed 4-momentum transfer q^2 as the proton kinetic energy T_{P_l} goes to zero. According to the Chew–Low conjecture [28] the residue at this pole is given by the product of the transition amplitudes connecting the two groups of particles in Fig. II.10 to the intermediate neutron on its mass shell. In this case the residue of the pole at $\Delta^2 = M_N^2$ is the product of the amplitude for neutron–electron scattering times the amplitude for deuteron $\leftrightarrow$ neutron $+$ proton. Since the amplitude for $D \leftrightarrow N+P$ can be expressed in terms of the normalization of the asymptotic deuteron wave function, the cross-section for Fig. II.10 has a second order pole at $\Delta^2 = M_N^2$ whose residue is a known multiple of the electron–neutron scattering cross-section. In this way by programming experiments for fixed q^2, the neutron structure can in principle be determined.

The relation between this extrapolation procedure of Chew and Low and the analysis of Durand is now clear. For protons emerging in the backward cone about $\mathbf{q}$ in the centre-of-mass system of the recoiling nucleons. the transition amplitude is near the pole at $\cos\theta = \cos\theta_0$, or $T_{P_l} = T_{P_{l0}}$, corresponding to the one-neutron intermediate state in Fig. II.10 and is dominated by the second or neutron scattering term in equation (2.6). The closer the experimental parameters approach this pole the less important are the contributions from the pole in the crossed reaction, corresponding to proton scattering, and the less important are the contributions from the branch cuts arising from higher mass intermediate states, such as neutron plus pion, which correspond to final state interactions as expressed by the correlation factor $f(\mathbf{r}_N - \mathbf{r}_P)$ in the form factor integrals in equation (2.6). This result can be seen from equation (2.6) as well as from the field theory formalism. Note that at the pole, the integral over the deuteron ground state wave function diverges since the asymptotic exponential decay of $\psi_0(r)$ for $r \to \infty$ is compensated by the exponential increase of $\exp i\mathbf{k}_{P,N} \cdot \mathbf{r}$ for imaginary $\mathbf{k}_{P,N}$ at the pole $T_{l_0} = k_0^2/2M = -1{\cdot}1$ MeV. The form factor integral then becomes infinite upon integration over all space since $f(r) \rightarrow 1$ for $r \gg$ inter-nucleon force range. The final state interaction contributes a finite additive term arising from the difference $(f(r)-1)$ which vanishes for large r. This term corresponds to the finite contributions from the higher branch cuts in Fig. II.11 and is relatively less and less significant as one approaches the pole for the one-nucleon state. Hence at the pole, only the asymptotic normalization of the deuteron wave function (i.e. the zero momentum amplitude in the Fourier transform of the wave function) appears in the calculated cross-section and this can in fact also be removed by taking a ratio of extrapolations for emerging neutrons as well as protons.

The explicit calculation of the formula for the residue at the pole at $\Delta^2 = M_N^2$ in Fig. II.10 proceeds as follows. The matrix element corresponding to this diagram is

$$ME = g(p_P)(ME)_{eN} \tag{2.8}$$

where p_P is the proton recoil momentum in the laboratory co-ordinates, and at the pole $\Delta^2 = M_N^2$, $(ME)_{eN}$ represents just the electron–neutron scattering amplitude on the mass shell [31]. The amplitude $g(p_P)$ is the projection of the initial deuteron wave function on the recoil proton plane wave state and is given by

$$(\varphi_{p_P}^*(\mathbf{r}_P, t), \psi_g(\mathbf{r}_P, \mathbf{r}_N, t)) = g(p_P)\varphi_{p_N}(\mathbf{r}_N, t).$$

Comparing with the earlier discussion of equation (2.6) it is seen that equation (2.8) corresponds to the second or neutron scattering term and $g(p_P)$ is just the last factor there, expressing the amplitude for a spectator proton to emerge with $\mathbf{p}_P$ from the deuteron. Near the pole the internucleon correlation, $f(r)$, may be neglected as discussed in the preceding paragraph [32].

To a very good approximation g may be expressed in terms of the deuteron radius $1/\alpha$ and triplet effective range r_0 by [28], [33],

$$g(p_P) = \frac{2}{M_N^2-\Delta^2}\sqrt{\frac{8\pi\alpha}{1-\alpha r_0}} \equiv \frac{\sqrt{(4\pi M_D)}\Gamma}{(M_N^2-\Delta^2)}.$$

The differential cross-section for scattering of the electron into energy–angle interval $d\Omega_{c'}\, dE_{e'}$ and of the recoil spectator proton into kinetic energy interval dT_{P_l} in the laboratory system is then, as $T_{P_l} \to T_{P_{l0}}$,

$$\frac{d^3\sigma}{d\Omega_{e'}\, dE_{e'}\, dT_{P_l}} = \frac{2\pi M_D \Gamma^2}{4\pi^2 (M_N^2 - \Delta^2)^2} \left(\frac{k_0^r}{k_0}\right) \left(\frac{d\sigma_{Ne}(q^2)}{d\Omega_{e'}}\right) \frac{E_N M_P}{2\sqrt{(E_N^2 - M_N^2)}}$$

$$= \frac{M_D \Gamma^2}{4\pi (M_N^2 - \Delta^2)^2} \left(\frac{k_0^r}{k_0}\right) \frac{(M_N + k_0) M_P}{\sqrt{\{k_0(k_0 + 2M_N)\}}} \left(\frac{d\sigma_{Ne}(q^2)}{d\Omega_{e'}}\right) \qquad (2.9)$$

where k_0 and k_0^r represent the incident electron energy in the laboratory system and rest system of the intermediate target neutron, respectively. To complete the kinematics one writes, in terms of the square sum of the final electron-plus-neutron 4-momenta ω^2,

$$k_0^r M_N = \sqrt{(\tfrac{1}{4}\omega^4 - \tfrac{1}{2}\omega^2 M_N^2 + \tfrac{1}{4} M_N^4)} = \tfrac{1}{2}(\omega^2 - M_N^2)$$

where, as always, terms proportional to the electron rest mass are neglected. The neutron structure is then determined for fixed q^2 by the extrapolation

$$\left(\frac{d^3\sigma}{d\Omega_{e'}\, dE_{e'}\, dT_{P_l}}\right) \frac{8\pi (M_N^2 - \Delta^2)^2}{M_D M_P} \left(\frac{M_N k_0}{\omega^2 - M_N^2}\right) \frac{\sqrt{\{k_0(k_0 + 2M_N)\}}}{k_0 + M_N}$$

$$\xrightarrow[\Delta^2 \to M^2]{} \Gamma^2 \frac{d\sigma_{Ne}(q^2)}{d\Omega_{e'}}.$$

The ratio of extrapolations for $T_{P_l} \to T_{P_{l0}}$ and $T_{N_l} \to T_{N_{l0}}$ removes Γ, the normalization of the asymptotic wave function of the deuteron, and fixes the neutron structure in terms of measured proton form factors. Moreover the absolute magnitude of the extrapolation to the proton pole may be studied as a check upon the quantitative validity of the entire procedure in the polology analysis since there is accurate independent information on the electron–proton scattering from the free proton target measurements, and Γ is well known from the low energy nucleon–nucleon interactions.

In résumé of this section, coincidence measurements on the inelastic scattering of electrons from deuterons offer the possibility of considerably sharpening the determination of neutron electromagnetic structure. The main experimental problems they pose are due to the necessity of detecting slow protons (or equivalently fast neutrons with high energy resolution), and to the small cross-section. For example, the ratio in (2.9) of the coincidence cross-section to that for elastic electron–neutron scattering into a given solid angle, integrated over recoil proton energies of 5 to 20 MeV and over a 10 MeV resolution width for final electrons is $\sim\frac{1}{2}\%$, for 650 MeV incident electrons.

In conclusion a variation on the polology theme of Chew and Low with an apparent experimental advantage may be proposed. It consists of inelastic electron scattering from H^3 and from He^3, with the detection, in coincidence, of the scattered electron and of the spectator deuteron:

$$\begin{aligned} e+\mathrm{H}^3 &\rightarrow e'+N+D \quad &\text{(a)} \\ e+\mathrm{He}^3 &\rightarrow e'+P+D. \quad &\text{(b)} \end{aligned} \qquad (2.10)$$

The ratio of extrapolations to the pole at a deuteron laboratory kinetic energy $T_{D_l} = -2$ MeV for these two reactions again measures neutron in terms of proton form factors [34]. These processes offer two experimental advantages relative to (2.6) and (2.9) for deuteron scattering. (1) In measuring the ratio of (a) to (b) in (2.10) the same detection equipment may be used since slow deuterons are collected in both cases, and one need only change the target material. (2) The counting rate may be increased relative to (2.9) since it may not be necessary to extrapolate so close to the pole at -2 MeV. This is because the competing matrix elements in (2.6) for neutron and proton scattering are comparable except near the pole where one of them dominates. Here however the competing amplitude contributing to the cross-section (2.10) is electron–deuteron elastic scattering which, in the energy region of interest for nucleon structure, is considerably reduced owing to the large deuteron size. Therefore one is not forced to very low deuteron recoil energies to be sure that the process is dominated by electron scattering from neutrons or protons respectively in the two cases of H^3 and He^3 targets. The first order effects of all but coulomb corrections will disappear in the ratio of (2.10a) to (2.10b); the coulomb corrections can be computed and will be at most a few per cent due to the small value of total charge and to the fact that the relative velocities of all particles are large. Once again the applicability of this procedure can be directly checked (at least in principle) by study of (2.10b) and its analysis in terms of known proton structure and of low energy proton deuteron scattering.

4 [35]. Elastic electron–deuteron scattering may be mentioned briefly as a source of corroborative evidence on neutron structure. However theoretical attempts to draw quantitative conclusions regarding neutron form factors from this process again run into the fundamental difficulty that the relativistic two-nucleon problem is still unsolved. At present the best one can do is to treat the deuteron in the non-relativistic limit as a static bound system of two Pauli nucleons and deduce from measurements of the elastic cross-section the product of the nucleon form factors and the fourier transform of the square of the deuteron's wave function. A detailed analysis and critique of this approximation has been given by Blankenbecler [36]. For not too large scattering angles charge scattering dominates and what is measured is

$$[F_1^N(q^2)+F_1^P(q^2)]^2F_D^2(\mathbf{q})$$

where

$$F_D(\mathbf{q}) = \int \psi_g(\mathbf{r})^* e^{i\mathbf{q}.\mathbf{r}}\psi_g(\mathbf{r})\, d^3\mathbf{r}$$

is commonly called the deuteron ground state form factor. The sum of the nucleon charge form factors appears here because the two nucleons scatter coherently in an elastic process. Note that the combination

$$F_1^N+F_1^P = F_1^s$$

is just the isotopic scalar charge form factor.

McIntyre [35] and collaborators have carried through an extensive programme of elastic scattering from the deuteron and their results are presented in Fig. II.12. The theoretical curves in this figure are drawn with the assumption that the neutron charge distribution vanishes identically for all values of q^2 and shows the influence of the proton form factor and of various deuteron models in fitting the data. Conversely, were there a known $F_D(q^2)$ this experiment would provide $F_1^s(q^2)$ and hence in conjunction with proton scattering measurements,

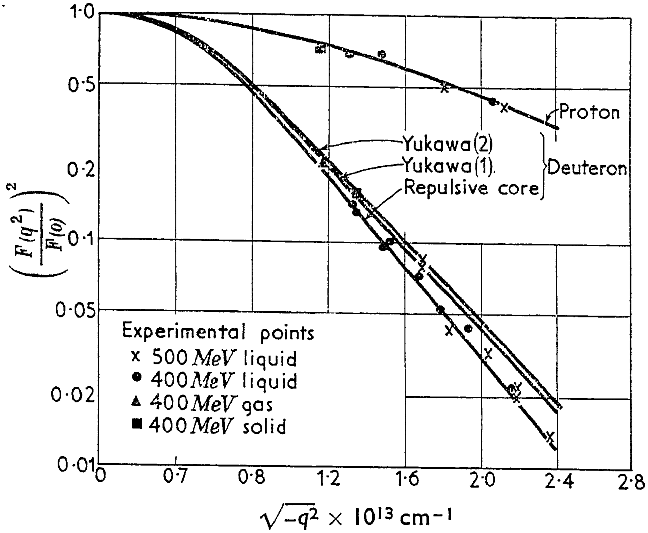

FIG. II.12. Elastic electron-deuteron scattering data presented as a ratio of experimental results to theoretical prediction for a point deuteron composed of point nucleons. The upper curve labelled proton indicates the proton form factor for comparison. The theoretical curves for three different deuteron models are constructed with the assumption that the neutron charge distribution vanishes and hence represent $[F_1^P(q^2)F_D(q^2)]^2$. The argument of the deuteron ground state form factor is taken to be the four momentum transfer, or the three momentum transfer in the centre of mass system. (Taken from J. A. McIntyre and G. R. Burleson [35]).

$F_1^N(q^2)$. The following examples indicate the sensitivity of these results to various assumed $F_1^N(q^2)$, consistent with the observation that $\langle r^2\rangle_{1,N} \rightarrow 0$. First note that with the assumptions that $\langle r^2\rangle_{1,N} = 0$, $\langle r^2\rangle_{1,P} = (0{\cdot}8f)^2$, and that the higher moments of the neutron's charge distribution cancel those of the proton, the above curves are decreased to less than $\frac{1}{3}$ of their drawn values at the highest q-values. Secondly it follows from the analysis of Schiff [37] that if a neutron has a charge distribution with $\langle r^2\rangle_{1,N} = 0$ and with no more than $-0{\cdot}1e$ at a distance of one meson compton wavelength from the origin, the cross-section is reduced by more than 60 per cent at the high q values indicated in Fig. II.12.

It is tempting to proceed further and attempt to draw quantitative conclusions concerning the neutron charge distribution. That the dangers in so doing are considerable, however, is apparent from calculations of Blankenbecler [36] and of Bernstein [38]. Their (different) relativistic and exchange current corrections to the usual description of the deuteron as two statically bound Pauli nucleons produced corrections of different signs but of magnitude comparable with the difference between the curves drawn in Fig. II.12 for different deuteron models. These corrections limit, at present, elastic deuteron scattering as a source of information on neutron structure. Once this is known from other measurements such as, perhaps, the inelastic cross-section for electrons on deuterons, elastic scattering will provide sensitive measurements of properties of the deuteron system itself.

Friedman, Kendall and Gram [39] have performed elastic scattering experiments designed to provide new information on neutron magnetic moment structure. They work at larger scattering angles in order to emphasize the magnetic interaction and form ratios of cross-sections for different energies and angles, corresponding to the same momentum transfer, in order to isolate the magnetic from the charge scattering, as was discussed earlier for the electron–proton scattering. Fig. II.13 summarizes their results.

These ratios have two main virtues. First of all they are sensitive to a difference in the neutron and proton moment structures. This is seen from the following elastic scattering formula, adapted from Jankus, which treats the deuteron non-relativistically:

$$\frac{d\sigma}{d\Omega} = 4\frac{d\sigma_0}{d\Omega}\,F_D^2(F_1^s)^2\left\{1+\frac{2}{3}\frac{|\mathbf{q}^2|}{4M^2}\left[2\tan^2(\tfrac{1}{2}\theta)\right.\right.$$
$$\left.\left.\times\left(1+\frac{2MF_2^s}{F_1^s}\right)^2+\left(\frac{2MF_2^s}{F_1^s}\right)^2\right]\right\}$$

where

$$\frac{d\sigma_0}{d\Omega} = \left(\frac{e^2}{8\pi E_0}\right)^2 \frac{\cos^2(\frac{1}{2}\theta)}{\sin^4(\frac{1}{2}\theta)} \frac{1}{1+\dfrac{2E_0}{M^2}\sin^2(\frac{1}{2}\theta)}. \tag{2.11}$$

Because the anomalous static nucleon moments almost completely cancel in the deuteron any difference in their structures for $q^2 \neq 0$ shows up magnified at large angles by its sizable contribution to elastic scattering. Also if the experiments are performed at not too high energies so that very little recoil energy is transferred to the deuteron and hence the three- and four-momentum transfers differ by very little, the deuteron wave function and structure disappear in the ratio of cross-sections (2.11) at different angles. However there still remains the difficulty that the relativistic corrections to the description of the deuteron are unknown [25], [36]. They

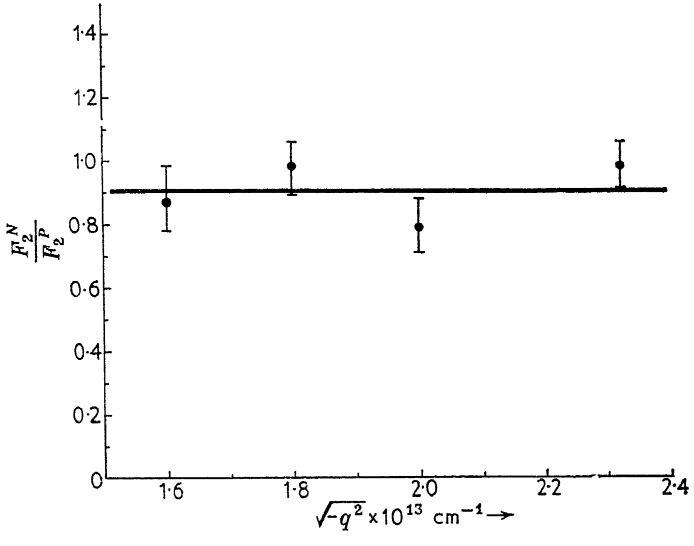

FIG. II.13. Ratio $F_2^N(q^2)/F_2^P(q^2)$ as determined by elastic electron deuteron scattering. The experimental data are analysed here according to equation (2.11) with the additional simplifying assumptions that $F_1^P(q^2)/F_1^P(0) = F_2^P(q^2)/F_2^P(0)$, which is consistent with experiment (see Fig. II.5) and that $F_1^N(q^2) = 0$. (We quote here the preliminary analysis of Friedman, Kendall, and Gram, [39].)

may not be at all insignificant in a process such as this where one is working with very small cross-sections.

In discussing the elastic deuteron scattering, the first Born approximation has been used. The validity of this approximation can be defended here to order 1/137 as in the case of the electron–proton scattering. Schiff [40], Lewis [41], and Valk and Malenka [42] have studied the dispersion contribution associated with the possibility of virtually disintegrating the deuteron in the intermediate state in a second Born approximation and found this to be small.

5 [26], [43]. The process of pion production in electron–nucleon collisions,

$$e+P \rightarrow e'+\begin{cases} P+\pi^0 \\ N+\pi^+ \end{cases} \tag{2.12}$$

offers two unique possibilities as a probe of nucleon structure. First, as a probe of neutron electromagnetic form factors, it is free of complications of the two-nucleon problem which have been analysed in previous paragraphs. Secondly, it offers the possibility of measuring the electromagnetic structure of the pion. In the theoretical analysis developed in the following chapter, it becomes apparent that a theoretical discussion of nucleon structure hinges upon pion structure; in particular, approximate dispersion theoretic calculations yield nucleon form factors as integrals involving pion structure. The pion form factor is then of great interest, not only in its own right, but because theory leads to an approximate relation between pion and nucleon form factors which in principle, at least, can be directly checked by experiment.

Before outlining the theoretical campaign from process (2.12) to actual form factors, it should be pointed out that with present experimental limitations it does not appear to be feasible to use electron production of pions to probe the pion form factors. However, new data on neutron structure can be obtained this way. The first study of electron production of pions as a nucleon structure probe was given by Fubini, Nambu and Wataghin [44], using the method of dispersion theory.

Again to lowest order (1st Born approximation) in the electromagnetic coupling, the amplitude for (2.12) can be expressed, as seen in Fig. II.14, as the amplitude for pion production by a virtual photon of 4-momentum q_μ:

$$T_{kq} = eA_\mu^{(e)}(q)\langle p_2 k^{(-)}|j_\mu(0)|p_1\rangle.$$

The matrix element of the photon current operator j_μ is taken between initial proton and final nucleon plus pion states and differs from the photo meson production matrix element only by virtue of the non-vanishing photon q^2 and of the fact that its scalar product is taken with the Møller potential of the scattered electron, which has longitudinal and scalar as well as transverse components. These differences are reflected by the presence of electromagnetic form factors in the inhomogeneous terms in the dispersion analysis of the amplitude $\langle p_2 k^{(-)}|j_\mu(0)|p_1\rangle$. The inhomogeneous terms come from the one-particle intermediate states shown in Fig. II.15. These terms exhibit poles for the one-particle intermediate states. The locations of these poles are at energies for which the intermediate particles have a squared 4-momentum equal to the square of their mass; i.e. they are 'on the mass shell,' and the

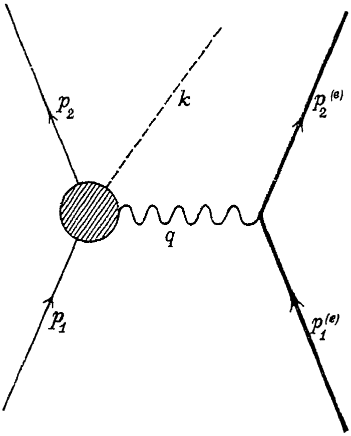

FIG. II.14. Diagram for the process (equation (2.12)).

residues at these poles are known coefficients expressing the amplitude for pion emission by a nucleon multiplied by the electromagnetic form factors. In Fig. II.15(a and b), the pole occurs for a 'real' intermediate nucleon and the residue depends

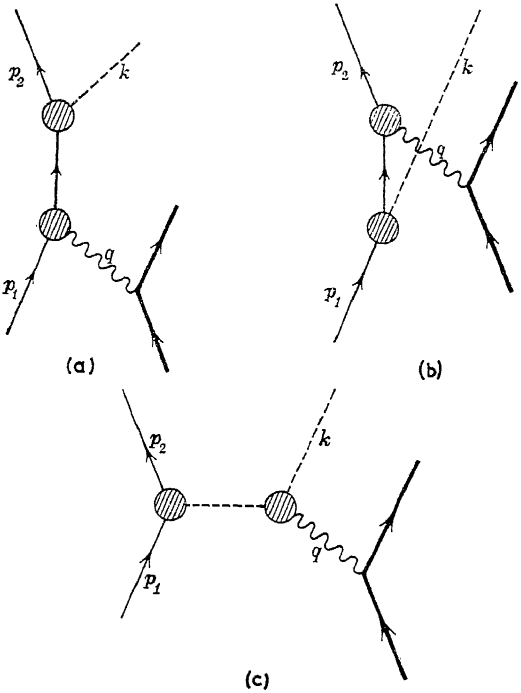

Fig. II.15. Diagrams producing poles in the process (equation (2.12)). Figure (c) occurs only for charged pion production.

on the nucleon form factors; in the third diagram the pole corresponds to a real charged pion and measures the pion form factor [45].

Just as in the earlier discussion of inelastic electron–deuteron scattering, there exists no rigorous proof of these analyticity properties. They follow from the Mandelstam [29] conjecture of a two-dimensional spectral representation in scattering (in this case of a virtual photon to a pion) and are valid at least in perturbation theory.

The work of Fubini, Nambu and Wataghin actually preceded that of Mandelstam and was carried out in the framework of the dispersion theory method applied to the energy but not the momentum transfer in the electron–pion production amplitude. Within this more limited 'one-dimensional' dispersion theory approach it is easy to see that the first two graphs in Fig. II.15 produce poles at energies $(p_2+k)^2 = M^2$ and $(p_1-k)^2 = M^2$, respectively; or in an invariant notation, at $\nu = \pm\nu_B$, where $\nu \equiv -(p_1+p_2) \,.\, q/2M$ and

$$\nu_B \equiv k \,.\, q/2M. \tag{2.13}$$

Fig. II.15c gives a pole in the momentum transfer variable $\Delta^2 = (p_2-p_1)^2 = (q-k)^2 = m_\pi^2$ corresponding to exchange of the pion on its mass shell. Its contribution to the dispersion relations in the energy variable appears in the form of a general polynomial in ν which the 'one-dimensional' dispersion relations themselves leave, in general, arbitrary, but which can be tied down to the form predicted by perturbation theory.

No such arbitrariness remains in the Mandelstam representation which is a two-dimensional dispersion relation in both variables ν and Δ^2 and which specifies the residues at all poles in ν and Δ^2. This has already been seen explicitly in the deuteron inelastic scattering discussion which considered both the direct and crossed reaction and located the corresponding poles and specified their residues.

The residue in the pole at $\Delta^2 = m_\pi^2$, which corresponds to elastic electron–pion scattering, is evidently proportional to $F_\pi(q^2)$. Since this is unknown, experiments to measure nucleon structure must be programmed so as to emphasize the role of diagrams (a) and (b) relative to (c). Conversely, in principle one can programme to emphasize (c) by extrapolating in the Chew–Low manner to its pole at $\Delta^2 = m_\pi^2$ and thereby measuring F_π. In either case, the theoretical problem is well defined here and free of the two-body complications presented by the deuteron. Both in its theoretical and experimental aspects, however, there is at present much need of refinement before this can serve as a quantitative tool in electromagnetic structure investigations.

Until now, the experimental investigations of Panofsky and Allton [43] have aimed at exploring the nucleon form factors under conditions such that the pion scattering term of Fig. II.15(c) is of secondary importance. These experiments detected only the scattered electron energy and angle and the runs were programmed by varying momentum transfer q^2 for fixed energy of the recoiling pion-nucleon system.

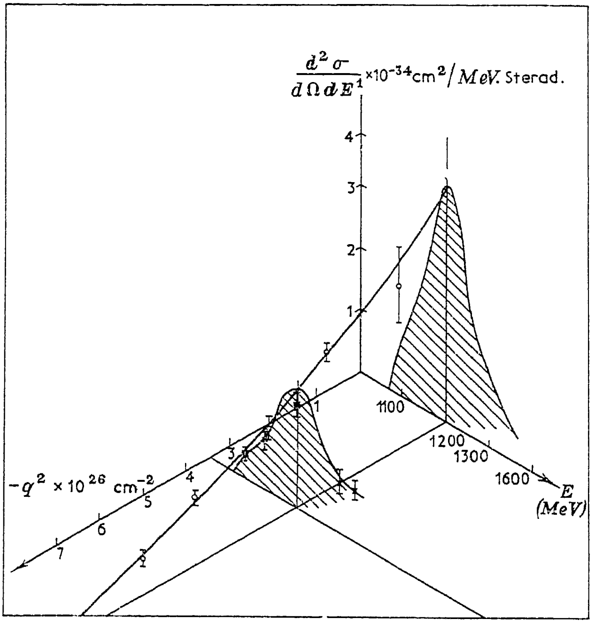

FIG. II.16. Cross-section for electron production of mesons as a function of momentum transfer q^2 and of the relative pion-nucleon energy E. The shaded curve at $q^2 = 0$ is theoretically computed for photo-meson production. (The curve and experimental points are taken from Panofsky and Allton, [43].)

Fig. II.16 shows the cross-section behaviour and some recent data plotted as a function of two variables, q^2 and E, the total pion plus nucleon energy in their centre-of-mass system. By riding down the peak of the curve, for fixed E, one measures predominantly the isovector part of the moment form factor. This is because ~75% of the cross-section at resonance comes from magnetic dipole absorption. The matrix element for this is proportional to

$$[F_2^P(q^2)-F_2^N(q^2)]\sin\delta_{33}(E)e^{i\delta_{33}(E)};$$

therefore only the form factors vary with q^2 and the phase shift is constant for fixed E. An experimental programme which rides down the ledge of Fig. II.16 near threshold is feasible and measures predominantly S-wave π^+-production (via the Kroll–Ruderman term), and hence

$$F_1^P(q^2)-F_1^N(q^2) = F_1^v(q^2).$$

Theoretical difficulties in this programme centre about the problem of obtaining accurate solutions to the dispersion relations. Considerable calculational effort is called for and is being devoted to surmounting this obstacle [46]. In addition an experimental programme has been undertaken to detect protons in coincidence with the electrons. This will permit the charged and neutral pion processes to be separated experimentally [47] and will also contribute to a sharpening in the interpretation possible for this process.

With the feasibility of coincidence studies comes the possibility of an extrapolation procedure to the poles (2.13) of Fig. II.15, which gives the form factors directly as in the earlier deuteron discussion.

For the first diagram the pole corresponding to the real intermediate nucleon occurs as in (2.13) at a recoil energy of the pion given by

$$(p_2+k)^2 = M^2 \quad \text{or} \quad t_{\pi_{\text{rec}}} = -m_\pi+m_\pi^2/2M$$

where $t_{\pi_{\text{rec}}}$ is the pion kinetic energy in the centre-of-mass system of the recoil nucleon and pion, $(\mathbf{p}_2+\mathbf{k} = 0)$, and is sufficiently far removed from the physical region as to discourage application of the extrapolation procedure.

Extrapolation to the nucleon pole in Fig. II.15(b) is also ruled out on practical grounds since it occurs at $(p_1-k)^2 = M^2$ or $t_{\pi_l} = -m_\pi+m_\pi^2/2M$ where t_{π_l} is the pion kinetic energy in the laboratory system [48].

From this it appears that direct, detailed application of the dispersion relations as formulated by Fubini, Nambu, and Wataghin is required in order to extract the nucleon form factors from electron–pion production data.

The pole in Fig. II.15(c) lies closer to the physical region and invites closer inspection as a possible procedure for determining the pion structure. In a manner entirely parallel to the discussion given earlier for the deuteron break-up, one finds this pole at an angle in the $\mathbf{p}_2+\mathbf{k} = 0$ co-ordinate system at

$$\cos\theta = \frac{E_{p_1}E_{p_2}-M^2+\frac{1}{2}m_\pi^2}{\sqrt{(E_{p_1}^2-M^2)}\sqrt{(E_{p_2}^2-M^2)}} > 1,$$

or at a kinetic energy of nucleon recoil in the laboratory system $T_{2_l} = -m_\pi^2/2M$. Frazer [49] has made a detailed statistical analysis of the feasibility of the Chew–Low extrapolation procedure being applied here to measure F_π and has found that an order of magnitude improvement beyond the present experimental accuracy is required. If achieved, direct experimental observation of $F_\pi(q^2)$ for spacelike momentum transfers will be possible. Actually, as the theoretical analysis of Chapter III will show, it is knowledge of the pion form factor for time-like $q^2>0$ that must be inserted into a calculation of the nucleon structure. Such would result from the same extrapolation procedure applied to the reaction

$$\pi^-+P\rightarrow N+e^++e^-$$

since the virtual photon in this case produces a pair with time-like momentum. This experiment unfortunately appears to be beyond experimental possibilities at present.

In conclusion, then, electron–pion production is a desirable probe of nucleon structure. It is free of the complications of the two-nucleon problem and in addition offers the possibility of measuring the pion electromagnetic size which enters into dispersion theoretic calculations of the nucleon form factors. However at this time both theoretical and experimental refinements are necessary.

CHAPTER III

CALCULATIONS OF NUCLEON FORM FACTORS [50]

THEORETICAL attempts to understand the electromagnetic structure of nucleons on the basis of meson theory originated, naturally enough, with perturbation theory calculations in the meson–nucleon coupling strength [51]. The agreement achieved was, to say the least, unimpressive, which was not surprising in view of the size of the meson–nucleon coupling constant. In conjunction with the development of improved methods of calculation with meson theory, the next theoretical work on the electromagnetic structure was done within the framework of the static theory of Chew and Low [52]. Several limitations are, of course, inherent to any discussions based on a static source theory, so only certain features of the structure could be predicted on the basis of the Chew–Low theory. These limitations were finally lifted, in principle at least, by the advent of the dispersion theory [53]. This language allows one to set up the nucleon form factor problem in terms of a set of equations of relatively simple structure, from which all the earlier calculations can be easily derived as straightforward approximations. The language allows, also, a number of improvements on the earlier theories, although it is certainly true that so far no really unimpeachable solution has been found by the dispersion method either.

1. The theoretical discussion of the form factors may be begun, then, by developing the dispersion theory approach, without slighting any of the earlier methods which will appear as appropriate limiting cases.

The dispersion theory is based on certain statements about the analyticity properties of the form factors, considered as functions of a complex momentum transfer squared. Specifically, form factors, e.g. $F_1(q^2)$, have been defined for real values of the variable q^2. One may define functions, which will be denoted by $F_1(z)$, which are the analytic continuations into the complex plane of the functions $F_1(q^2)$ defined on the real axis, with

$$F_1(q^2) = \lim_{z \to q^2 + i\epsilon} F_1(z).$$

The properties of the analytic continuation which will be needed are

(i) $F_1(z)$ is analytic in the closed upper half z plane, except for a branch cut on the positive real axis, for $z \geqslant 4m_\pi^2$.

(ii) $F_1(z)$ (or in some cases $F_1(z)/z$) vanishes as $z \to \infty$ anywhere in the upper half plane.

As yet no rigorous proof of either of these statements exists for the case of interest here, though proofs are available for a few somewhat similar cases [53], [54]. That the statements are true for any order of perturbation theory, however, can be proved [55], and it is generally felt that the present lack of a complete proof independent of the perturbation expansion reflects the difficulty of constructing such a proof, not the falseness of statements (i) and (ii).

In the interest of simplicity the above properties of $F_1(z)$ will be demonstrated in the lowest order of perturbation theory only.

To simplify the algebra, assume that protons, mesons and photons are all spin zero bosons. The fact that spin is present in the actual case changes none of the properties of interest in the calculation which will be carried out; it serves merely to force the use of two form factors, and to require a lot of spinology. For this case, then, the form factor (remember again that there is only one for a spinless proton) is directly given by the Feynman matrix element for the reaction $\gamma + P \to P$, where the photon is allowed to be virtual. To lowest order, this matrix element is calculated from the two Feynman diagrams of Fig. III.1. To illustrate the argument consider only Fig. III.1(a). Upon writing out the matrix element corresponding to this diagram one gets as its contribution to the form factor the expression

$$F(q^2) \sim \int d^4k \, \frac{1}{k^2 - m_\pi^2} \, \frac{1}{(k+q)^2 - m_\pi^2} \, \frac{1}{(p-k)^2 - M^2}. \qquad (3.1)$$

Since it is of interest only to demonstrate the properties of the analytic continuation of F into the complex plane, constant factors may be ignored; several such factors have been dropped here. In accordance with the conventional Feynman rules, remember also that the masses in the propagators of equation (3.1) are considered to have a small negative imaginary part, as a reminder of how to treat the singularities.

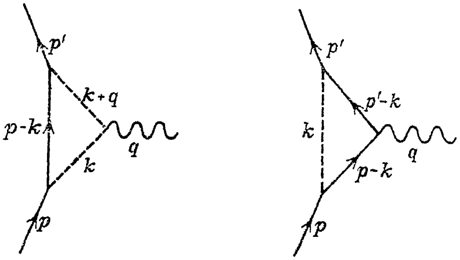

(a) (b)

FIG. III.1. Feynman diagrams for the lowest order perturbation theory contribution of virtual mesons to the nucleon form factors.

It is worth observing, in addition, that the integral of equation (3.1) converges; this is not the case for the actual problem, including the correct spins, so that it is there necessary to renormalize the vertex to produce a finite answer. Again, however, this is a minor complication and of no interest for the purposes under discussion.

The expression (3.1) may now be rewritten by use of the familiar identity used in calculating Feynman diagrams:

$$\frac{1}{a_1 a_2 a_3} = 2\int_0^\infty dx_1\, dx_2\, dx_3\, \frac{\delta(1-x_1-x_2-x_3)}{(a_1x_1+a_2x_2+a_3x_3)^3}.$$

For this case,

$$a_1x_1+a_2x_2+a_3x_3 = k^2+2k\,.\,(qx_2-px_3)-m_\pi^2(1-x_3)+q^2x_2$$

so that

$$F(q^2) \sim \int_0^\infty dx_1\, dx_2\, dx_3 \delta(1-\textstyle\sum x_i)\int d^4k'\left(\frac{1}{k'^2+\Delta}\right)^3$$

where

$$\begin{aligned} k' &= k+k_0 \\ k_0 &= qx_2-px_3 \\ \Delta &= -k_0^2-m_\pi^2(1-x_3)+q^2x_2 \\ &= q^2[x_2(1-x_2)-x_2x_3]-M^2x_3^2-m_\pi^2(1-x_3). \end{aligned}$$

The last equality follows because $p^2 = M^2, p'^2 = (p+q)^2 = M^2$, and therefore $2p \,.\, q = -q^2$. Performing the integral on d^4k' gives

$$F(q^2) \sim \int\limits_0^1 dx_3 \int\limits_0^{1-x_3} dx_2 \frac{1}{\Delta}$$

which may be rewritten as

$$F(q^2) \sim \int\limits_0^1 x\,dx \int\limits_0^1 dy \frac{1}{(q^2+i\epsilon)x^2y(1-y)-M^2(1-x)^2-m_\pi^2x} \tag{3.2}$$

by use of the substitutions

$$\begin{aligned} y &= x_2/x \\ x &= 1-x_3. \end{aligned}$$

The imaginary part from the masses is here exhibited explicitly; since the coefficients of $-M^2$, $-m_\pi^2$, and q^2 are all positive, the overall effect of the small negative imaginary part in M and m_π is to introduce a small positive imaginary part $i\epsilon$ into the denominator as shown.

The way to continue $F(q^2)$ into the complex plane is now clear; one defines a function $F(z)$ by equation (3.2) with $q^2+i\epsilon$ replaced by z. Evidently $F(z)$ is analytic in the entire upper half plane, excluding the real axis; evidently $F(z) \to 0$ as $z \to \infty$; and evidently

$$\lim_{z \to q^2+i\epsilon} F(z) = F(q^2).$$

Thus $F(z)$ is the analytic continuation of $F(q^2)$ into the complex plane, and the region of analyticity is all z for which the denominator in equation (3.2) does not vanish. The denominator vanishes if

$$z = \frac{M^2(1-x)^2+m_\pi^2x}{x^2y(1-y)};$$

in view of the range of x and y, this can happen for all z which are real and greater than $4m_\pi^2$. In conclusion $F(z)$ is analytic in the entire plane with the exception of a branch cut on the positive real axis from $4m_\pi^2$ to ∞.

This verifies conditions (i) and (ii) in lowest order perturbation theory; as stated already, they may also be verified in any finite order.

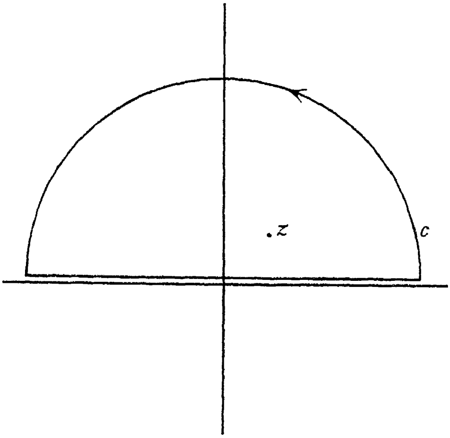

Fig. III.2. Contour in the complex plane used in deriving dispersion relations for form factors.

Return now to the general case and accept once and for all the properties (i) and (ii). First consider the case in which $F(z)$ itself vanishes as $z \to \infty$ in the upper half plane.

By Cauchy's theorem,

$$F(z) = \frac{1}{2\pi i} \oint_c \frac{F(\omega)}{\omega - z} \, d\omega$$

where c is the contour shown in Fig. III.2. Since $F(z)$ vanishes at ∞, the contribution of the semicircle at infinity is zero. Then, since the quantity of interest is $F(q^2)$,

$$F(q^2) = \lim_{\epsilon \to 0} \frac{1}{2\pi i} \int_{-\infty}^{\infty} \frac{F(q'^2)}{q'^2 - q^2 - i\epsilon} \, dq'^2$$

where the integration is now along the real axis, and the contour has been made to approach it from the upper half plane. Using the symbolic identity

$$\lim_{\epsilon\to 0}\frac{1}{x-i\epsilon} = p\frac{1}{x}+i\pi\,\delta(x) \tag{3.3}$$

where p means principal value, this becomes

$$F(q^2) = \frac{1}{\pi i}p\int\limits_{-\infty}^{\infty}\frac{F(q'^2)}{q'^2-q^2}\,dq'^2.$$

Now taking the real part of this equation gives

$$\text{Re } F(q^2) = \frac{1}{\pi}p\int\limits_{-\infty}^{\infty}\frac{\text{Im } F(q'^2)}{q'^2-q^2}\,dq'^2$$

or equivalently

$$F(q^2) = \frac{1}{\pi}\int\limits_{-\infty}^{\infty}\frac{\text{Im } F(q'^2)}{q'^2-q^2-i\epsilon}\,dq'^2.$$

The limit $\epsilon\to 0$ is to be understood from now on.

If there is a region of the real axis in which $\text{Im } F(q^2) = 0$, the above equation may be used to define the analytic continuation of $F(z)$ into the lower half plane. To be precise, define

$$F(z) = \frac{1}{\pi}\int\limits_{-\infty}^{\infty}\frac{\text{Im } F(q'^2)}{q'^2-z}\,dq'^2 \tag{3.4}$$

for an arbitrary z. Now let z approach the real axis, from above and below, in a region where $\text{Im } F(q'^2) = 0$. The same value is obtained, so equation (3.4) in fact defines the analytic continuation of $F(z)$ into the lower half plane, across this region of the real axis. If, on the other hand, z is allowed to approach the real axis from above and below at a point where $\text{Im } F$ does not vanish, one obtains from (3.3) and (3.4),

$$\lim_{\epsilon\to 0}\left(F(z)\big|_{z=q^2+i\epsilon}-F(z)\big|_{z=q^2-i\epsilon}\right) = 2i\,\text{Im } F(q^2).$$

$\left(\text{Here remember that Im } F(q^2) = \text{Im}\left\{\lim\limits_{z\to q^2+i\epsilon} F(z)\right\}.\right)$

Thus the analytic function $F(z)$, defined in the entire plane, has a branch cut across which the discontinuity of the function is $2i\,\text{Im } F(q^2)$. Elsewhere on the real axis $F(q^2)$ is real [56]. By assumption this branch cut exists for $q^2 \geqslant 4m_\pi^2$, so that finally,

$$F(q^2) = \frac{1}{\pi} \int\limits_{4m_\pi{}^2}^{\infty} \frac{\operatorname{Im} F(q'^2)}{q'^2 - q^2 - i\epsilon}\, dq'^2 \tag{3.5}$$

for the physical form factor itself.

If only $F(z)/z$ is assumed to vanish as $z \to \infty$, the application of Cauchy's theorem to this function instead of to $F(z)$ itself, together with a trivial modification of the previous discussion to allow for the pole introduced at $z = 0$, produces a slightly different equation, namely:

$$F(q^2) = F(0) + \frac{q^2}{\pi} \int\limits_{4m_\pi{}^2}^{\infty} \frac{\operatorname{Im} F(q'^2)}{q'^2(q'^2 - q^2 - i\epsilon)}\, dq'^2. \tag{3.6}$$

Both of these equations are called dispersion relations; the first is said to be an unsubtracted, the second, a once subtracted dispersion relation.

2. The dispersion relations are obviously not sufficient in themselves to be used as the basis for any calculations. It is necessary to find in addition an expression for Im $F(q^2)$, or what is equivalent, for the discontinuity of $F(z)$ across the branch cut. It is also necessary to decide which kind of dispersion relation, subtracted or unsubtracted, to use for any given F, and if a subtracted one is used, to decide on the value of $F(0)$.

To obtain the imaginary parts and to discuss the question of subtractions it is convenient to return to the original definition of the form factors. They were given by (neglecting isotopic spin for the moment)

$$\langle p' | j_\mu(0) | p \rangle = \frac{1}{\sqrt{(4E_{p'}E_p)}} (\bar{u}_{p'} | \gamma_\mu F_1(q^2) + i\sigma_{\mu\nu} q_\nu F_2(q^2) | u_p)$$

and may be rewritten in a different form [57]:

$$\langle p' | j_\mu(0) | p \rangle = -\frac{i}{\sqrt{2E_p}} \int d^4x e^{-ip.x}$$
$$\langle p' | (\bar{\psi}(x), j_\mu(0))_+ | 0 \rangle (-i\overleftarrow{\not\nabla}_x - M) u_p.$$

Here the $+$ symbol denotes the time ordering of the two field operators. The differential operator may be moved through the time ordering with the effect of adding an extra term coming from the operation of the time derivative on the step functions implied by the time ordering. Explicitly

$$
\begin{aligned}
(i\nabla_x - M)(\psi(x)j_\mu(0))_+ \\
&= (i\nabla_x - M)(\psi(x)j_\mu(0)\eta(x_0) + j_\mu(0)\psi(x)\eta(-x_0)) \\
&= (j_N(x), j_\mu(0))_+ + i\gamma_0\,\delta(x_0)[\psi(x), j_\mu(0)]
\end{aligned}
$$

where $$\eta(x_0) = \begin{cases} 1 & x_0 > 0 \\ 0 & x_0 < 0. \end{cases}$$

For the standard meson theory, the commutator may be evaluated directly [58];

$$\delta(x_0)[\psi(x), j_\mu(0)] = \frac{e_0}{Z_3^{\frac{1}{2}}}\gamma_0\gamma_\mu\psi(0)\delta^4(x)$$

where e_0 is the unrenormalized electric charge; $e_0 Z_3^{\frac{1}{2}} = e$, the physical renormalized charge. Thus

$$
\begin{aligned}
\langle p'|j_\mu(0)|p\rangle &= -\frac{i}{\sqrt{(2E_p)}}\int d^4x e^{-ip.x}\langle p'|(\bar{j}_N(x), j_\mu(0))_+|0\rangle u_p \\
&\quad + \frac{e_0}{Z_3^{\frac{1}{2}}}\frac{1}{\sqrt{(2E_p)}}\langle p'|\bar{\psi}(0)|0\rangle\gamma_\mu u_p \\
&= -\frac{i}{\sqrt{(2E_p)}}\int d^4x e^{-ip.x}\langle p'|(\bar{j}_N(x)j_\mu(0))_+|0\rangle u_p \\
&\quad + \frac{e_0}{Z_3^{\frac{1}{2}}}\frac{1}{\sqrt{(4E_{p'}E_p)}}(\bar{u}_{p'}|\gamma_\mu|u_p). \qquad (3.7)
\end{aligned}
$$

Several alternatives suggest themselves for the forms of F_1 and F_2. Perturbation theory [51] indicates that $F_1(q^2)$ diverges logarithmically as $q^2 \to \infty$ while $F_2(q^2) \to 0$; if this were the case, a subtracted dispersion relation would be required for F_1, while an unsubtracted one would do for F_2. As a result of the term proportional to e_0 in equation (3.7), which contributes an additive constant $e_0/Z_3^{\frac{1}{2}}$ to F_1, another possibility is that the integral in equation (3.7) vanishes as $q^2 \to \infty$, so that $F_1 \to e_0/Z_3^{\frac{1}{2}}$. In this event a subtracted relation is again needed for F_1, but $e_0/Z_3^{\frac{1}{2}}$ could be computed from it. In either event, the use of a subtracted relation for F_1 introduces no difficulty since the necessary constant $F_1(0)$ is just the electron charge e. It could also be the case that $F_1 \to 0$, allowing the use of the unsubtracted form (3.5) for F_1. In this case one might hope to be able to get some information about the charge, which now appears as an integral over Im F_1 [59]. Finally, there is no proof that either F_1 or F_2 or both do not diverge so badly as $q^2 \to \infty$ that dispersion relations with even more than one subtraction must be used. In any case, it will be assumed at this point that F_2 satisfies an unsubtracted, and F_1 a subtracted, dispersion relation; a subtracted relation for F_1, it should be noted, does not preclude the stronger statement that $F_1 \to 0$ with the consequent validity of an unsubtracted relation.

Aside from the e_0 term in equation (3.7), then, evaluation of the integral results in

$$\begin{aligned}\langle p'|j_\mu(0)p\rangle = \\ -\frac{1}{\sqrt{(2E_p)}}\sum_n \biggl\{ & \frac{\langle p'|\bar{j}_N(0)|n\rangle\langle n|j_\mu(0)|0\rangle}{E_n - p_0' + p_0 - i\epsilon}(2\pi)^3\,\delta^3(\mathbf{P}_n - \mathbf{p}' + \mathbf{p}) \\ & + \frac{\langle p'|j_\mu(0)|n\rangle\langle n|\bar{j}_N(0)|0\rangle}{E_n - p_0 - i\epsilon}(2\pi)^3\,\delta^3(\mathbf{P}_n - \mathbf{p})\biggr\} u_p. \qquad (3.8)\end{aligned}$$

In deriving this a complete set of Heisenberg states of energy E_n and momentum P_n, denoted $|n\rangle$, has been inserted. The choice of boundary conditions on these states is a matter of convenience. From equation (3.8) an explicit formula for the imaginary parts of the form factors can now be obtained. First consider the second term. The denominator can vanish only if

$$P_n^2 = p^2 = M^2.$$

It is easy to see that this condition can be satisfied only if the state n is a one-nucleon state; if it is such a state, however, $\langle n|\bar{j}_N(0)|0\rangle = 0$, so the second term is never singular. To see this, note that if $\langle n|$ is one nucleon of momentum n, then

$$\begin{aligned}\langle n|\bar{j}_N(0)|0\rangle &= \overline{(i\not{\nabla}_x - M)\langle n|\psi(x)|0\rangle|_{x=0}} \\ &= \overline{(i\not{\nabla}_x - M)\frac{1}{\sqrt{(2E_n)}}u_n e^{in.x}|_{x=0}} \\ &= -\frac{1}{\sqrt{(2E_n)}}\bar{v}_n(\varkappa + M) = 0.\end{aligned}$$

by the Dirac equation. It therefore contributes nothing to the discontinuity of the form factors.

In the first term, a singularity can occur if

$$P_n^2 = (p'-p)^2 = q^2,$$

i.e. only for positive real values of q^2. The discontinuity in this term, then, occurs only if $q^2 \geqslant 4m_\pi^2$ (assuming the state n = two pions to be the state of lightest mass which appears), which coincides with the position of the branch cut obtained from the perturbation diagram in which the pion absorbs the photon. The value of the discontinuity is

$$\begin{aligned} -\frac{1}{\sqrt{(2E_p)}} \sum_n \langle p'|\bar{j}_N(0)|n\rangle\langle n|j_\mu(0)|0\rangle(2\pi)^3\delta^3(\mathbf{P}_n-\mathbf{p}) & \\ \times\left(\frac{1}{E_n-q_0-i\epsilon}-\frac{1}{E_n-q_0+i\epsilon}\right)u_p & \\ = -i\,\frac{1}{\sqrt{(2E_p)}}\sum_n (2\pi)^4\,\delta^4(P_n-q)\langle p'|\bar{j}_N(0)|n\rangle\langle n|j_\mu(0)|0\rangle u_p. & \end{aligned}$$

Since the discontinuity in F equals $2i$ Im F, there results

$$\begin{aligned} (\bar{u}_{p'}|\,\mathrm{Im}\,F_1(q^2)\gamma_\mu+i\,\mathrm{Im}\,F_2(q^2)\sigma_{\mu\nu}q_\nu|u_p) & \\ = -\sqrt{(\tfrac{1}{2}E_{p'})}\sum_n (2\pi)^4\,\delta^4(P_n-q)\langle p'|\bar{j}_N(0)|n\rangle\langle n|j_\mu(0)|0\rangle u_p. & \quad (3.9) \end{aligned}$$

The discontinuities, or imaginary parts, then, receive contributions from various intermediate states n. It is convenient to symbolize these contributions pictorially as shown in Fig. III.3. Evidently the delta function in (3.9) implies that a given state contributes only for q^2 greater than the rest mass of that state. If it is desired, the form factors may, as mentioned in Chapter I, be defined in terms of the production process $\gamma \rightarrow N+\bar{N}$; this allows the deduction again of equation (3.9) with u_p replaced by the antiparticle spinor $v_{\bar{p}}$. The corresponding diagrams are then altered by having the incident nucleon line turned around, to become an outgoing antinucleon of momentum $\bar{p}$, so that $q^2 = (p'+\bar{p})^2$. This description will generally be used in what follows.

A final complication is to include both neutrons and protons by introducing the isotopic spin and isotopic scalar and vector form factors. How this is done has already been discussed in the first chapter; therefore, it will suffice here to say that it is only necessary to replace Im $F_{1,2}$ by Im $F^s_{2,1}+\tau_3$ Im $F^v_{1,2}$ in equation (3.9) if charge independence is assumed.

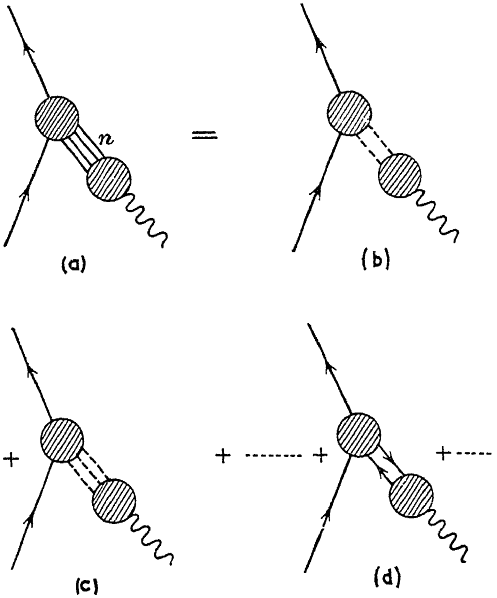

FIG. III.3. Diagrams representing the contributions of various intermediate states to the imaginary parts of the nucleon form factors as given in equation (3.9). (a) is a general state n; (b) is the two-pion, (c) the three-pion, and (d) the nucleon-antinucleon state.

The problem is set up, then, by combining equation (3.9) with the four dispersion relations

$$F_1^{s,v}(q^2) = \tfrac{1}{2}e + \frac{q^2}{\pi}\int\limits_{4m_\pi^2}^{\infty} \frac{\operatorname{Im} F_1^{s,v}(q'^2)}{q'^2(q'^2-q^2-i\epsilon)}\,dq'^2$$

$$F_2^{s,v}(q^2) = \frac{1}{\pi}\int\limits_{4m_\pi^2}^{\infty} \frac{\operatorname{Im} F_2^{s,v}(q'^2)}{q'^2-q^2-i\epsilon}\,dq'^2. \tag{3.10}$$

One additional observation should be made about the above equations, and that is, that Im F_1^s and Im F_2^s vanish for

$q'^2 \leqslant 9m_\pi^2$; thus the thresholds on the dispersion integrals for the scalar form factors should be changed from $4m_\pi^2$ to $9m_\pi^2$. To see this, recall that the contribution to Im F from any given intermediate state is given by equation (3.9). Consider the lightest intermediate states, which are those containing only π mesons, in that equation. The contribution of a state of $n\pi$ mesons is proportional to the amplitude that a photon produces n pions, times the amplitude that n pions are absorbed by a nucleon line. It will be proved that this state contributes only to the isotopic vector from factors if n is even, and only to the isotopic scalar form factors if n is odd.

Since the state of n mesons is produced by a photon, it must have zero total charge and be odd under charge conjugation. The pions may be described as created by the Hermitian fields φ_1, φ_2, φ_3 defined by

$$\varphi_1 = \frac{1}{\sqrt{2}}(\varphi+\varphi^*)$$

$$\varphi_2 = \frac{1}{\sqrt{2}}i(\varphi-\varphi^*)$$

$$\varphi_3 = \varphi_0$$

in terms of the usual charged and neutral fields φ and φ_0 [60]. Now φ creates negative charge, φ^* creates positive charge, and φ_0 zero charge. Then both φ_1 and φ_2 create a linear combination of positive and negative charge. In order that the total charge of the state of n mesons be zero, therefore, the number of particles of type 1 (created by φ_1) plus the number of type 2 must be even. Under charge conjugation, that is, the interchange of positive and negative charge, $\varphi \rightarrow \varphi^*$ and $\varphi_0 \rightarrow \varphi_0$, and so $\varphi_1 \rightarrow \varphi_1$, $\varphi_2 \rightarrow -\varphi_2$, $\varphi_3 \rightarrow \varphi_3$. If the state is to be odd under charge conjugation, then, the number of 2's must be odd, and therefore so must the number of 1's. Finally, mesons of type 1, 2 and 3 absorb on the nucleon line with isotopic operators τ_1, τ_2 and τ_3, respectively. Therefore the total isotopic operator for the n-meson state is $\tau_1^{\text{odd}}\tau_2^{\text{odd}}\tau_3^{\text{n}-\text{even}} = \tau_3^{\text{n}-\text{odd}} = \tau_3$ if n is even, and $=1$ if n is odd. Thus n even or odd leads to an isotopic vector or scalar form factor, and consequently the lightest state which contributes to a scalar form factor is the three-pion state, with a threshold $9m_\pi^2$.

The dispersion relations may be used to derive expressions for, e.g. the 'radii' of the charge and current distributions. These, it will be remembered, were defined by

$$\langle r^2\rangle = \frac{6}{F(0)}\frac{d}{dq^2}F(q^2)|_{q^2=0}. \tag{3.11}$$

If F satisfies a dispersion relation, either subtracted or unsubtracted,

$$F'(0) \equiv \left(\frac{dF}{dq^2}\right)\Big|_{q^2=0} = \frac{1}{\pi}\int^{\infty}\frac{\operatorname{Im} F(q'^2)}{q'^4}\,dq'^2. \tag{3.12}$$

If in addition F were to satisfy an unsubtracted dispersion relation, one could write

$$F(0) = \frac{1}{\pi}\int^{\infty}\frac{\operatorname{Im} F(q'^2)}{q'^2}\,dq'^2. \tag{3.13}$$

Now, if Im $F(q'^2)$ is everywhere positive, equations (3.11, 3.12, and 3.13) provide a bound on the radius, given by

$$\langle r^2\rangle \leqslant \frac{6}{(2m_\pi)^2} \quad \text{for the vector radii}$$

$$\langle r^2\rangle \leqslant \frac{6}{(3m_\pi)^2} \quad \text{for the scalar radii.}$$

Since there is no theoretical reason whatever to believe that Im $F(q'^2)$ does not change sign, however, these bounds are useless, and the radii will not be discussed further. However, if Im $F(q'^2)$ were positive definite, one could obtain predictions about the behaviour of F itself which may be tested by experiment. For example, if one computes the curvature of $1/F$ [61], one obtains

$$\frac{d^2}{d(q^2)^2}\frac{1}{F(q^2)} \equiv \left(\frac{1}{F(q^2)}\right)''$$
$$= 2\pi\frac{\left(\displaystyle\int\frac{\operatorname{Im} F}{(q'^2-q^2)^2}\right)^2-\displaystyle\int\frac{\operatorname{Im} F}{q'^2-q^2}\int\frac{\operatorname{Im} F}{(q'^2-q^2)^3}}{\left(\displaystyle\int\frac{\operatorname{Im} F}{q'^2-q^2}\right)^3}.$$

If Im $F(q'^2) \geqslant 0$ everywhere, and if $q^2 \leqslant 0$, which is the region in which $F(q^2)$ is measured, the denominator here is positive. The numerator may be rewritten as

$$-\tfrac{1}{2}\int dq'^2 \int dq''^2 \text{Im } F(q'^2) \text{ Im } F(q''^2) \frac{1}{q'^2-q^2}\frac{1}{q''^2-q^2} \times \left(\frac{1}{q'^2-q^2}-\frac{1}{q''^2-q^2}\right)^2,$$

which, under the same assumptions, is $\leqslant 0$. Thus, a positive definite imaginary part for a form factor satisfying an unsubtracted dispersion relation requires the reciprocal of the form factor to be concave downward in the region of spacelike q^2. Present experimental evidence is still too scanty to test the validity of this prediction. A somewhat easier comparison with experiment seems to be afforded by the curvature of $\log F(q^2)$ rather than of $1/F(q^2)$ [62]; namely

$$(\log F)'' = -F\left(\frac{1}{F}\right)'' + \left(\frac{F'}{F}\right)^2,$$

which is positive under the above assumptions. Additional experimental information on the charge and moment form factors separately is required to test either of these results.

3. Up to this point no approximations have been necessary (provided one accepts the assumed analyticity properties of the form factors); equation (3.9), together with the dispersion relations, are a formally correct set of equations from which the form factors can, in principle, be determined. A practical calculation of the form factors, however, will of course require some approximations in the use of equation (3.9) to determine the imaginary parts. It is convenient to begin the second—i.e. the approximate—phase of the theoretical discussions by indicating how the perturbation theory calculations follow from the general formalism.

Perturbation theory takes the view that only terms with the smallest number of powers of g, the meson nucleon coupling constant, will be of importance. It requires only a moment's thought to convince oneself that the only intermediate states in equation (3.9) which contribute to order g^2 are the two-pion and the nucleon–antinucleon states. All other states are at least of order g^4. Fig. III.4 illustrates this. To evaluate the Im F's to order g^2, then, it is necessary to drop all but these two intermediate states in equation (3.9) and to replace the matrix elements which appear in the states retained by their lowest-order values. Thus, one should use, e.g. for the contribution of the two-pion intermediate state, the expression

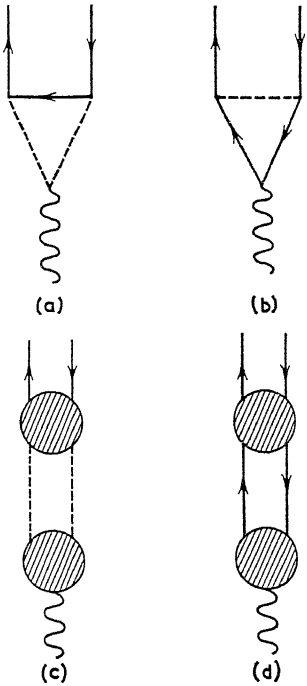

Fig. III.4. (a) and (b) show the two Feynman graphs contributing to the form factors to order g^2, (c) and (d) are the corresponding diagrams indicating which intermediate states the same graphs contribute to in the dispersion relation language.

$$(\bar{u}_{p'}|\text{Im } F_1^v\tau_3\gamma_\mu + i\text{ Im } F_2^v\tau_3\sigma_{\mu\nu}q_\nu|v_{\bar{p}})_{2\pi}$$
$$= -\sqrt{(\tfrac{1}{2}E_{p'})}\int\frac{d^3q_1}{(2\pi)^3}\int\frac{d^3q_2}{(2\pi)^3}\sum_{\sigma_1,\sigma_2=1}^{3}(2\pi)^4\,\delta^4(q_1+q_2-q)$$
$$\times\langle p'|\bar{j}_N(0)v_{\bar{p}}|q_1\sigma_1,\,q_2\sigma_2\rangle\langle q_1\sigma_1,\,q_2\sigma_2|j_\mu(0)|0\rangle \quad (3.14)$$

(where q_1, q_2 and σ_1, σ_2 are the momenta and charges of the two intermediate π's), and write, to order g^2,

$$\begin{aligned}
&\langle q_1\sigma_1 q_2\sigma_2|j_\mu(0)|0\rangle \\
&\qquad = -\frac{1}{\sqrt{(4\omega_1\omega_2)}}\, ie(q_{1\mu}-q_{2\mu})(\delta_{\sigma_1 1}\delta_{\sigma_2 2}-\delta_{\sigma_1 2}\delta_{\sigma_2 1}) \\
&\langle p'|\bar{j}_N(0)v_{\bar{p}}|q_1\sigma_1,\, q_2\sigma_2\rangle \\
&\qquad = \frac{1}{\sqrt{(8E_{p'}\omega_1\omega_2)}}\, (\bar{u}_{p'}|g\gamma_5\tau_{\sigma_1}\frac{1}{\not{p}'-\not{q}_1-M}\, g\gamma_5\tau_{\sigma_2}|v_{\bar{p}}).
\end{aligned}$$

A small amount of algebra, together with the identity

$$\int dq_{10}\,\delta(q_1^2-m_\pi^2)\eta(q_{10}) = \frac{1}{2\omega_{q_1}};$$

permits a more convenient form for equation (3.14):

$$\begin{aligned}
&(\bar{u}_{p'}|\tau_3 \operatorname{Im} F_1^v\gamma_\mu + i\tau_3 \operatorname{Im} F_2^v\sigma_{\mu\nu}q_\nu|v_{\bar{p}})_{2\pi} \\
&\qquad = \frac{ieg^2}{8\pi^2}\Bigg(\bar{u}_{p'}\Big|\int d^4q_1\int d^4q_2\,\eta(q_{10})\eta(q_{20}) \\
&\quad \times \sum_{\sigma_1,\sigma_2=1}^{3} \delta(q_1^2-m_\pi^2)\,\delta(q_2^2-m_\pi^2)\,\delta^4(q_1+q_2-q)\,\tau_{\sigma_1}\gamma_5\frac{1}{\not{p}'-\not{q}_1-M} \\
&\qquad\quad \times\tau_{\sigma_2}\gamma_5(q_{1\mu}-q_{2\mu})(\delta_{\sigma_1 1}\delta_{\sigma_2 2}-\delta_{\sigma_1 2}\delta_{\sigma_2 1})\Big|v_{\bar{p}}\Bigg).
\end{aligned} \tag{3.15}$$

It is interesting to observe that this is nothing more than the standard Feynman amplitude for the diagram of Fig. (III.4(a)), multiplied by $2\pi^2$ and with the Feynman propagators of the intermediate mesons replaced according to

$$\frac{1}{q_1^2-m_\pi^2} \to \eta(q_{10})\delta(q_1^2-m_\pi^2).$$

A similar result appears if one calculates to order g^2 the nucleon–antinucleon state contribution in equation (3.9).

It is a definitely non-trivial task to show directly that this modification in the Feynman matrix element is what is required to give its imaginary part. For a Feynman matrix element with a single propagator, the analogous identification is simple, because the small negative imaginary part in the mass in each propagator produces the identity

$$\frac{1}{q^2-m_\pi^2+i\epsilon} = \frac{1}{q^2-m_\pi^2} - i\pi\delta(q^2-m_\pi^2),$$

from which one sees that the imaginary part is clearly obtained by the replacement

$$\frac{1}{q^2-m_\pi^2} \rightarrow -\pi\delta(q^2-m_\pi^2).$$

However no such simple argument works in the present example, where three propagators appear.

If now these expressions are used to evaluate Im $F_{1,2}^{s,v}$ to order g^2, and the resulting functions are inserted into the dispersion relations, the usual perturbation theory is obtained [51]. It should, perhaps, be remarked that it is the usual *renormalized* perturbation theory which is obtained; this approach through the dispersion relations is automatically finite at every stage and expresses the answer directly in terms of renormalized quantities.

It may be worthwhile to indicate how this derivation of the perturbation result goes in a bit more detail. In equation (3.15), use the fact that

$$\frac{1}{\not{p}'-\not{q}_1-M} = \frac{\not{p}'-\not{q}_1+M}{(p'-q_1)^2-M^2}$$

and then write

$$(\bar{u}_{p'}|\gamma_5(\not{p}'-\not{q}_1+M)\gamma_5|v_{\bar{p}}) = (\bar{u}_{p'}|-\not{q}_1|v_{\bar{p}}).$$

Next observe that

$$\sum_{\sigma_1\sigma_2}\tau_{\sigma_1}\tau_{\sigma_2}(\delta_{\sigma_1 1}\delta_{\sigma_2 2}-\delta_{\sigma_1 2}\delta_{\sigma_2 1}) = \tau_1\tau_2-\tau_2\tau_1 = 2i\tau_3.$$

Inserting these relations in equation (3.15) yields

$$\text{Im } F_1^v\gamma_\mu + i \text{ Im } F_2^v\sigma_{\mu\nu}q_\nu = \frac{eg^2}{2\pi^2}\int d^4Q\eta(K_0+Q_0)\eta(K_0-Q_0)$$
$$\times\,\delta((K+Q)^2-m_\pi^2)\delta((K-Q)^2-m_\pi^2)\not{Q}Q_\mu\frac{1}{(P-Q)^2-M^2}$$

where

$$\begin{aligned}Q &= \tfrac{1}{2}(q_1-q_2)\\ K &= \tfrac{1}{2}q = \tfrac{1}{2}(q_1+q_2) = \tfrac{1}{2}(p'+\bar{p})\\ P &= \tfrac{1}{2}(p'-\bar{p}).\end{aligned}$$

Before evaluating the integral over d^4Q it is convenient to carry out the spinology, and identify Im F_1 and Im F_2 separately. This is easily done and results in

$$\begin{aligned}\operatorname{Im} F_1^v(q^2) &= \frac{eg^2}{2\pi^2}\int d^4Q\,\delta((K+Q)^2-m_\pi^2)\,\delta((K-Q)^2-m_\pi^2)\\ &\quad\times\frac{1}{(P-Q)^2-M^2}\left[\frac{(P\,.\,Q)^2-P^2Q^2}{2P^2}+M^2\frac{P^2Q^2-3(P\,.\,Q)^2}{2P^4}\right]\\ \operatorname{Im} F_2^v(q^2) &= \frac{eg^2}{2\pi^2}M\int d^4Q\,\delta((K+Q)^2-m_\pi^2)\,\delta((K-Q)^2-m_\pi^2)\\ &\quad\times\frac{1}{(P-Q)^2-M^2}\left[\frac{P^2Q^2-3(P\,.\,Q)^2}{2P^4}\right].\end{aligned}$$

Finally, evaluating these integrals gives at last

$$\begin{aligned}\operatorname{Im} F_1^v(q^2) &= \frac{eg^2}{8\pi}\frac{q_\pi^2}{\sqrt{(q^2q_N^2)}}\left\{\frac{2}{y_0}\left(1-\frac{1}{y_0}\tan^{-1}y_0\right)\right.\\ &\quad\left.-\frac{q^2}{4q_N^2}\left[\tan^{-1}y_0-\frac{3}{y_0}\left(1-\frac{1}{y_0}\tan^{-1}y_0\right)\right]\right\}\end{aligned}$$

and

$$\begin{aligned}\operatorname{Im} F_2^v(q^2) &= -M\frac{eg^2}{8\pi}\frac{q_\pi^2}{\sqrt{(q^2q_N^2)}}\frac{1}{q_N^2}\\ &\quad\times\left\{\tan^{-1}y_0-\frac{3}{y_0}\left(1-\frac{1}{y_0}\tan^{-1}y_0\right)\right\}\end{aligned} \qquad (3.16)$$

where

$$y_0 = \frac{2q_\pi q_N}{\frac{1}{2}q^2-m_\pi^2}$$

and

$$q_\pi = \sqrt{(q^2/4-m_\pi^2)}, \qquad q_N = \sqrt{(q^2/4-M^2)}.$$

These expressions are rather complicated, and the derivation of them has been presented in some detail because the techniques of calculation are typical of the type of algebra necessary in using these dispersion relations, not because these particular results are of any great significance.

As indicated above, the results quoted here are only for the meson current contribution to the perturbation result in Fig. III.4(c). Similar calculations will produce the answer for the nucleon current part, Fig. III.4(d).

This perturbation calculation gives the following values for, e.g., the static anomalous magnetic moments [51].

$$\mu_P^a = \mu_v + \mu_s = \cdot 036\left(\frac{g^2}{4\pi}\frac{e}{2M}\right)$$

$$\mu_N^a = -\mu_v + \mu_s = -\cdot 26\left(\frac{g^2}{4\pi}\frac{e}{2M}\right).$$

The agreement with the experimental values is not startling, as is only to be expected from a solution obtained by an expansion in powers of 15. The difficulty comes from a large isotopic scalar contribution by the nucleon current; i.e. from the second of the two perturbation diagrams, Fig. III.4(b). Note that the meson current contributes only to the isotopic vector part, its second-order contribution being $1\cdot 6(e/2M)$ for $g^2/4\pi = 15$. This result is increased by less than 10% when fourth order terms in the meson–nucleon coupling constant are included. On the other hand, the fourth order contribution from the nucleon current greatly alters the second order results of $-1\cdot 55(e/2M)$ and $+\cdot 57(e/2M)$ to ~ 0 and $4\cdot 4(e/2M)$ for the isoscalar and isovector parts, respectively. It is therefore necessary to look for an improved approximation method.

4. The dispersion theory approach, as outlined above, is not a foundation which suggests that a perturbation expansion is a very natural kind of approximation to try. A more plausible scheme might be as follows. Observe that a particular intermediate state in equation (3.9) contributes only with a threshold equal to the square of the total rest mass of that state. Thus, a heavy state appears only for large q'^2 in the Im F's; in fact, for $4m_{\pi^2} \leqslant q'^2 \leqslant 16\, m_\pi^2$, the Im F's are given exactly by only the 2π intermediate state. The heavy state contributions in the dispersion integrals may therefore be small, due to the denominator $(q'^2 - q^2)$ in the dispersion integral, particularly

if one is only interested in evaluating the form factors at the negative values of q^2 for which they are measured. The dispersion relation approach is based on the hope, then, that it is a sensible approximation to drop the effects of heavy intermediate states in equation (3.9). It may be mentioned that the subtracted dispersion relation has an extra power of q'^2 in the denominator which provides an additional weighting against heavy state contributions to the imaginary parts. One would therefore expect to have more confidence in this approximation scheme if used in conjunction with the subtracted form of the dispersion relation.

An argument such as the above, is, of course, hardly convincing; nevertheless it seems more reasonable than the perturbation theory. Thus the next try might be to say that only the lightest state counts; that is the 2π state for the vector form factors, and the 3π state for the scalar form factors. Consider first the isotopic vector case; so return to equation (3.9), drop all but the 2π state, but now do not replace the remaining amplitudes by perturbation theory. When this is done, and the limit $M \rightarrow \infty$ (i.e. the static nucleon limit) is taken, the results of calculations made with the Chew–Low form of the static theory are reproduced [52], [53]. Since the two-pion state will be discussed shortly, there is no point in going into the algebraic details here. Suffice it to say that the values of the static anomalous moments obtained from this theory are

$$\mu_P^a = -\mu_N^a \sim 2\left(\frac{e}{2M}\right).$$

(Since the two-pion state is a pure isotopic vector, the proton and neutron moments are of course equal and opposite; the static theory is totally incapable of discussing the isoscalar moments.) These numbers result for a static theory coupling constant

$$f^2 = 0{\cdot}08 = (m_\pi/2M)^2(g^2/4\pi)$$

and a cutoff

$$\omega_{\text{Max}} \sim 6m_\pi.$$

This result is somewhat more encouraging than that of perturbation theory; however, talking in terms of the static theory is always rather unsatisfactory since these results all depend sensitively on cutoffs and are not gauge invariant, among other shortcomings; in addition in this application the static theory has been shown to introduce serious kinematical errors [63].

The previous discussion has sketched briefly how the results of both perturbation theory and the static meson theory may be derived from the general formalism of dispersion relations. The natural question to be discussed next, then, is how to improve on these approximations.

The partial success of the static theory, within its obvious limitations, supports the hope that the approximation of sticking to the lightest intermediate state, even in the relativistic case, may not be too absurd, at least if one confines oneself to properties of the form factors for small momentum transfers. This hope may be reinforced by looking in some detail at a particular heavy intermediate state, that of a nucleon–antinucleon pair, and showing that it is unlikely that this state, at least, contributes in a very important way in determining the low momentum transfer form factors. The reason that limitations may be placed on the effect of the nucleon–antinucleon state is more easily illustrated by discussing the case where the spin of the particles is neglected The essential features of the argument are all present in this case; the presence of spin only serves to complicate the algebra.

It is obvious, from equation (3.9) and the interpretation of this equation in terms of pictures, such as shown in Fig. III.3, that the contribution to the imaginary parts of the form factors from the $N\bar{N}$ state is proportional to the nucleon form factor itself times the $N\bar{N}$ scattering amplitude. Since the threshold of this contribution is $q'^2 = 4M^2$, the total centre-of-mass energy of the $N\bar{N}$ scattering process is always greater than or equal to $2M$, so the amplitude appearing is actually a physically observable quantity [64]. In addition, the initial nucleon and antinucleon of this scattering have been produced by a photon, which has spin one. So, in their centre-of-mass system, only the amplitude for scattering in a state odd under charge conjugation and of total angular momentum one will be relevant. For the case of the actual spins, this limits the scattering to be in the $3S_1$ and $3D_1$ states; for the illustration problem, where the nucleons are given spin zero, the scattering is then in the P state. Thus one may write, in the fictitious case,

$$\operatorname{Im} F(q'^2)_{N\bar{N}} = F(q'^2)^* \sin \delta e^{i\delta}, \tag{3.16}$$

where δ is the P wave $N\bar{N}$ scattering phase shift, evaluated as a total centre-of-mass energy given by $\sqrt{(q'^2)}$. Two comments are necessary concerning this equation: first, only one form factor is involved. This is because spin zero nucleons have only a charge form factor and no moment form factor. Second, the right-hand side involves F^*, not F. This may be understood by referring back to equation (3.9), and observing that if the matrix element of the nucleon current is to represent $N\bar{N}$ scattering, the intermediate nucleon–antinucleon state in equation 3.9 must be a state with outgoing wave boundary conditions [65]. But this means that the photon current matrix element has as its final state an outgoing $N\bar{N}$ pair instead of an ingoing one; since the form factors were originally defined in terms of the matrix element of the photon current with ingoing boundary conditions, F^* rather than F appears here. To be specific, the relation of the matrix element

$$\langle p'\overline{p}^{(-)}|j_\mu(0)|0\rangle$$

where the final state has ingoing boundary conditions, to the matrix element

$$\langle p'\overline{p}^{(+)}|j_\mu(0)|0\rangle$$

in which the final state differs only in that it has outgoing boundary conditions, may be obtained from time reversal invariance. The form factor for spin zero nucleons is defined in terms of the first matrix element by

$$\langle p'\overline{p}^{(-)}|j_\mu(0)|0\rangle = \frac{1}{\sqrt{(4E_{p'}E_{\overline{p}})}}\,(p'-\overline{p})_\mu F(q^2).$$

Then, to evaluate the second matrix element, note

$$\begin{aligned}\langle \mathbf{p}', \bar{\mathbf{p}}^{(+)}|j_\mu(0)|0\rangle &= \langle \mathbf{p}', \bar{\mathbf{p}}^{(+)}|T^{-1}Tj_\mu(0)T^{-1}T|0\rangle \\ &= \langle -\mathbf{p}', -\bar{\mathbf{p}}^{(-)}|j_\mu(0)_T|0\rangle^*\end{aligned}$$

where $j_\mu(0)_T$ is the time reverse Heisenberg electromagnetic current [66], and

$$j_\mu(0)_T = \begin{array}{rl} j_\mu(0) & \text{if } \mu \text{ is the time component} \\ -j_\mu(0) & \text{if } \mu \text{ is a space component.}\end{array}$$

Therefore,

$$\begin{aligned}\langle \mathbf{p}'\bar{\mathbf{p}}^{(+)}|j_\mu(0)|0\rangle &= \pm\langle -\mathbf{p}', -\bar{\mathbf{p}}^{(-)}|j_\mu(0)|0\rangle^* \\ &= \pm\left(\left(\frac{1}{\sqrt{4E_{p'}E_{\bar{p}}}}\right)(\pm(p'-\bar{p})_\mu)F(q^2)\right)^*\end{aligned}$$

where

$$\pm(p'-\bar{p})_\mu = \begin{array}{rl} (p'-\bar{p})_\mu & \text{if } \mu \text{ is the time component} \\ -(p'-\bar{p})_\mu & \text{if } \mu \text{ is a space component.}\end{array}$$

Thus finally

$$\langle \mathbf{p}'\bar{\mathbf{p}}^{(+)}|j_\mu(0)|0\rangle = \frac{1}{\sqrt{(4E_p\, E_{\bar{p}})}}(p'-\bar{p})_\mu F(q^2)^*;$$

that is, the only effect of using outgoing states instead of ingoing states is to replace F by F^*.

Consider the contribution, now, of this $N\bar{N}$ state to some low-energy property of the form factor, e.g. the radius. This is given by

$$\begin{aligned}\langle r^2\rangle_{N\bar{N}} &= \frac{6}{F(0)}\left.\frac{dF_{N\bar{N}}}{dq^2}\right|_{q^2=0} \\ &= \frac{6}{F(0)}\frac{1}{\pi}\int\limits_{4M^2}^{\infty}\frac{\operatorname{Im} F_{N\bar{N}}(q'^2)}{q'^4}\,dq'^2.\end{aligned}$$

Now $\operatorname{Im} F_{N\bar{N}}(q'^2)$ is given by equation (3.16); hence

$$|\operatorname{Im} F_{N\bar{N}}(q'^2)| \leqslant |F(q'^2)|.$$

If $F(q'^2)$ is assumed bounded, e.g. by its value at zero, there results

$$\langle r^2\rangle_{N\bar{N}} \leqslant \frac{6}{\pi}\int\limits_{4M^2}^{\infty}\frac{dq'^2}{q'^4} = \frac{3}{2\pi M^2}. \tag{3.17}$$

Such a limitation is called a 'unitarity limitation,' because it has its origin in the statement that $|\sin\delta e^{i\delta}| < 1$. In the actual case of spin $\frac{1}{2}$ nucleons, similar limitations may be derived effectively by the method indicated, though the derivation is complicated by a certain amount of algebra. These limitations exist for the radii, static moments, etc. If they are valid, they imply, owing to the large mass of the nucleon, that the $N\bar{N}$ state contributes little to the low-energy properties of the form factor [67].

Several things should be emphasized, however, to avoid undue joy at this result. First, limitations can be imposed only on the moments of F, so nothing is said about the effect of the $N\bar{N}$ state on the behaviour of F at higher momentum transfers, say comparable to M^2. Second, to get the limitations, it was necessary to assume that $|F|$ itself was bounded; in fact bounded by a value comparable to its value at the origin. This assumption is not necessarily correct. For example, if one rewrites equation (3.16) in the form (taking δ to be real, for the moment)

$$\operatorname{Im} F = \tan\delta \operatorname{Re} F,$$

it becomes less obvious that there should be a bound. Only if we say $\operatorname{Re} F$ becomes zero when δ goes through $\frac{1}{2}\pi$ do we get back the bound on $\operatorname{Im} F$. But it is not necessarily more reasonable to say $|F|$ is bounded and therefore $\operatorname{Re} F \to 0$ than that $\operatorname{Re} F$ is finite at resonance, which implies $|F|$ is unbounded. All in all, then, these unitarity limitations must be taken with at least a small grain of salt [68].

In any case, for one reason or another, one may try to adopt the optimistic view that only the two-pion intermediate state is important. This, of course, restricts the discussion to the isotopic vector form factors; the scalar ones will be discussed later.

5. Analytically, the two-pion contribution to the imaginary parts of the form factors is completely given by equation (3.14), where the two matrix elements

$$\langle q_1\sigma_1,\, q_2\sigma_2^{(+)}|j_\mu(0)|0\rangle$$

and

$$\langle p'|\bar{j}_N(0)v_{\bar{p}}|q_1\sigma_1 q_2\sigma_2^{(+)}\rangle$$

are treated exactly and not replaced by perturbation theory. The corresponding diagram representation Fig. III.3(b) gives a pictorial idea of what is involved in calculating this contribution. As the picture indicates, the desired contribution will involve the amplitudes for the processes

$$\gamma \to \pi + \pi$$

and

$$\pi + \pi \to N + \bar{N}.$$

The first of these is the electromagnetic form factor of the *pion*; to evaluate this one could pursue the same type of attack that is being attempted on the nucleon form factors.

Define, to be specific, the pion form factor by

$$\langle q_1\sigma_1, q_2\sigma_2^{(-)}|j_\mu(0)|0\rangle$$
$$= \frac{-i}{\sqrt{(4\omega_1\omega_2)}}(q_1-q_2)_\mu(\delta_{\sigma_1 1}\delta_{\sigma_2 2}-\delta_{\sigma_1 2}\delta_{\sigma_2 1})F_\pi((q_1+q_2)^2). \qquad (3.18)$$

This is the same form that was used in the simplified discussion of the unitarity limitations imposed on the nucleon–antinucleon state, when the nucleons were taken to be spinless. It is perhaps worthwhile to indicate how invariance arguments show this form to be the correct one.

The matrix element $\langle q_1\sigma_1, q_2\sigma_2^{(-)}|j_\mu(0)|0\rangle$ is a Lorentz vector, and depends only on the 4-vectors q_1 and q_2. It is therefore a linear combination of (q_1+q_2), and (q_1-q_2). If $\nabla_\mu j_\mu = 0$ is imposed, the combination (q_1+q_2) is clearly impossible. From the two vectors one can form three scalars, and with the two mass conditions $q_1^2 = q_2^2 = m_\pi^2$ only one independent scalar remains, which may be taken to be $(q_1+q_2)^2$. As far as the isotopic dependence is concerned, it has already been shown that the two pions must be in a $T = 1$ state; hence the factor

$$\delta_{\sigma_1 1}\delta_{\sigma_2 2}-\delta_{\sigma_1 2}\delta_{\sigma_2 1}.$$

The remaining factors of $-i/\sqrt{(4\omega_1\omega_2)}$ are put in explicitly so that $F_\pi(0) = e$, the physical meson charge.

One may then write a dispersion relation for F_π, and derive an expression analogous to equation (3.9) for Im F_π, which one may attempt to evaluate in some approximation. Now the approximation which is being used for the nucleon form factor includes only the intermediate state of the lowest mass. It therefore seems reasonable to try the same approximation for the pion form factor. This intermediate state is just the two-pion state. Thus, in this approximation, one has exactly the situation which was used as an example to illustrate the use of the unitarity conditions in limiting the nucleon–antinucleon contributions to the imaginary part of the nucleon form factors; it is therefore possible to write immediately, to the accuracy of keeping just the two-pion state,

$$\operatorname{Im} F_\pi(q'^2) = F_\pi^*(q'^2) \sin \delta e^{i\delta} \tag{3.19}$$

where δ is the P-wave $\pi\pi$ scattering phase shift.

One comment is worth making here before proceeding. Equation (3.19), together with the fact that Im F_π is of course a real number, implies that F_π has the phase δ. Now equation (3.19) is just an approximation, so in general this statement is not exact; however (3.19) is correct for $q'^2 \leqslant 16m_\pi^2$ (below threshold for the next possible state, that of four pions), so in the region $4m_\pi^2 \leqslant q'^2 \leqslant 16m_\pi^2$ it is in fact a rigorous result that the phase of F_π is δ.

Coupling (3.19) with the dispersion relation for the pion form factor gives the equation

$$F_\pi(q^2) = e + \frac{q^2}{\pi} \int\limits_{4m_\pi^2}^{\infty} \frac{\tan \delta \operatorname{Re} F_\pi(q'^2)}{q'^2(q'^2 - q^2 - i\epsilon)}\, dq'^2.$$

This equation may in fact be solved exactly for F_π in terms of δ [69]. In order to minimize the algebra while explicitly demonstrating the method of solution it is convenient to work with the unsubtracted form of the dispersion relation. Then the equation is

$$F_\pi(x) = \frac{1}{\pi} \int\limits_{x_0}^{\infty} \frac{\tan \delta(x') \operatorname{Re} F_\pi(x')}{x' - x - i\epsilon}\, dx'$$

with the restriction $F_\pi(0) = e$. Define

$$F_\pi(z) = \frac{1}{\pi} \int\limits_{x_0}^{\infty} \frac{\tan \delta(x') \operatorname{Re} F_\pi(x')}{x' - z}\, dx';$$

thus $F_\pi(z)$ is the analytic continuation of $F_\pi(x)$ into the complex plane. Clearly if

$$F_\pi(x)_\pm \equiv \lim_{z \to x \pm i\epsilon} F_\pi(z)$$

then

$$F_\pi(x) = F_\pi(x)_+;$$

also

$$\text{Re } F_\pi(x)_+ = \text{Re } F_\pi(x)_- = \text{Re } F_\pi(x).$$

Now, assuming again that δ is real, one can write as before

$$\text{Im } F_\pi(x)_\pm = \pm \tan \delta(x) \text{ Re } F_\pi(x).$$

Thus

$$F_\pi(x)_\pm = (1 \pm i \tan \delta(x)) \text{ Re } F_\pi(x),$$

so that

$$\frac{F_\pi(x)_+}{F_\pi(x)_-} = \frac{1+i \tan \delta}{1-i \tan \delta}.$$

Now define

$$L(z) = \log F_\pi(z).$$

Then $L(z)$ is analytic, since $F_\pi(z)$ is (except that $L(z)$ has a branch cut on the positive real axis from x_0 to ∞), provided $F_\pi(z)$ has no zeros. The discontinuity across this branch cut is

$$L_+(x) - L_-(x) = \log \frac{F_\pi(x)_+}{F_\pi(x)_-} = 2i\,\delta(x).$$

Then, using a subtracted dispersion relation for $L(z)$, assuming $L(z)/z \to 0$ as $z \to \infty$,

$$L_+(x) = L(0) + \frac{x}{\pi} \int_{x_0}^{\infty} \frac{\delta(x')}{x'(x'-x-i\epsilon)}\, dx',$$

or, finally, replacing x by q^2 again,

$$F_\pi(q^2) = e \exp \frac{q^2}{\pi} \int_{4m_\pi^2}^{\infty} \frac{\delta(\sqrt{q'^2})}{q'^2(q'^2-q^2-i\epsilon)}\, dq'^2$$

since

$$e^{L(0)} = F(0) = e.$$

This same result would not be much more difficult to obtain even if the subtracted form of the dispersion relation for F_π were retained. F_π could consequently be considered known, if the P-wave $\pi\pi$ phase shift were known at all energies. What can be said about this phase shift will be discussed later.

6. To complete the calculation of the two-pion contribution to the Im $F_{1,2}^{s,v}$ s, the annihilation amplitude for the reaction

$$\pi+\pi\rightarrow N+\bar{N}$$

is required. This amplitude is, analytically, the matrix element

$$\langle p'|\bar{j}_N(0)v_{\bar{p}}|q\sigma_1,\, q_2\sigma_2^{(+)}\rangle.$$

By the usual invariance arguments, this may be expressed in terms of four unknown scalar functions of the two independent scalar variables which can be formed from the three vectors p', q_1 and q_2, viz:

$$\begin{aligned}\langle p'|\bar{j}_N(0)v_{\bar{p}}|q_1\sigma_1,\, q_2\sigma_2^{(+)}\rangle\\ &= \frac{1}{\sqrt{(8E_{p'}\omega_1\omega_2)}}\left(\bar{u}_{p'}\middle|\left(A^+\,\delta_{\sigma_1\sigma_2}+A^-\frac{[\tau_{\sigma_1},\,\tau_{\sigma_2}]}{2}\right)\right.\\ &\qquad\left.+\left(B^+\delta_{\sigma_1\sigma_2}+B^-\frac{[\tau_{\sigma_1},\,\tau_{\sigma_2}]}{2}\right)\left(\frac{\not{q}_1+\not{q}_2}{2}\right)\middle|v_{\bar{p}}\right).\end{aligned}$$

Here $A^{\pm}$ and $B^{\pm}$ are functions of, for example, $q^2 = (q_1+q_2)^2 = 4K^2$ and $(p'-q_2)^2 \equiv W^2$. The use of this expression, together with the definition of the pion form factor from equation (3.18) allows the two-pion contribution to the Im F's to be given explicitly in terms of $A^{\pm}$, $B^{\pm}$ and F_π by equation (3.14). The algebra necessary to accomplish this is identical with that used in the derivation of the perturbation theory from equation (3.14) and will not be repeated here. The result is [53]

$$\begin{aligned}\operatorname{Im} F_1^v(q^2) &= [M\alpha(q^2)+\beta_1(q^2)+M^2\beta_2(q^2)]\overset{*}{F}_\pi(q^2)\\ &\equiv J_1(q^2)\overset{*}{F}_\pi(q^2),\\ \operatorname{Im} F_2^v(q^2) &= [\alpha(q^2)+M\beta_2(q^2)]\overset{*}{F}_\pi(q^2)\\ &\equiv J_2(q^2)\overset{*}{F}_\pi(q^2),\end{aligned}$$

where

$$\alpha(q^2) = -\frac{1}{4\pi^2}\int d^4Q\, \delta((K+Q)^2-m_\pi^2)\, \delta((K-Q)^2-m_\pi^2)$$
$$P\,.\,Q/P^2A^-(W^2, q^2),$$
$$\beta_1(q^2) = -\frac{1}{4\pi^2}\int d^4Q\, \delta((K+Q)^2-m_\pi^2)\, \delta((K-Q)^2-m_\pi^2)$$
$$((P^2Q^2-(P\,.\,Q)^2)/2P^2)B^-(W^2, q^2),$$
$$\beta_2(q^2) = -\frac{1}{4\pi^2}\int d^4Q\, \delta((K+Q)^2-m_\pi^2)\, \delta((K-Q)^2-m_\pi^2)$$
$$((3(P\,.\,Q)^2-P^2Q^2)/2P^4)B^-(W^2, q^2).$$

Here P, Q, K are defined as before, namely:

$$P = \tfrac{1}{2}(p'-\bar{p}), \qquad Q = \tfrac{1}{2}(q_1-q_2),$$
$$K = \tfrac{1}{2}(q_1+q_2) = \tfrac{1}{2}(p'+\bar{p}) = q/2,$$

so $W^2 = (P+Q)^2$.

One approach to the evaluation of $J_1(q^2)$ and $J_2(q^2)$ which has been attempted is based on the following observation. The annihilation amplitude in question, in terms of which $A^{\pm}$, $B^{\pm}$ and hence J_1 and J_2 are defined, may be re-expressed as

$$\langle p'|\bar{j}_N(0)v_{\bar{p}}|q_1\sigma_1,\, q_2\sigma_2^{(+)}\rangle = \langle p',\, -q_2\sigma_2^{(-)}|\bar{j}_N(0)v_{\bar{p}}|q_1\sigma_1\rangle.$$

The right hand side of this equation is nothing more than the matrix element for pion–nucleon scattering, from an initial state consisting of a nucleon $-\bar{p}$ and a meson $q_1\sigma_1$ to a final state of a nucleon p' and a meson $-q_2\sigma_2$. Since the final meson, for example, has negative energy, this is not a physically observable scattering process. Nevertheless, it is in principle possible, using dispersion relations for meson–nucleon scattering, to extrapolate the four functions $A^{\pm}$, $B^{\pm}$ from their measured values in the physical region for meson-nucleon scattering to the range of variables required in the present calculation. This extrapolation has not, however, yielded very good results in practice, as there are a number of ambiguities and divergences connected with the method [53]. This approach will therefore not be pursued further here.

More fruitful results can be obtained on the basis of making another assumption, which is that the functions J_1 and J_2 satisfy dispersion relations in q^2. This assumption is the same as the statement that each partial wave amplitude in a scattering process satisfies a dispersion relation. It is impossible to justify this assumption rigorously, as it was impossible to justify the dispersion relations for the form factors themselves. However, the assumption may be made quite plausible through the Mandelstam representation [70]. The details of the use of Mandelstam's representation to justify, at least in part, the necessary properties of J_1 and J_2 is too complicated to be entered into here—since there is no rigorous proof anyway one might as well just accept the assumption in the form most convenient for present purposes [71].

Therefore, the next move will be to investigate the consequences of the statement that J_1 and J_2 satisfy dispersion relations; namely

$$J_1(q^2) = \frac{1}{\pi}\int_{-\infty}^{\infty}\frac{\operatorname{Im} J_1(q'^2)}{q'^2-q^2-i\epsilon}\,dq'^2,$$

and similarly for J_2.

To proceed from this point it is easiest to return to the interpretation of J_1 and J_2 in terms of the annihilation process $\pi+\pi\rightarrow N+\bar{N}$; thus they may be written pictorially as in Fig. III.5(a).

The contribution of the two-pion intermediate state, shown in Fig. III.5(b) is as before

$$\begin{aligned}\operatorname{Im} J_1 &= J_1^* \sin\delta e^{i\delta}\\ \operatorname{Im} J_2 &= J_2^* \sin\delta e^{i\delta}\end{aligned} \tag{3.20}$$

where δ is again the $J = 1$ $T = 1$ pion–pion scattering phase shift [72]. It is convenient to separate this term out explicitly.

The contribution to the Im J's not included by the two-pion intermediate state can be formally added in by writing

$$\operatorname{Im} J_{1,2} = J_{1,2}^* \sin\delta e^{i\delta} + \operatorname{Im} J'_{1,2}. \tag{3.21}$$

For example, as can easily be seen by inspection of Fig. III.5(b), the two-pion state does not include the perturbation contribution (order g^2, Fig. III.5(c)) to $\text{Im}\, J$; it will therefore be contained in $\text{Im}\, J'$.

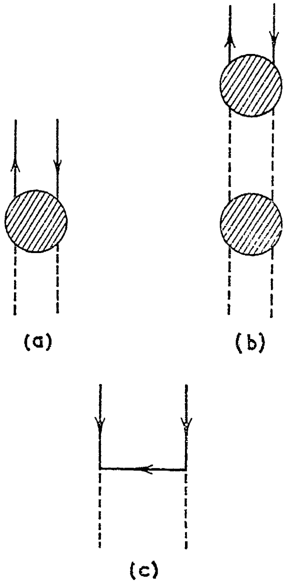

FIG. III.5. (a) shows symbolically the amplitudes J_1 and J_2; (b) shows the two-pion contribution to $\text{Im}\, J_1$, and $\text{Im}\, J_2$, and (c) shows the perturbation theory Feynman graph contributing to J_1 and J_2.

7. Now the development may be completed as follows. Recall that the pion form factor satisfied a very similar relationship,

$$\text{Im}\, F_\pi = F_\pi^* \sin \delta e^{i\delta}, \tag{3.22}$$

within the framework of the approximations used in dealing with it. If both F_π and J_1, say, satisfy dispersion relations, so does [73] J_1/F_π.

Now $\text{Im}\, J'_{1,2}$ receives contributions from diagrams similar to Fig. III.5(b), but with the two-pion intermediate state replaced by any other allowed state. The lightest of these is four pions, with a threshold at $16m_\pi^2$, so that $\text{Im}\, J'_{1,2}$ does not vanish above $q^2 = 16m_\pi^2$. In addition, it can be shown from the Mandelstam representation that $\text{Im}\, J'_{1,2}$ is non-zero for

$q^2 \leqslant 4m_\pi^2(1-m_\pi^2/4M^2)$. In the region $0 \leqslant q^2 \leqslant 4m_\pi^2(1-m_\pi^2/4M^2)$, $\text{Im}\, J'_{1,2}$ is determined solely by the perturbation diagram, Fig. III.5(c). These results are derived in Appendix B.

In the region $4m_\pi^2 \leqslant q^2 \leqslant 16m_\pi^2$, then, $J^*_{1,2} \sin\delta e^{i\delta}$ is itself real. If it is assumed to be real for all q^2, then

$$\text{Im}\left(\frac{J_{1,2}}{F_\pi}\right) = \frac{\text{Re}\, F_\pi}{|F_\pi|^2} \frac{\text{Im}\, J'_{1,2}}{\cos^2\delta} = \frac{\text{Im}\, J'_{1,2}}{\text{Re}\, F_\pi}.$$

Thus one obtains

$$J_{1,2}(q^2) = F_\pi(q^2)\frac{1}{\pi}\int \frac{dq'^2}{q'^2-q^2-i\epsilon} \frac{\text{Im}\, J'_{1,2}(q'^2)}{\text{Re}\, F_\pi(q'^2)}.$$

The integration here, of course, runs over the region of q'^2 for which $\text{Im}\, J'_{1,2}(q'^2)$ does not vanish. As yet this expression is still too 'exact' to be useful, since, $\text{Im}\, J'_{1,2}$ contains everything.

A not too far fetched approximation now suggests itself. Namely one might try to retain in $\text{Im}\, J'_{1,2}(q'^2)$ only the contribution of order g^2, and replace $\text{Re}\, F_\pi(q'^2)$ by its lowest order value, namely e. The best argument for the validity of this approximation is that attempts have been made to include more details of $\text{Im}\, J'_{1,2}$ and $\text{Re}\, F_\pi$ and these refinements do not produce significant changes, at least for J_2. With this approximation, then, plus the observation that

$$\frac{1}{\pi}\int \frac{\text{Im}\, J_{1,2}(q'^2)_{\text{BA}}}{q'^2-q^2-i\epsilon}\, dq'^2 = J_{1,2}(q^2)_{\text{BA}}$$

(the subscript BA means Born Approximation), the final answer is obtained:

$$J_{1,2}(q^2) = \frac{1}{e} F_\pi(q^2) J_{1,2}(q^2)_{\text{BA}}.$$

Inserting this back in the expressions for the imaginary parts of the nucleon form factors yields, finally:

$$\text{Im}\, F^v_{1,2}(q^2) = \frac{1}{e^2}|F_\pi(q^2)|^2\, \text{Im}\, F^v_{1,2}(q^2)_{\text{BA}}. \tag{3.23}$$

The Born Approximation results for $\text{Im}\, F_1^v$ and $\text{Im}\, F_2^v$ were derived much earlier (see equations (3.16) [74].

It remains, then, to see how well this approximation agrees with experiment. The results obtained depend on the P-wave $\pi\pi$ phase shift through F_π, and nothing is yet known experimentally about this phase shift. One might start therefore, by asking what kind of a phase shift is necessary to fit the experimental results. Frazer and Fulco [71] have used a two parameter resonance formula for the pion–pion scattering, and have determined values for the position and width of the resonance which give agreement with the experimental isotopic vector moment structure as well as with the static moment value since they use the unsubtracted form for the calculation of $F_2^v(q^2)$ in equation (3.16). Their results are shown in Figs. III.6, 7 and 8. They find that if δ goes through 90° at a value q'^2 of the order of $12m_\pi^2$ to $16m_\pi^2$, in a fairly sharp resonance, agreement can be achieved. It is significant that

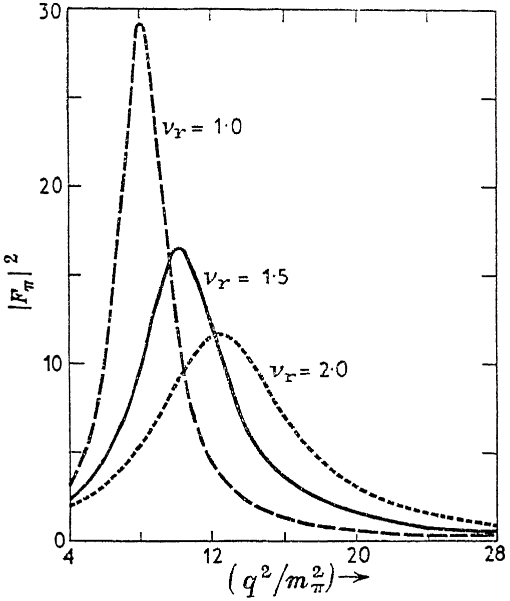

FIG. III.6. Pion form factors resulting from various choices of the $\pi\pi$ resonance in the $T = 1\ J = 1$ state. (The graph is taken from Frazer and Fulco, [71].)

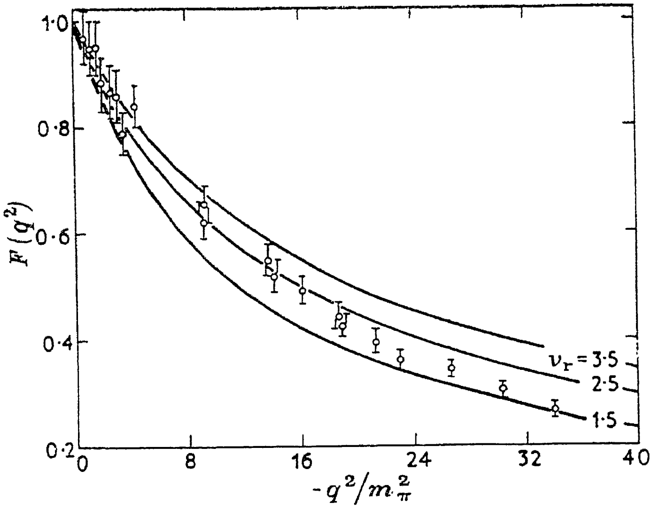

FIG. III.7. A comparison of the proton isotopic vector form factors (assuming $F_1^p/F_1^p(0) = F_2^p/F_2^p(0)$) resulting from various choices of the $\pi\pi$ resonance with experiment. The comparison is probably meaningful only for small values of q^2. (Taken from Frazer and Fulco, [71].)

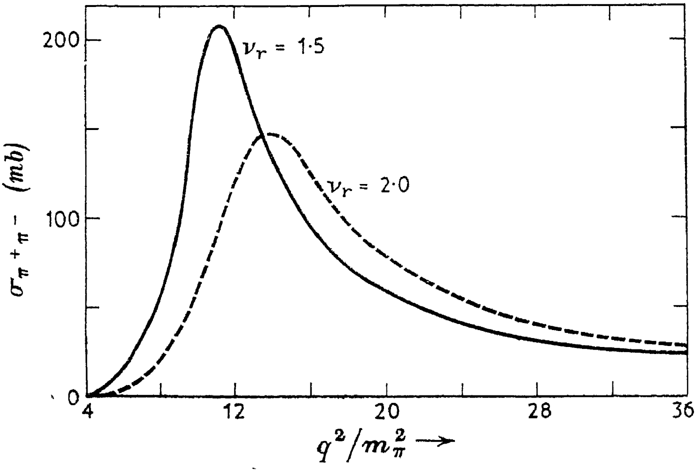

FIG. III.8. Two choices for the $T = 1$ $J = 1\pi\pi$ cross-section used in fitting the nucleon structure. (Taken from Frazer and Fulco, [71].)

they are unable to obtain agreement without such a resonance; its existence, then, may be said to be a prediction of the dispersions approach *within the approximations which have been outlined above.*

It is perhaps even more significant that if a subtracted dispersion relation is used for the moment, which should tend to improve the validity of the two-pion approximation, a resonance is still necessary; in fact, even if two subtractions are made a fit to the experiments is impossible without appreciable $\pi\pi$ scattering [75].

The basic question is then reduced to whether or not experimental or theoretical information about δ implies the presence of this resonance. In retrospect, what has been achieved by the analysis of the form factors is a relation between two experiments, the nucleon structure and $\pi\pi$ scattering. If eventually $\pi\pi$ scattering experiments are not consistent with the nucleon structure, one will have to decide between accepting the assumptions involved in the present calculation, and dropping quantum electrodynamics or meson theory entirely.

At present, experimental information on $\pi\pi$ scattering is non-existent though some experiments have been proposed [76]. Various theoretical calculations have been made or are in progress [77]. As an example of the kind of agreement which can be obtained through some of these theoretical estimates of $\pi\pi$ scattering, together with the approximations outlined above, Figs. III.9 and III.10 are shown. The theoretical curves here are obtained on the basis of equations (3.23) combined with δ obtained from a determinantal calculation, assuming a point four-pion interaction of the form $\lambda(\sum_{i=1}^{3}\varphi_i^2)^2$. The agreement seems nice, but is deceptive as the curves have been normalized to one at $q^2 = 0$. The actual zero value may be expressed by saying that the theoretically predicted isotopic vector anomalous magnetic moment is 0.8 magnetons, instead of the experimental 1·85 magnetons.

Note that the neglect of heavy mass intermediate states, which affect the Im F_2's only at large q'^2, are more likely to influence the value of $F_2^v(0)$ than the shape of $F_2^v(q^2)$. This may be seen by returning to the subtracted dispersion relation (3.6), namely

$$F_2^v(q^2) = F_2^v(0)+\frac{q^2}{\pi}\int\frac{\text{Im } F_2^v(q'^2)}{q'^2(q'^2-q^2-i\epsilon)}\,dq'^2.$$

The integrand is now weighted by an extra power of $(q'^2)^{-1}$

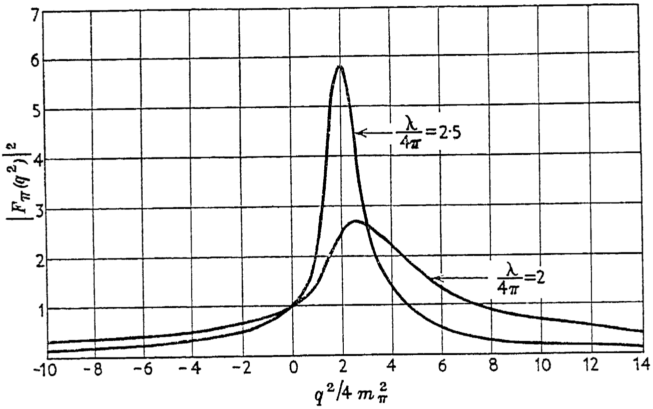

FIG. III.9. Pion form factors obtained from an assumed pion point interaction $\lambda(\varphi\,.\,\varphi)^2$. (Taken from Baker and Zachariasen, [77].)

against large q'^2, but $F_2^v(0)$ cannot be predicted, and must be taken from experiment:

$$F_2^v(0) = 1{\cdot}85\frac{e}{2M}.$$

An optimist would be satisfied with the prediction of the shape, and say that of course inclusion of heavy states might allow the evaluation of the moment as well by going back to an unsubtracted relation. A pessimist will, on the other hand, insist that it is a shortcoming of the present calculation that the predicted moment misses by a factor of 2.

With regard to the charge isovector form factor theoretical predictions are again made from equations (3.23). However, because of the lack of symmetry between the experimental charge structure of the neutron and proton, it is evident that there are sizable scalar contributions to the observed charge structures. Therefore experimental information on F_1^v is largely lacking, so comparison with the theoretical predictions is difficult. The best information on the neutron charge structure, as discussed in Chapter II, is that the charge radius is ~zero, indicating that for small q^2 the proton charge structure coincides with the isovector charge structure. This is in agreement with the results of Frazer and Fulco [71].

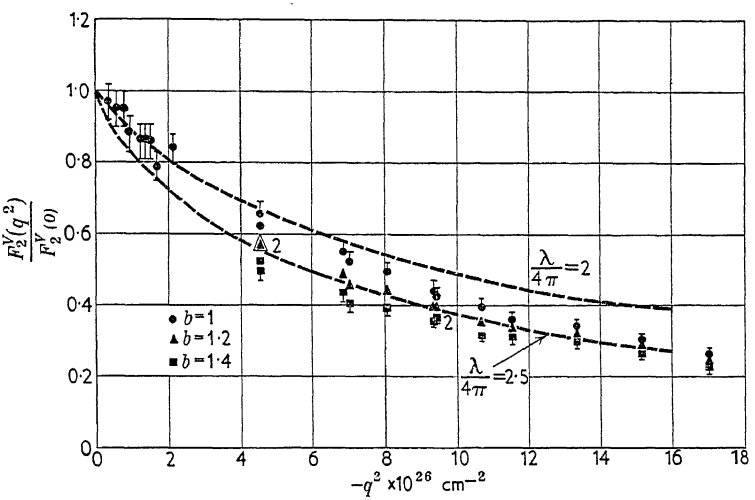

FIG. III.10. The predictions of the $\lambda(\varphi \, . \, \varphi)^2$ π-π coupling for the nucleon isotopic vector form factors, superimposed on the experimental results from Fig. II.5. (Taken from Baker and Zachariasen, [77].)

This completes all there is to say at present about the isotopic vector form factors. To add to this a discussion of the theoretical results which exist on the scalar form factors is simple owing to their scarcity. If the unitarity argument is accepted, it seems proper to rule out the nucleon–antinucleon intermediate state as providing much of the scalar form factors. If this philosophy is extended to exclude all heavy states, one is presumably left with the three-pion state as the culprit. It is so difficult to even estimate the size or properties of what this state gives that the scalar form factor problem remains totally un-understood.

In order that this state explain the observed properties, it must provide sizable charge effects but almost no contribution to the moments. Some crude estimates of the three-pion state contributions, based on perturbation theory [78] and on the static meson theory [79] exist, but none have this feature. Generally, a scalar static moment emerges which is of the order of 50 times too large.

Moreover, it is disturbing to have to call upon a three-pion intermediate state to play a major role in the charge structure analysis. One wonders then whether it is a valid approximation to neglect, say, the four-pion state as has been done on the basis of the threshold arguments given in the above dispersion approach to the isovector form factors.

To conclude, then, theoretical understanding of the form factors on the basis of meson field theory is fairly meagre; totally so for the scalar form factors, less so for the vector ones. Predictions, on the basis of certain approximations, can be made for the vector form factors; these then agree or disagree with experiment depending on whether or not there is an appropriate resonance in the $\pi\pi$ scattering.

CHAPTER IV

VALIDITY OF QUANTUM ELECTRODYNAMICS AND EFFECT ON NUCLEON STRUCTURE INTERPRETATION

Up to this point the entire discussion has proceeded on the tacit assumption that electron–proton scattering, and the other experiments mentioned in Chapter II, all are explicable in terms of nucleon electromagnetic structure. In Chapter I this structure was defined; in Chapter II experimental information about it was discussed; in Chapter III theoretical predictions about it were made. As was explained in Chapter III, it remains a question whether or not the presently fashionable dispersion theoretic calculations actually offer the possibility of a *quantitative* comparison between theory and experiment. This question can only be answered by reliable calculations of the effects of higher mass intermediate states. At any rate the dispersion approach does have the virtue of producing a result directly susceptible of experimental test: the requirement of a sharp resonance in the $J = 1$ $T = 1$ state of pion–pion scattering. Evidence of such a resonance is now being sought. However even if one is found with the correct energy and width to fit F_2^v, the charge radius of the neutron still demands a theoretical understanding which at present is totally lacking.

Since there exists then the possibility that pion physics as now known [80] may not be able to account for the proton and neutron structures inferred from the experimental data, one is led to inquire into the possibility of other interpretations of these observations. Consider the electron–proton scattering experiments; they have yielded the most complete, accurate data and their analysis is free of all nuclear physics complications and pion interaction models. The *only* alternative to the interpretation of electron–proton scattering in terms of proton structure is in terms of a modification in the present theory of quantum electrodynamics of the electron and the photon. A finite extension of the electron's charge distribution for example would show itself by replacing the proton form factors in the Rosenbluth formula (I.10) by products of an electron times a proton form factor [81].

There would be two direct and significant consequences of accounting for the observed structure wholly or largely by electron size:

(1) In order to achieve agreement with the isovector moment distribution it was necessary in (3.19) and (3.23) to introduce a fairly sharp $\pi\pi$ resonance for a total energy of the two pions $\approx 3{\cdot}5 m_\pi$ in their centre of mass. This was required in order to enhance the absorptive amplitude Im $F_2^v(q^2)$ for small

values of q^2 as seen in Fig. III.6. This in turn led to a spread out distribution, which may be made evident by re-expressing (1.11) with (3.5):

$$e_2^v(r) = \frac{1}{4\pi^2}\int\limits_{4m_\pi^2}^{\infty} dq'^2\,\mathrm{Im}\,F_2^v(q'^2)\,\frac{e^{-\sqrt{(q'^2)}r}}{r}.$$

Therefore it follows that, by attributing much if not all of the observed structure to the electron, one obviates the requirement of the resonant pion–pion interaction.

(2) The very puzzling difference between the proton and neutron charge sizes would disappear.

What direct evidence is there then for finite electron size or for modifications of any sort in the theory of quantum electrodynamics? So far, none; indeed it is supported by very precise measurements [82]. The magnetic moment of the electron including radiative corrections is accurate to better than one part in 10^{-5}:

$$g_{\text{exptl}} = 2(1{\cdot}001162 \pm 4\times 10^{-6})$$

$$g_{\text{theor}} = 2\left(1+\frac{\alpha}{2\pi} - 0{\cdot}328\,\frac{\alpha^2}{\pi^2}\right) = 2(1{\cdot}0011596) \qquad (4.1)$$

and calculations and observations on the Lamb shift are in agreement with an accuracy of $\approx 0{\cdot}2$ megacycles [83].

These however are low energy experiments and probe possible electron size or quantum electrodynamic modifications only with a very crude yardstick whose unit of measure is the electron compton wavelength: $\hbar/mc \approx 3{\cdot}8\times 10^{-11}$ cm. In order to test the validity of the theory down to distances of less than 10^{-13} cm, such as enter into the nucleon structure analysis, large momentum transfer experiments are required. They contain a small invariant length (corresponding to $\hbar$ divided by the invariant 4-momentum transfer) against which to measure the small distance behaviour. In fact, at present, it is the electron–proton scattering experiments themselves which supply the most severe test of quantum electrodynamics at small distances since they show that modifications are limited to distances of $\lesssim \frac{1}{3}\times 10^{-13}$ cm (corresponding to a root mean square radius of $0{\cdot}8\times 10^{-13}$ cm which is conventionally quoted as the proton 'size' on the assumption of a point electron) [84].

How then is it possible to extend the limits of one's knowledge of quantum electrodynamics and to decide unambigously if the 'size' deduced from electron–proton scattering experiments is in fact the structure of the proton or if it is an indication of deviations from the theory of photons and electrons as now formulated?

One possibility mentioned earlier is that of using the electron–proton scattering itself as a consistency check on the theory by performing three measurements at different energies and angles corresponding to the same q^2. As remarked by Feynman [85] it would no longer necessarily be the case that only two functions, $F_1(q^2)$ and $F_2(q^2)$ summarize the electron–proton scattering data if there are contributions to their interaction corresponding to the exchange of other than vector photons, or if electrons and protons can virtually combine to form a boson. To this may be added the observation that the same conclusion would also follow if the electron were to develop an anomalous moment structure for large q^2.

The Rosenbluth formula may be generalized to allow for such a possibility in which case (1.10) becomes

$$\frac{d\sigma}{d\Omega} = \frac{1}{4(4\pi)^2E_0^2}\frac{\cos^2(\frac{1}{2}\theta)}{\sin^4(\frac{1}{2}\theta)}\frac{1}{1+2\dfrac{E_0}{M}\sin^2(\frac{1}{2}\theta)}$$

$$\times\biggl\{[f_1+2mf_2]^2\biggl[F_1^2-\frac{q^2}{4M^2}(2\{F_1+2MF_2\}^2\tan^2(\tfrac{1}{2}\theta)+\{2MF_2\}^2)\biggr]$$

$$+2mf_2\biggl[-2f_1-\frac{q^2}{4m^2}\,2mf_2\biggr]\biggl[(F_1^2-q^2F_2^2)\sin^2(\tfrac{1}{2}\theta)$$

$$+2MF_2\tan^2(\tfrac{1}{2}\theta)\left(\frac{q^2}{4M^2}\right)\biggl(2F_1+2MF_2\biggl[1+\frac{q^2}{4M^2}\biggr]\biggr)\biggr]\biggr\},$$

where f_1 and f_2 are form factors for the electron and m has been put equal to zero everywhere except for the one large term indicated [86]. Since this formula contains three different angular terms, for $2mf_2 \neq 0$, it allows a more general analysis of the observations in terms of three invariant functions of q^2.

It is therefore of great interest to establish whether or not the scattering data can be completely summarized in terms of only two functions by constructing three (or more) experimental ratios of the scattering at fixed q^2. If not, one may attribute it to an anomalous electron–proton interaction such as discussed by Feynman or to an anomalous electron moment f_2 as indicated above. This latter possibility is unlikely to show up in the scattering experiments however, because the measurements of the electron g value, (4.1), agree to better than one part in 10^5 with electrodynamic predictions. Therefore, unless the anomalous moment f_2 peaks up for large space like q^2, it follows that $f_2 < 10^{-5}\, e/2m$ and $(2mf_2)^2 q^2/4m^2 < 10^{-4} e^2$ for 500 MeV electron energies.

In order to test for electron form factors or for other possible types of breakdown in quantum electrodynamics it is necessary to turn to different experiments. It is conceivable for example that the photon propagator has to be modified at small distances, indicating a departure from Coulomb's law. This would mean a change in the Feynman propagator for a photon of four momentum q^2 [87]:

$$\frac{1}{q^2} \rightarrow \frac{C(q^2)}{q^2} = \frac{1}{q^2}\,(1 \pm d^2 q^2 + \ldots). \tag{4.2}$$

Another possibility is to alter the electron–positron propagator at small distances, or large momenta, in a similar fashion; there must in fact be a connection between electron size, or form factors, and alterations in the behaviour of the propagator of the electron–positron field in order to maintain a differential current conservation law [88].

Such modifications may be studied directly by electron–electron, electron–positron or by photon–electron (compton) scattering. The Feynman diagram, Fig. IV.1, for electron–electron scattering shows that it probes electron size and the photon propagator as a function of the momentum transfer. The diagrams for compton scattering, Fig. IV.2, show that the virtual particle in this process is the electron, so that what is probed here is the electron propagator at small distances.

For these processes to probe the structure of quantum electrodynamics at distances $\leqslant 10^{-13}$ cm it is necessary to achieve momentum transfers of ≈ 200 MeV/c. In experimental arrangements scattering from target electrons most of the energy is in the centre-of-mass motion and the momentum transfer is limited by $\{2mE_0\}^{\frac{1}{2}}$. Therefore a 40 BeV accelerator is required in order to realize the necessary momentum transfer [89]. As such energies are not now available in the laboratory one has two choices—either to increase the energy available in the centre of mass by replacing the target with a colliding beam, or to 'embed' the interesting Feynman graphs

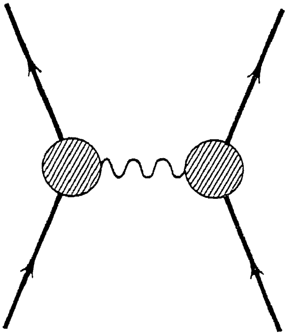

FIG. IV.1. Diagram representing the single photon exchange contribution to electron–electron scattering.

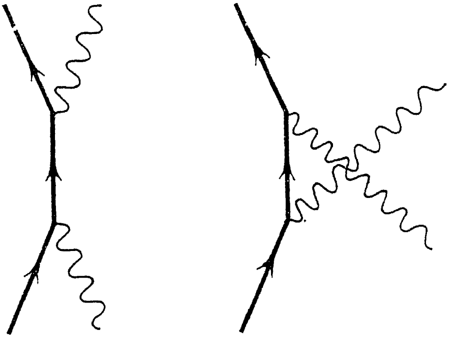

FIG. IV.2. Feynman graphs for compton scattering: $\gamma+e \rightarrow \gamma+e$.

of Fig. IV.1,2 in more complicated processes which avoid the centre-of-mass problem by using heavy target particles.

The first of these alternatives is now being pursued at Stanford for electron–electron scattering [90]. Two beams of 500 MeV electrons are formed in intersecting storage rings and their collisions studied by counting pairs of electrons emerging back to back in coincidence at various scattering angles. A detailed analysis of the radiative corrections to the Möller cross-section has been carried out by Tsai [91] for experimental parameters of interest here. If there is any disagreement between theory and experiment, it will have to be attributed to finite electron size or to modifications of the photon propagator. Since momentum transfers of up to 700 MeV/c will be realized, this experiment, if successful to a 10% accuracy, will be an enormously high resolution probe to distances of 10^{-14} cm. At present this project is in the construction stage and it is hoped that data taking will start during 1961.

The second alternative of achieving large 4-momentum transfers at present laboratory energies by using a heavy target particle is also being pursued [82], [92]. In particular, Richter has measured large angle production of electron–positron pairs by photons incident on hydrogen; further experiments aiming for greater precision and higher energies are now in progress. These serve as probes of quantum electrodynamics in the following way. If quantum electrodynamics is valid it is possible to summarize the proton's structure in terms of measured $F_1(q^2)$ and $F_2(q^2)$. This is seen in the Feynman diagrams for pair production, Fig. IV.3. These graphs show that only the electromagnetic vertex of a physical proton appears. Therefore any disagreement between theory and experiment can be interpreted only in terms of modifications in quantum electrodynamics, and a comparison between theory and experiment yields new information on the small distance behaviour of the virtual intermediate electron–positron line. The present agreement between theory and experiment indicates no modification in the electron propagator at distances $\approx 10^{-13}$ cm. Further experimental refinements are anticipated to lower this limit by a factor ≈ 3.

These large angle pair studies provide direct information only on the electron propagator. The photon propagator and electron structure appear together with the proton structure as in the elastic scattering [93].

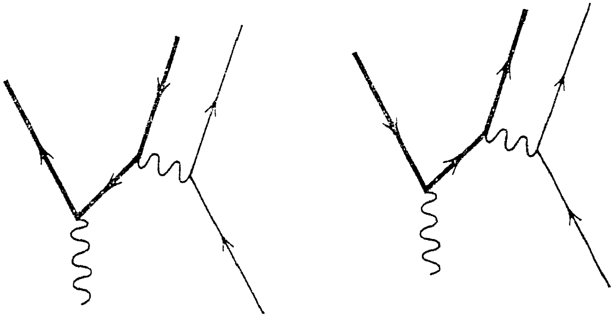

FIG. IV.3. Feynman graphs for pair production: $\gamma + P \rightarrow e + \bar{e} + P$.

In order to investigate electron size and the photon propagator further consider another experimental arrangement in which the pair is produced by an incident electron, i.e. trident production. Fig. IV.4 shows a typical Feynman graph.

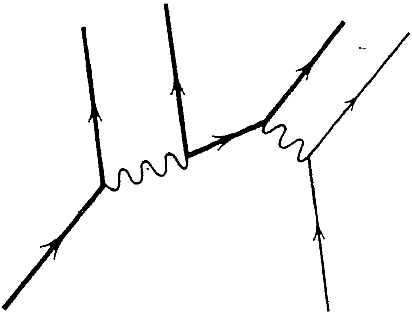

FIG. IV.4. A Feynman graph contributing to trident production: $e + P \rightarrow e + e + \bar{e} + P$.

By tying the photon of Fig. IV.3 on to an incident electron the photon propagator and electron vertex are introduced. It has been shown [94] that the ratio of this to pair production provides a sensitive test of these structures and hence of the interpretation of the electron–proton scattering experiments in terms of proton structure.

In conclusion then three points may be repeated:

(1) It remains for experiment to verify unambiguously the analyses of the electron–proton scattering and of the other experiments discussed in terms of nucleon structure in Chapter II.

(2) It remains for theory to verify that the theoretical approximation scheme is appropriate for a quantitative comparison with experiment.

(3) If (1) and (2) are fulfilled, it remains finally for experiment to verify the $\pi\pi$ resonance in the $J = 1$, $T = 1$ state predicted by the dispersion analysis of the isovector form factors.

APPENDIX A

It is desired to verify the relation used in equation (3.7) or more generally, to prove the identity

$$\langle\beta^{(-)}|0|\alpha p^{(+)}\rangle = \sum_n \delta_{\beta,np}\langle n^{(-)}|0|\alpha^{(+)}\rangle$$
$$-i\int d^4x\langle\beta^{(-)}|(0\bar{\psi}(x))_+|\alpha^{(+)}\rangle(\overleftarrow{-i\not{\nabla}_x-m})\,\frac{u_p}{\sqrt{(2E_p)}}\,e^{-ip.x}. \qquad \text{(A.1)}$$

The notation here needs some explanation: $|\alpha^{(+)}\rangle$ and $\langle\beta^{(-)}|$ are arbitrary Heisenberg states with the indicated boundary conditions; $|\alpha p^{(+)}\rangle$ is a state containing, in addition to whatever is contained in $|\alpha^{(+)}\rangle$, a nucleon of momentum p. 0 is an arbitrary Heisenberg operator, and $\psi(x)$ is the renormalized Heisenberg nucleon field operator. In the first term, the symbol $\delta_{\beta,np}$ is meant to be zero unless the state $|\beta\rangle$ contains the nucleon of momentum p, and if $|\beta\rangle$ does contain the nucleon p, the state $|n\rangle$ is to represent everything in $|\beta\rangle$

other than this nucleon. The first term in equation (A.1), then, represents the possibility of the nucleon p not interacting with anything, but just passing from the initial to the final state as a free particle.

The proof of equation (A.1), which is generally referred to either as the 'contraction rule,' or the 'reduction formula,' is not difficult, and is sketched in what follows [95].

Consider the matrix element $\lim\limits_{x_0 \to -\infty} \langle \beta^{(-)} | (0\bar{\psi}(x))_+ | \alpha^{(+)} \rangle$. Then

$$\lim_{x_0 \to -\infty} \langle \beta^{(-)} | (0\bar{\psi}(x))_+ | \alpha^{(+)} \rangle = \sum_n \langle \beta^{(-)} | 0 | n^{(+)} \rangle \lim_{x_0 \to -\infty} \langle n^{(+)} | \bar{\psi}(x) | \alpha^{(+)} \rangle. \tag{A.2}$$

Now, since $\psi(x) \to \psi_{\text{in}}(x)$ as $x_0 \to -\infty$,

$$\lim_{x_0 \to -\infty} \langle n^{(+)} | \bar{\psi}(x) | \alpha^{(+)} \rangle = \lim_{x_0 \to -\infty} \int \frac{d^3\mathbf{p}}{(2\pi)^3} \frac{1}{\sqrt{(2E_p)}} (\bar{u}_p e^{ip.x} \delta_{n,\alpha p} + \bar{v}_p e^{-ip.x} \delta_{np,\alpha}). \tag{A.3}$$

It should be noted that no factors of Z_2 appear here since ψ is the renormalized field. If (A.3) is substituted into (A.2), and the Fourier transform is inverted, one obtains

$$\langle \beta^{(-)} | 0 | \alpha p^{(+)} \rangle = \lim_{x_0 \to -\infty} \int d^3\mathbf{x} \langle \beta^{(-)} | (0\bar{\psi}(x))_+ | \alpha^{(+)} \rangle \gamma_0 \frac{u_p}{\sqrt{(2E_p)}} e^{-ip.x}. \tag{A.4}$$

Now observe the identity

$$f(x) = -i \int d^4y f(y) (\overrightarrow{i \not{\nabla}_y - m}) K_+(y, x),$$

which holds since the nucleon propagator K_+ satisfies

$$(i\not{\nabla}_y - m) K_+(y, x) = i\delta^4(y - x).$$

A partial integration may be performed in this identity, yielding

$$f(x) = -i \int d^4y f(y) (\overleftarrow{-i\not{\nabla}_y - m}) K_+(y, x) + \int d^3y f(y) \gamma_0 K_+(y, x) \Big|_{y_0 = -\infty}^{y_0 = +\infty} \tag{A.5}$$

Equation (A.5) may now be applied to $\langle\beta^{(-)}|(0\bar{\psi}(x))_+|\alpha^{(+)}\rangle$ in equation (A.4). Using the fact that

$$\int d^3\mathbf{x} K_+(y, x)\gamma_0 \frac{u_p}{\sqrt{(2E_p)}} e^{-ip.x} = \begin{cases} \dfrac{u_p}{\sqrt{(2E_p)}} e^{-ip.y} & y_0 > x_0 \\ 0 & y_0 < x_0 \end{cases}$$

one finds

$$\langle\beta^{(-)}|0|\alpha p^{(+)}\rangle = \lim_{y_0 \to +\infty} \int d^3\mathbf{y} \langle\beta^{(-)}|(0\bar{\psi}(y))_+|\alpha^{(+)}\rangle\gamma_0 \frac{u_p}{\sqrt{(2E_p)}} e^{-ip.y}$$
$$-i\int d^4y \langle\beta^{(-)}|(0\bar{\psi}(y))_+|\alpha^{(+)}\rangle(\overleftarrow{-i\not\nabla_y}-m) \frac{u_p}{\sqrt{(2E_p)}} e^{-ip.y}. \qquad (A.6)$$

The first term in (A.6) may be rewritten as sketched below. Write

$$\lim_{y_0 \to +\infty} \langle\beta^{(-)}|(0\bar{\psi}(y))_+|\alpha^{(+)}\rangle$$
$$= \lim_{y_0 \to +\infty} \sum_n \langle\beta^{(-)}|\bar{\psi}(y)|n^{(-)}\rangle\langle n^{(-)}|0|\alpha^{(+)}\rangle;$$

now $\lim\limits_{y_0 \to +\infty} \bar{\psi}(y) = \bar{\psi}_{\text{out}}(y)$, so that the same algebraic manipulations as were used to arrive at (A.4) from (A.2) may be used to replace the first term in (A.6) by

$$\sum_n \delta_{np,\beta}\langle n^{(-)}|0|\alpha^{(+)}\rangle.$$

This completes the verification of equation (A.1).

APPENDIX B

In this appendix, a more complete discussion of the regions in which Im J' is non-zero will be presented. This is equivalent to discussing the singularities of the annihilation amplitude for the reaction $\pi+\pi \to N+\bar{N}$. It will facilitate the discussion to assume, as has been done before, that nucleons have spin zero. The amplitude for this reaction is then a single scalar function of two variables, which may conveniently be chosen to be

$$s = q^2 = (q_1+q_2)^2$$

and

$$t = (q_1-p_1)^2.$$

Here the two meson 4-momenta are denoted q_1 and q_2; those of the nucleons p_1 and p_2. Thus the amplitude for the annihilation may be written

$$\frac{A(s,t)}{\sqrt{(8E_{p_2}\omega_{q_1}\omega_{q_2})}} = \langle p_2|j_N(0)|q_1q_2{}^{(+)}\rangle. \tag{B.1}$$

In terms of s and t, the angle of scattering in the centre-of-mass system is

$$\cos\theta = \frac{t+s/2-m_\pi^2-M^2}{2\sqrt{(s/4-m_\pi^2)}\sqrt{(s/4-M^2)}}. \tag{B.2}$$

A particular partial wave amplitude for the process is then obtained by

$$A_l(s) = \int\limits_{-1}^{1} A(s,t)P_l(\cos\theta)\,d(\cos\theta); \tag{B.3}$$

the integration over $d(\cos\theta)$ may be replaced by one over dt by virtue of equation (B.2). It is one of these partial wave amplitudes, specifically the $l = 1$ amplitude, which is the analogue of the functions J_1 and J_2 discussed in Chapter III. The fact that the nucleon spin has been ignored is responsible for the appearance of only one function here instead of two; however the kinematics have not been affected, so that the singularities of A_1 which will be obtained here are identical with those of the actual functions J_1 and J_2.

If the contraction rule is applied to the annihilation amplitude, then as in the derivation of equation (3.8), one obtains

$$\frac{A(s,t)}{\sqrt{(4E_{p_2}\omega_{q_2})}} = \sum_n \left\{\frac{(2\pi)^3\delta^3(\mathbf{P}_n-\mathbf{q}_1-\mathbf{q}_2)\langle p_2|j_N|n\rangle\langle n|j_\pi|q_1\rangle}{E_n-\omega_1-\omega_2+i\epsilon} + \frac{(2\pi)^3\delta^3(\mathbf{P}_n+\mathbf{q}_2-\mathbf{p}_2)\langle p_2|j_\pi|n\rangle\langle n|j_N|q_1\rangle}{E_n-E_2+\omega_2+i\epsilon}\right\}. \tag{B.4}$$

Equation (B.4) may be thought of as the decomposition of the $\pi+\pi \rightarrow N+\bar{N}$ amplitude into the processes $\pi+\pi \rightarrow n \rightarrow N+\bar{N}$ (the first term) and $\pi \rightarrow n+N$ followed by $\pi+n \rightarrow N$ (the second term). Now, the first term will be singular if

$$P_n = q_1+q_2,$$

that is, if

$$P_n^2 = (q_1+q_2)^2 = s.$$

Since the lightest state n here consistent with the various conservation laws is two pions, the first term is singular when

$$s = P_n^2 \geqslant 4m_\pi^2.$$

The next heaviest state is four pions, which produces a singularity for

$$s \geqslant 16m_\pi^2;$$

thus for $4m_\pi^2 \leqslant s \leqslant 16m_\pi^2$ all of the singularities in the first term of (B.4) are due to the two-pion intermediate state, pictured in Fig. III.5(b).

The second term in (B.4), on the other hand, is singular if

$$P_n = p_2 - q_2 = q_1 - p_1;$$

in other words, if

$$P_n^2 = (q_1 - p_1)^2 = t.$$

Here the lightest allowed state is one nucleon, for which $P_n^2 = M^2$, and which therefore produces a pole at $t = M^2$. In diagrams, this is represented by Fig. III.5(c). The next state is one nucleon and one pion, for which $P_n^2 \geqslant (M + m_\pi^2)^2$, so there are singularities from the second term of (B.4) for

$$t \geqslant (M + m_\pi^2)^2.$$

This term is illustrated in Fig. (B.1).

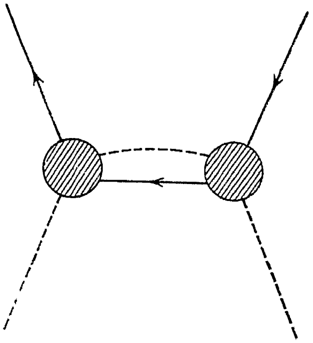

FIG. B.1. Graph illustrating the one nucleon one meson intermediate state contributing to the second term of equation (B.4).

Now singularities will occur in $A_l(s)$, according to equation (B.3), either when $A(s, t)$ is singular as a function of s, or when the integration over $\cos\theta$, or equivalently t, includes a region of t for which $A(s, t)$ is singular in t. It is the assumption of the Mandelstam representation that no further singularities exist in $A_l(s)$.

$A_l(s)$ will then have singularities for $s \geqslant 4m_\pi^2$, of which those between $4m_\pi^2$ and $16m_\pi^2$ are due only to the two-pion state contribution to the first term of (B.4). It will also have singularities whenever the range

$$-1 \leqslant \frac{t+\frac{1}{2}s-m_\pi^2-M^2}{2\sqrt{(s/4-m_\pi^2)}\sqrt{(s/4-M^2)}} \leqslant 1$$

is consistent with $t = M^2$ or $t \geqslant (M+m_\pi)^2$. It is possible to have $t = M^2$ in this range when

$$s \leqslant 4m_\pi^2(1-m_\pi^2/4M^2);$$

it is possible to have $t \geqslant (M+m_\pi)^2$ when

$$s \leqslant 0.$$

The singularities of $A_l(s)$ between 0 and $4m_\pi^2(1-m_\pi^2/4M^2)$ are therefore all due to the single nucleon pole in the second term of (B.4).

Finally, as has been indicated in Chapter III, Im $A_l(s)$ is proportional to the discontinuity of $A_l(s)$; thus Im $A_l(s)$, or equivalently Im $J_{1,2}$ of the actual problem will be non-zero if $s \geqslant 4m_\pi^2$, or $s \leqslant 4m_\pi^2(1-m_\pi^2/4M^2)$. Since Im $J'_{1,2}$ is the same as Im $J_{1,2}$ with the two-pion state omitted, Im $J'_{1,2}$ will be non-zero for $s \geqslant 16m_\pi^2$ or $s \leqslant 4m_\pi^2(1-m_\pi^2/4M^2)$.

NOTES

[1] The following notation will be consistently used: 4-vectors are denoted a, or a_μ, or $(a_0, \mathbf{a})$. The scalar product is defined as

$$a \, . \, b = a_0 b_0 - \mathbf{a} \, . \, \mathbf{b} = a_\mu b_\mu;$$

raising and lowering of indices will be suppressed. The Dirac matrices are defined by

$$\gamma_\mu = (\beta, \beta\boldsymbol{\alpha}), \qquad \gamma_5 = \gamma_0\gamma_x\gamma_y\gamma_z$$

and

$$\sigma_{\mu\nu} = \tfrac{1}{2}i(\gamma_\mu\gamma_\nu - \gamma_\nu\gamma_\mu).$$

The symbol $\not{a}$ will be used for $a\,.\,\gamma = a_\mu\gamma_\mu$. The operator ∇_μ is $\left(\frac{\partial}{\partial t}, -\boldsymbol{\nabla}\right)$; thus the free Dirac equation is written ($\hbar = c = 1$)

$$(i\not{\nabla}-M)\psi = 0.$$

The spinors which are used are normalized to $\bar{u}_p u_p = 2M$ for positive energy solutions where $\bar{u} = u^*\gamma_0$, and $\bar{v}_p v_p = -2M$ for negative energy solutions. All field operators which appear are renormalized Heisenberg fields; Heisenberg states are denoted $|p\rangle$, for example, for a single particle of momentum $\mathbf{p}$.

[2] The combination $\frac{1}{q^2}\langle p_f^{(e)}|\int d^4x j_\mu^{(e)}(x)e^{iq.x}|p_i^{(e)}\rangle$ is what one usually refers to as the Møller potential, $A_\mu^{(e)}(q)$, of the scattered electron.

[3] S. Schweber, H. Bethe, and F. de Hoffmann, *Mesons and Fields* Vol. 1 (Row Peterson and Co., Evanston, Ill. 1955), p. 119.

[4] Here

$$F_{\mu\nu}^{(e)} \equiv \nabla_\nu A_\mu^{(e)} - \nabla_\mu A_\nu^{(e)} = i[q_\nu A_\mu^{(e)} - q_\mu A_\nu^{(e)}].$$

[5] M. N. Rosenbluth, *Phys. Rev.*, **79**, 615 (1950); in writing this the electron rest mass is set to zero; i.e. $m^2/q^2 \to 0$.

[6] The experimental basis for these definitions is this. The zero energy limit of the amplitude for Compton scattering, i.e., the Thomson limit, is proportional to $\frac{F_1^2(0)}{M} = e^2/M$. This comes from the two Feynman diagrams

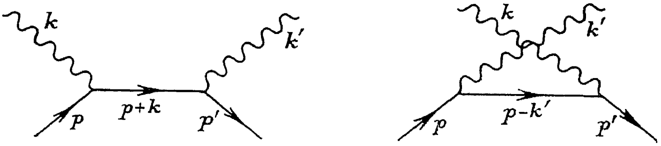

which for zero photon energy measure just the product of two vertices connecting physical (because $\lim\limits_{k\to 0}(p\pm k)^2 = M^2$) proton states and also measure $F_1(0)$ since $q^2 = 0$ for real photons. $F_2(0)$ is determined by measurement of the proton magnetic moment in an external magnetic field.

[7] J. Hamilton, 'The Theory of Elementary Particles' (Oxford 1959), Chapter VI.

[8] It is customary to define a neutron charge radius as follows:

$$\langle r^2\rangle_{1,N} = 6F_1^N(q^2)'|_{q^2=0}/F_1^P(0)$$

$$= \frac{6}{e}F_1^N(q^2)'|_{q^2=0}.$$

[9] R. Hofstadter, *Annual Rev. Nuclear Science*, **7**, 231 (1957); R. Hofstadter, F. Bumiller and M. Yearian, *Rev. Mod. Phys.*, **30**, 482 (1958); E. E. Chambers and R. Hofstadter, *Phys. Rev.*, **103**, 1454 (1956); R. Hofstadter and R. W. McAllister, *Phys. Rev.*, **98**, 217 (1955), **102**, 851 (1956); G. W. Tautfest and W. K. H. Panofsky, *Phys. Rev.*, **105**, 1356 (1957). R. W. McAllister, *Phys. Rev.*, **104**, 1494 (1956). See also E. Clementel and C. Villi, *Nuovo Cimento*, **4**, 1207 (1956) and Yennie, Lévy and Ravenhall, *Rev. Mod. Phys.*, **29**, 144 (1957); R. Hofstadter and R. R. Wilson: *9th Ann. Int. Conf. on High Energy Physics at Kiev*, 1959.

[10] There may, of course, be more than one intersection. The figure shows only that in the first quadrant.

[11] J. Schwinger, *Phys. Rev.*, **76**, 790 (1949). This radiative correction has been observed directly in the absolute measurements of electron–proton scattering cross-sections as carried out with low resolution by Tautfest and Panofsky [9] to an accuracy of 2 per cent, and with high resolution by McAllister [9] to an accuracy of 6 per cent.

[12] D. Yennie, D. G. Ravenhall and R. Wilson, *Phys. Rev.*, **95**, 500 (1954) and unpublished calculations referred to in Yennie, Lévy and Ravenhall, *Rev. Mod. Phys.*, **29**, 144 (1957).

[13] S. Drell and M. Ruderman, *Phys. Rev.*, **106**, 561 (1957); S. Drell and S. Fubini, *Phys. Rev.*, **113**, 741 (1959).

[14] Y. Yamaguchi (unpublished), Karzas, Watson and Zachariasen, *Phys. Rev.*, **110**, 253 (1958).

[15] Yamagata, Auerbach, Bernardini, Fuosofo, Hansen and Odian, *Bull. Am. Phys. Soc.*, Ser. II, **1**, 350 (1956).

[16] L. L. Foldy, *Rev. Mod. Phys.*, **30**, 471 (1958).

[17] E. Fermi and L. Marshall, *Phys. Rev.*, **72**, 1139 (1947); Hammermesh, Ringo and Wattenberg, *Phys. Rev.*, **85**, 483 (L) (1942).

[18] Havens, Rabi and Rainwater, *Phys. Rev.*, **72**, 634 (1947), **82**, 345 (1951); Melkonian, Rustad and Havens, *Phys. Rev.*, **114**, 1571 (1959).

[19] Harvey, Hughes and Goldberg, *Phys. Rev.*, **87**, 220 (A) (1952), **88**, 163 (A) (1952); Hughes, Harvey, Goldberg and Stafne, *Phys. Rev.*, **90**, 497 (L) (1953).

[20] R. Hofstadter, F. Bumiller and M. R. Yearian, *Rev. Mod. Phys.*, **30**, 482 (1958); Yearian and Hofstadter, *Phys. Rev.*, **110**, 552 (1958), **111**, 934 (1958).

[21] S. Sobottka, *Phys. Rev.*, **118**, 831 (1960).

[22] V. Z. Jankus, *Phys. Rev.*, **102**, 1586 (1956); R. Blankenbecler, *Phys. Rev.*, **111**, 1684 (1958); A. Goldberg, *Phys. Rev.*, **112**, 618 (1958); L. Durand III, *Phys. Rev.*, **115**, 1020 (1959).

[23] The neutron contribution to (2.5) is $\approx 30\%$ of that of the proton for $q^2 > (2.5)^2 \times 10^{26}$ cm^{-2} corresponding to scattering of 600 MeV electrons through 60°. For such parameters the Rosenbluth cross-section is dominated by the $(F_1 + 2MF_2)^2 \tan^2(\frac{1}{2}\theta)$

term corresponding to scattering by the total Dirac plus Pauli moment.

[24] There are of course also the experimental difficulties associated with an accurate subtraction procedure in (2.5) which permits

$$d\sigma_N/d\Omega_{e'} = \int dE_{e'} \frac{d^2\sigma_P}{dE_{e'}\, d\Omega_{e'}} - d\sigma_P/d\Omega_{e'}$$

to be stated with small experimental errors.

[25] These remarks are amplified in R. Blankenbecler, *Phys. Rev.*, **111,** 1684 (1958); S. Drell: *8th Ann. Int. Conf. on High Energy Physics at CERN* (1958).

[26] W. K. H. Panofsky, *8th Ann. Int. Conf. on High Energy Physics at CERN* (1958).

[27] It should be cautioned that only qualitative significance is to be assigned to these results as they are based on a non-relativistic approximate treatment of the intricate nucleon–nucleon interaction operating in both the deuteron and in the final state.

[28] G. Chew and F. Low, *Phys. Rev.*, **113,** 1640 (1959).

[29] S. Mandelstam, *Phys. Rev.*, **112,** 1344 (1958), **115,** 1741, 1752 (1949). The cuts with the so called anomalous thresholds have not been included here. These occur whenever one is dealing with a loosely bound structure such as the deuteron. The first of these cuts starts at $\Delta^2 \approx M_N^2 + 2m_\pi^2$, in other words at $T_{P_{1a}} \approx -\frac{m_\pi^2}{M_D} \approx -10$ MeV. See for example reference 55.

[30] The differences between M_N, M_P, and $\frac{1}{2}M_D$ are exhibited only when they are significant.

[31] Spin factors are suppressed here. They are irrelevant for the discussion of unpolarized cross-sections.

[32] These remarks may all be paraphrased in the language of field theory. Since the following chapter is largely devoted to the development of this language and its application to the electromagnetic vertex, it will suffice only to mention here that one is calculating the amplitude for deuteron break-up by a virtual photon represented by a Møller potential $A_\mu^{(e)}(q)$:

$$T = eA_\mu^{(e)}(q)\langle p_P p_N | j_\mu(0) | p_D\rangle$$

with j_μ the photon current operator. If the reduction formula is applied to bring the proton field operator explicitly into the matrix element there results

$$T = -\frac{eA_\mu^{(e)}}{\sqrt{(2E_p)}}\, \bar{u}_p \sum_n \left\{ \frac{\langle p_N | j_N | n\rangle \langle n | j_\mu | p_D\rangle}{E_n - E_{p_P} - E_{p_N} - i\epsilon} + \frac{\langle p_N | j_\mu | n\rangle \langle n | j_N | p_D\rangle}{E_n + E_{p_P} - E_D - i\epsilon} \right\}$$

where $j_N = (i\nabla\!\!\!/ - M)\psi$. The pole for the one neutron intermediate state in Fig. II.10 arises from the second term for $|n\rangle$ a one neutron state with $M_N^2 = P_n^2 = (p_D - p_P)^2 = \Delta^2$. In the vicinity of this pole one has the limit

$$T \to \frac{-eA_\mu^{(e)}}{\sqrt{(2E_p)}}\,\bar{u}_p\,\frac{\langle p_N|j_\mu|n\rangle\langle n|j_N|p_D\rangle}{M_N^2-\Delta^2}\,(2E_n)$$

so that T is expressed as in (2.8) as the product of electron-neutron scattering times the amplitude for projecting the proton out of the deuteron. Pushing on further in the spirit of the polology game this second factor can be related to the pole in low energy neutron proton scattering in the triplet state in which the bound deuteron state appears as a pole for an extrapolated $-2{\cdot}2$ MeV bombarding energy.

[33] J. Blatt and V. Weisskopf, Theoretical Nuclear Physics (John Wiley and Sons, Inc., New York, 1952), p. 611.

[34] This is true on the basis of charge symmetry alone and does not require the full assumption of charge independence. The cross-section for this is readily adapted from equation (2.9). For (2.10*a*), for example, replace M_P everywhere by M_D and $M_D\Gamma^2$ by the corresponding asymptotic wave function normalization for H^3. The pole here occurs at $T_{D_l} = \dfrac{M_N^2-(M_{H^3}-M_D)^2}{2M_{H^3}} \approx -2$ MeV for the H^3 target, and similarly for the He^3 target. The anomalous threshold starts at $\Delta^2 \approx M_N^2+\frac{3}{2}m_\pi^2$ or at $T_{D_{l_a}} \approx -2\text{ MeV}-\frac{1}{4}m_\pi^2/M_N \approx -7$ MeV and is somewhat closer to the pole of interest than was the case for the deuterium experiment [29].

[35] J. A. McIntyre and S. Dhar, *Phys. Rev.*, **106,** 1074 (1957); J. A. McIntyre and G. R. Burleson, *Phys. Rev.*, **112,** 2077 (1958).

[36] R. Blankenbecler, Ph.D. Thesis, Physics Department, Stanford University (unpublished), 1958.

[37] L. I. Schiff, *Rev. Mod. Phys.*, **30,** 462 (1958).

[38] J. Bernstein, *Phys. Rev.*, **104,** 249 (1956).

[39] J. Friedman and H. Kendall and P. Gram, *Phys. Rev.*, **120,** 992 (1960).

[40] L. I. Schiff, *Phys. Rev.*, **98,** 756 (1955).

[41] R. R. Lewis, Jr., *Phys. Rev.*, **102,** 537, 544 (1956).

[42] H. S. Valk, *Nuovo Cimento*, **6,** 173 (1957); H. S. Valk and B. J. Malenka, *Phys. Rev.*, **104,** 800 (1956).

[43] W. Panofsky and E. Allton, *Phys. Rev.*, **110,** 1155 (1958); G. Ohlsen, *Phys. Rev.*, **120,** 584 (1960).

[44] S. Fubini, Y. Nambu, and V. Wataghin, *Phys. Rev.*, **111,** 329 (1958).

[45] As a spin zero particle, a pion has only one electromagnetic form factor. The most general gauge invariant form for the pion electromagnetic vertex is

$$\langle q_2\sigma_2|j_\mu|q_1\sigma_1\rangle = \frac{-i}{\sqrt{(4\omega_{q_1}\omega_{q_2})}}\,(q_2+q_1)_\mu(\delta_{\sigma_1 1}\delta_{\sigma_2 2}-\delta_{\sigma_1 2}\delta_{\sigma_2 1})F_\pi((q_2-q_1)^2)$$

where q and σ represent pion momentum and charge states. The form factor F_π is a function of the only invariant, the square of the four-momentum transfer; and the combination $(q_2+q_1)_\mu$ is the only four vector which can appear, since the further requirement of gauge invariance, and hence of a continuity equation, is expressed by

$$(q_2-q_1)_\mu \langle q_2\sigma_2 | j_\mu | q_1\sigma_1 \rangle = 0.$$

[46] Solutions to the dispersion relations are needed for large q^2 in order to probe form factors and for low E so that the 3–3 resonance dominates the contribution to the dispersion integrals. Large values of q^2 make the static approximation which has been used for the photo-meson production analysis ($q^2 = 0$) a much poorer approximation here. Fubini, Nambu, and Wataghin have formulated the dispersion relations covariantly taking into account the 3–3 resonance only in the evaluation of the absorptive amplitudes. A general method of solution is being explored now by Blankenbecler, Gartenhaus, Huff, and Nambu, *Nuovo Cimento*, **17,** 775 (1960).

[47] It is of no value in nucleon structure studies to detect the pion alone since the undetected electron will then emerge predominantly in the forward direction, corresponding to $q^2 \rightarrow 0$ as in photo production.

[48] It is approximately one-half of the way from the physical region to the start of the branch cut for the nucleon and pion state which starts at $t_{\pi_l} = -2m_\pi$. In terms of the angle θ between the pion and the direction of momentum transfer by the electron, $\mathbf{q}$, in the centre-of-mass system of the recoil nucleon and pion, the pole is found at

$$\cos\theta = -\frac{q_0 E_{p'} - \frac{1}{2}q^2}{\sqrt{(q_0^2-\mathbf{q}^2)}\sqrt{(E_{p'}^2-M^2)}} < -1$$

[49] W. R. Frazer, *Phys. Rev.*, **115,** 1763 (1959).

[50] For other theoretical reviews on this subject see: D. Yennie, M. Lévy, and D. Ravenhall, *Rev. Mod. Phys.*, **29,** 144 (1957); J. Bernstein and M. Goldberger, *Rev. Mod. Phys.*, **30,** 465 (1958); S. Drell, *8th Ann. Int. Conf. on High Energy Physics at CERN* (1958); L. I. Schiff, *9th Ann. Int. Conf. on High Energy Physics at Kiev* (1959).

[51] B. Fried, *Phys. Rev.*, **88,** 1142 (1952) and see Schweber, Bethe, and de Hoffmann, *Mesons and Fields* (Rowe Peterson & Co., Evanston, Ill. 1955).

[52] H. Miyazawa, *Phys. Rev.*, **101,** 1564 (1956); S. Fubini, *Nuovo Cimento*, **3,** 1425 (1956); F. Zachariasen, *Phys. Rev.*, **102,** 295 (1956); G. Salzman, *Phys. Rev.*, **105,** 1076 (1957); Blokhintsev, Barashenkov, and Barbashov, *JETP*, **36,** 1145 (1959); S. Trieman and R. Sachs, *Phys. Rev.*, **103,** 435 (1956).

[53] Chew, Karplus, Gasiorowicz, and Zachariasen, *Phys. Rev.*, **110**, 265 (1958); Federbush, Goldberger, and Trieman, *Phys. Rev.*, **112**, 642 (1958).

[54] Bremerman, Oehme, and Taylor, *Phys. Rev.*, **109**, 2178 (1958); R. Oehme, *Nuovo Cimento*, **4**, 1316 (1956).

[55] Y. Nambu, *Nuovo Cimento*, **6**, 1064 (1957), and **9**, 610 (1958); J. Bjorken, Ph.D. Thesis, Stanford University, 1959 (unpublished); R. Chisholm, *Proc. Camb. Phil. Soc.*, **48**, 300 (1952); L. Landau, *Nucl. Phys.*, **13**, 141 (1959).

[56] It should be noted that this is consistent with the reality property proved in Chapter I. The proof given there fails for $q^2>0$, when the form factors are defined in terms of the production amplitude $\gamma \rightarrow N+\bar{N}$, because of the difference between ingoing and outgoing boundary conditions.

[57] For a proof of this identity, see Appendix A.

[58] It should be noted that the field operators written in these equations are all renormalized Heisenberg fields.

[59] It can be shown that a finite charge renormalization $1 \geqslant Z_3 > 0$ implies the validity of the unsubtracted form of the dispersion relation. S. Drell and F. Zachariasen, *Phys. Rev.*, **119**, 463 (1960).

[60] S. Schweber, H. Bethe, and F. de Hoffmann, *Mesons and Fields*, vol. I (Row Peterson & Co., Evanston, Ill., 1955), sec. 13.

[61] J. Bernstein and M. Goldberger, *Rev. Mod. Phys.*, **30**, 465 (1958).

[62] J. Bjorken (private communication).

[63] J. D. Walecka, *Nuovo Cimento*, **11**, 821 (1959).

[64] As opposed to an extrapolation to negative kinetic energies as would be the case if $q'^2<4M^2$.

[65] J. Hamilton, 'The Theory of Elementary Particles,' Oxford, 1959, Chapter VI.

[66] N. Kemmer, J. Polkinghorne, and D. L. Pursey, Rep. on Prog. in Phys., **22**, 1959. The notation is intended to indicate the change of sign of the space momentum.

[67] The measured isovector magnetic moment form factor, for example, corresponds to a spread out distribution with a second moment $\langle r^2\rangle \sim (0{\cdot}8f)^2$ in a one parameter fit to the data. However, the "unitarity limit" (3.17) on the second moment is $(0{\cdot}14f)^2$; for higher moments $\langle (r^2)^l\rangle_{N\bar{N}}$ similar bounds $\sim \dfrac{1}{M^{2l}}$ emerge indicating a much more compact distribution than is observed.

[68] The neglect of heavy states has been shown to be correct, however, in a special model related to this problem. M. Baker and F. Zachariasen, *Phys. Rev.*, **119**, 438 (1960).

[69] R. Omnés, *Nuovo Cimento*, **8**, 316 (1958).

[70] S. Mandelstam, *Phys. Rev.*, **112**, 1344 (1958); **115**, 1741, 1752 (1959).

[71] This analysis has been carried out by W. Frazer and J. Fulco, *Phys. Rev. Lett.*, **2,** 365 (1959); *Phys. Rev.*, **115,** 1763 (1959); **117,** 1609 (1960).

[72] It is actually not obvious that the results quoted here are correct, since the four-particle vertex under discussion is not completely analogous to the three-particle vertex analysed before, and from which the analogue of equation (3.20) was obtained. However, if the Mandelstam representation is accepted, equation (3.20) can be obtained from it. See reference [70].

[73] It is assumed here that F_π has no zero, and that $J_1/F_\pi \rightarrow 0$ at ∞.

[74] Equations (3.23) are related to the static meson theory as follows: First of all, F_π is replaced by e, since the pion is a point particle and there is no $\pi\pi$ interaction in the static theory. Second, one keeps, in addition to the Born approximation diagram III.5(c) in $\operatorname{Im} J'$ the contribution of the one nucleon one pion state as shown in Fig. B.1 of Appendix B. Finally, the nucleon mass is sent to infinity, a cutoff on the dispersion integral is introduced, and pion nucleon scattering in the one pion one nucleon state is kept only in the resonant 33 state. Frazer and Fulco have shown that these rescattering corrections are not important in the relativistic analysis including a pion form factor.

[75] S. Fubini, *8th Int. Conf. on High Energy Physics at CERN* (1958), p. 35.

[76] G. Chew and F. Low, *Phys. Rev.*, **113,** 1640 (1959); C. Goebel, *Phys. Rev. Lett.*, **1,** 337 (1958); S. Drell and F. Zachariasen, *Phys. Rev. Lett.*, **5,** 66 (1960); F. and G. Salzman, *Phys. Rev.*, **120,** 599 (1960); I. Dremin, *JETP*, **39,** 130 (1960); S. Drell, *Phys. Rev. Lett.*, **5,** 342 (1960).

[77] G. Chew and S. Mandelstam, *Phys. Rev.*, **119,** 467, 478 (1960), M. Baker and F. Zachariasen, *Phys. Rev.*, **118,** 1659 (1960).

[78] K. Hiida, N. Nakanashi, Y. Nogami, and M. Uehara, *Prog. Theor. Phys.*, **22,** 247 and 351 (1959).

[79] B. Bosco and V. De Alfaro, *Phys. Rev.*, **115,** 215 (1959); I. Tamm, *9th Ann. Int. Conf. on High Energy Physics at Kiev* (1959).

[80] The difficult relation between the sizes of protons and neutrons may be resolved if the principle of charge symmetry is abandoned; for example, see D. Yennie, M. Lévy, and D. Ravenhall, *Rev. Mod. Phys.*, **29,** 144 (1957).

[81] The electromagnetic radiative corrections of Fig. II.3 may of course be partially summarized in terms of electron structure; these are included in the experimental analysis. What is meant here by electron structure are possible additional contributions due to modifications in the quantum electrodynamics.

[82] S. Drell, *Ann. Phys.* (New York), **4,** 75 (1958).

[83] P. Franken and S. Liebes, Jr., *Phys. Rev.*, **104,** 1197 (1956);

Schupp, Pidd, and Crane, *Bull. Am. Phys. Soc.*, Ser. II, **4,** 250 (1959) quoted by L. Lederman; C. M. Sommerfield, *Phys. Rev.*, **107,** 328 (1957); *Ann. of Physics* (New York), **5,** 26 (1958); A. Petermann, *Helv. Phys. Acta*, **30,** 407 (1957); *Nuclear Physics*, **3,** 689 (1957); **5,** 677 (1958); A. J. Layzer, *Phys. Rev. Lett.*, **4,** 580 (1960); H. Fried and D. Yennie, *Phys. Rev. Lett.*, **4,** 583 (1960).

[84] The distance quoted here is defined by $(\frac{1}{6}\langle r^2\rangle)^{\frac{1}{2}}$; i.e. by the coefficient of the square of the four momentum transfer q^2 in an expansion in powers of q^2 of the deviations from point particle predictions. The reader should recall the discussion of Chapter II which points out that this 'radius' is in fact not well measured directly, but is obtained if a smooth extrapolation of the results to small q^2 is assumed. See also reference [82], *op. cit.*

[85] R. P. Feynman, *8th Ann. Int. Conf. on High Energy Physics at CERN*, p. 25.

[86] A. I. Nikishov, *J. Exptl. & Theoretical Physics*, USSR, **36,** 1604 (1959), English Translation *JETP*, **9,** 1140 (1959), has given a more general formula including the terms which vanish as $m \to 0$.

[87] Throughout these remarks Lorentz invariance is presumed.

[88] The vertex and propagator are related by Ward's identity expressing the gauge invariance of the theory.

[89] For other estimates see: H. Salecker, *Z. Naturforsch.*, **8a,** 16 (1953); G. Andreassi, P. Budini, and I. Reina, *Nuovo Cimento*, **12,** 488 (1959); G. Furlan and G. Peresutti, *Nvovo Cimento*, **14,** 758 (1959). The relative merits of these experiments as probes of structure in quantum electrodynamics depend on the assumed models of possible deviations from the point theory.

[90] Barber, Gittleman, O'Neill, Panofsky, and Richter (in progress).

[91] Y. S. Tsai, *Phys. Rev.*, **120,** 269 (1960).

[92] J. Bjorken, S. Drell, and S. Frautschi, *Phys. Rev.*, **112,** 1409 (1958); I. A. Dyatlev, *JETP*, **35,** 154 (1958) (in Russian); B. Richter, *Phys. Rev. Lett.*, **1,** 114 (1958).

[93] Also there are no form factors at the vertex for absorbing the incident photon since the four momentum of a photon is zero.

[94] J. Bjorken and S. Drell, *Phys. Rev.*, **114,** 1368 (1959).

[95] Lehman, Symanzik and Zimmerman, *Nuovo Cimento*, **1,** 205, (1955). This paper also defines the in and out fields ψ_{in} and ψ_{out}.

NOTES ADDED IN PROOF

1. Page 66. R. Cutkosky (Tenth Annual International Conference on High Energy Physics at Rochester) has shown that such a replacement generally produces the absorptive part of any Feynman graph.

2. Page 85. Frautschi and Walecka [*Phys. Rev.* (1960) in press] and Bowcock, Cottingham and Lurie [*Nuovo Cimento*, **16,** 918 (1960)] have included the effect of $\pi\pi$ scattering on πN scattering, and find no significant effect on the large 33 phase shift. However Frautschi [*Phys. Rev. Letters*, **5,** 159 (1960)] has shown that with the Frazer-Fulco [71] parameters for the $\pi\pi$ interaction, unacceptable small P-wave phase shifts are found in the πN problem. Bowcock et al., on the other hand, determine the $\pi\pi$ interaction by fitting the energy dependence of the S-wave πN phase shifts and the radius, $\langle r^2\rangle_2$, of the magnetic form factor F_2^v, and find the $\pi\pi$ resonance at a higher energy (around $5m_\pi$) and narrower in width than

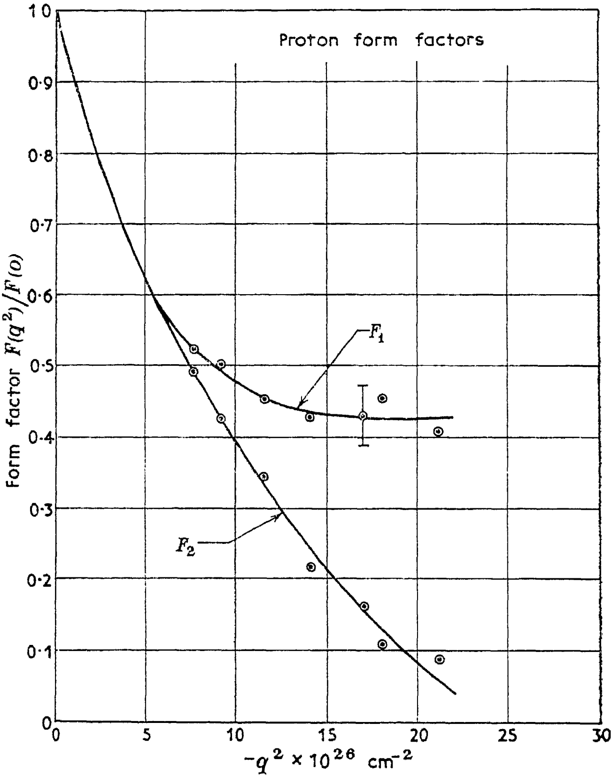

that of Frazer and Fulco, leading to too large a static magnetic moment by a factor of the order of two. These results indicate that the two-pion approximation may well be inadequate.

As yet there is no clear experimental evidence for or against the existence of the $\pi\pi$ resonance.

3. Page 19 and page 87. The latest experimental information on the proton form factors, as obtained from electron–proton scattering, is shown in the graph taken from Hofstadter, Bumiller and Croissiaux. These curves are in agreement with data by Beckelman, Cassels and Wilson, and by L. Hand. (Report to Tenth Annual International Conference on High Energy Physics at Rochester.)

   It is interesting that F_1 appears to be levelling off, indicating that approximately 40 per cent of the time a proton is a "proton." It is also worth noting that the shape of F_2, together with the results on page 64, shows that Im F_2 cannot be positive definite.

L. Hand, *Phys. Rev. Letts.*, **5**, 168 (1960).
Bumiller, Croissiaux, and Hofstadter, *Phys. Rev. Letts.*, **5**, 261, 263 (1960).
Wilson, Berkelman, Cassels, and Olson, *Nature*, **188**, 94 (1960).

UNIVERSAL LIBRARY

112 515

UNIVERSAL LIBRARY